Fall 12-2018

Host Mediated Mechanisms of Fungal Cell Spread in a Transparent Zebrafish Infection Model

Allison Scherer
allison.scherer@maine.edu

HOST MEDIATED MECHANISMS OF FUNGAL CELL SPREAD IN A TRANSPARENT ZEBRAFISH INFECTION MODEL

By

Allison Scherer

B.S. St Cloud State University, 2012

A DISSERTATION

Submitted in Partial Fulfillment of the

Requirements for the Degree of

Doctor of Philosophy

(in Microbiology)

The Graduate School

The University of Maine

December 2018

Advisory Committee:

Robert Wheeler, Associate Professor of Microbiology, Advisor

Julie Gosse, Associate Professor of Biochemistry

Clarissa Henry, Assistant Professor of Biological Sciences

Roger Sher, Research Associate Professor of Neurobiology, Stony Brook University

John Singer, Professor of Microbiology

HOST MEDIATED MECHANISMS OF FUNGAL CELL SPREAD IN A TRANSPARENT ZEBRAFISH INFECTION MODEL

By Allison Scherer

Dissertation Advisor: Dr. Robert Wheeler

An Abstract of the Dissertation Presented
in Partial Fulfillment of the Requirements for the
Degree of Doctor of Philosophy
(in Microbiology)

December 2018

Innate immunity has developed elegant processes for the detection and clearance of invasive fungal pathogens. Disseminated candidiasis is of significant concern for those with suppressed immune systems or indwelling medical equipment, and mortality in these groups approaches 70%. Poor patient outcomes have spurred the need to understand how this non-motile pathogen spreads in the host. Technical limitations have previously hindered our ability to visualize the role of innate immunity and host tissue barriers in the spread of *C. albicans in vivo*. Using the zebrafish model to overcome these limitations, we have examined three potential host-mediated mechanisms of dissemination: movement inside phagocytes ("Trojan Horse"), inflammation, and endothelial barrier disruption.

Both neutrophils and macrophages respond to yeast-locked and wild type *C. albicans* in our zebrafish infection model, and time lapse imaging has revealed that macrophages may support yeast spread in a "Trojan Horse" mechanism. Similarly, inflammation is associated with the influx of immune cells to the site of infection which often precedes dissemination events. Loss of immune cell response or inflammation does not alter dissemination dynamics, however, so other mechanisms of yeast spread are also involved. Time lapse imaging also demonstrated the role of the endothelium on direct uptake of yeast into the bloodstream, suggesting the endothelium aids in yeast escape. When blood flow is blocked, yeast continue to cross the endothelium, but

dissemination level is reduced. With loss of both phagocytes and blood flow, yeast disseminate but the distance traveled may be reduced. Together, our data suggests a two-step process: (1) yeast are brought across the endothelium with the assistance of phagocytes or direct uptake of host tissue, and then (2) utilize blood flow or phagocytes to travel to distant sites.

This suggests the host can contribute to the spread of yeast throughout the body. Surprisingly, innate immune cells do not always contain or kill the pathogen, instead allowing it grow if released in other tissues. This work will help to identify specific host and pathogen molecules which initiate cues for yeast uptake and spread, pinpointing areas for therapeutic targeting.

ACKNOWLEDGEMENTS

A generous amount of thanks goes to my advisor, Rob Wheeler. Thank you for pointing me in the right directions, allowing me to let go of the little stuff, and being a constant supporter of my crazy science dream! Additionally, my main project would not have been possible without the discussion and support of Team Yolk: Zachary Newman, Brittany Seman, Joshua Jones, Sony Manandhar, and Jessica Moore. Honorary team yolk members include Bailey Blair and Josh Kelly who made my late nights and early mornings with zebrafish mean something more than just pretty pictures. I would also like to thank Mark Nilan for fish care in the zebrafish facility, Michel Bagnat and Jieun Park for histology, and Julie Walter for help with data analysis.

To those that supported me on bad fish days (Yay fish!) or with technical experiment advice, thank you! I would like to specifically thank Remi Gratacap who worked with me through one of those painful projects and celebrated with me through the exciting ones. To Linda Archambault and Audrey Bergeron for technical advice, stimulating discussions, and general fish commiseration, thank you. I would also like to extend my thanks to the Henry lab for allowing me to tag along on microscope adventures, technical assists, and equipment use.

I would like to thank my husband Alex for sticking with me even when I make some questionable decisions resulting in late nights or an extra rabbit… Thank you for choosing to hang out with me every day! Thanks to my incredibly supportive parentals-in-law, Mae and Bob, for making sure we take care of ourselves, last minute frog and rabbit-sitting, and helping us with life's little hassles. And lastly, but probably most importantly, thank you to my parents for supporting my pursuit of fungus, general life advice, and for cheering me on from miles away. It was your encouragement that has brought me to these incredible new opportunities. Thank you!

TABLE OF CONTENTS

LIST OF TABLES

LIST OF FIGURES

CHAPTER 1

REVIEW OF THE LITERATURE

1.1 Fungi pathogens in pop culture and the natural environment

H.P. Lovecraft is better known for his captivating tales of a great being somewhere between an octopus and a dragon, called Cthulhu. One of his later, but not lesser, works concerns an alien race, the Mi-go, which are fungoid beings that most closely resemble crustaceans in appearance. For many years, authors and audiences have been fascinated by the unknown and carefully crafted stories of fungal pathogens. Since H.P. Lovecraft, audiences have been regaled with fungal pathogens. These often resemble the brain controlling Cordyceps in *The Girl with all the Gifts* by M. R. Carey, or the world dominating aerosolized spore of Aspergillus in *The Genius Plague* by D. Walton. These exaggerated fungal pathogens have even made it into children's stories as the main antagonist, as in the *Medusoid Mycelium* in the series *A Series of Unfortunate Events* by Lemony Snicket. It's not surprising that fungi are frequently depicted as the dubious and malevolent antagonist in these stories. There are many instances in nature where this is proven true.

Examples of fungal infections in nature are numerous. Frequently we hear about fungal infections related to warm humid places, but northeastern United States (US) has its own unique fungal pathogens. For example, the fungus *Ophidiomyces ophiodiicola* causes skin lesions in timber rattlesnakes found in the northeastern US. The fungus persists in soil as well as colonizing living hosts and has become a concern for pitvipers (Allender et al. 2015). Chytridiomycosis, caused by *Batrachochytrium dendrobatidis*, is associated with the death of amphibians across the world, including the US. Interestingly, Maine frogs may be less susceptible because their thermoregulatory behavior may allow frogs to raise their body temperature to levels that will retard the growth of the fungus. This may impede fungal growth and reduce frog death from fungal complications (Longcore et al. 2007). Fungal pathogens are prevalent in nature, and humans encounter these or similar fungal pathogens every day.

1.1.1 Opportunistic fungal pathogens in humans

Fungal pathogens in humans are frequently opportunistic in nature and take advantage of a weakened host state, specifically when the person is immunosuppressed in some way. The three most important fungal pathogens include Aspergillus, Cryptococcus, and Candida, but many more exist. Aspergillus and Cryptococcus are found in the soil and, when inhaled by immunocompromised people, can establish residence in the lung and brain, respectively (Brown et al. 2012). Candida, however, is often a commensal organism found on the mucosal surfaces on most healthy individuals. It becomes a pathogen that can establish cutaneous, mucosal, or systemic disease when the host becomes immune-suppressed such as through the use of broad spectrum antibiotics, chemotherapy treatment, or HIV/AIDS. Candida has become a serious public health concern as our medical technology has advanced and created growing immunocompromised populations (Brown et al. 2012; Pappas et al. 2018; Pfaller and Diekema 2007). *Candida albicans* and *Candida auris* are of particular concern as they have developed resistance to many antifungal drugs (Johnson et al. 2018; Pappas et al. 2018). Challenges that face the field include finding prevention strategies for developing candidemia, finding tools for early detection, and alternative therapeutics as our current antifungals become less potent to antifungal resistant strains (Pappas et al. 2018).

1.1.2 Tools that *Candida albicans* utilizes to persist in the host

Candida albicans has many strategies to evade the host immune system. Of note, is its ability to undergo morphogenetic conversion. *C. albicans* can grow as a small yeast, pseudohyphae, or in a long filamentous hyphal form (Sudbery, Gow, and Berman 2004). Hyphal locked or yeast locked mutant strains of *C. albicans* have been proposed to be less virulent than the wildtype Candida which suggests morphological switching plays a role in fungal virulence (Cheng et al. 2012). Hyphae have been generally regarded as more damaging to host tissue while yeast were suggested to be more prevalent as a commensal (Grubb et al. 2008). Previous work in our lab has demonstrated

that both morphologies of Candida are virulent in the zebrafish, and that yeast are more likely to disseminate (Seman et al. 2018). Temperature, pH, oxygen, and available nutrients impact the morphology of Candida. Genes associated with yeast-to-hyphae switch are numerous, but the yeast-promoting regulator, Nrg1, has a hypofilamentous phenotype which allows us to ask yeast-specific questions by manipulation of this regulator (Peters et al. 2014; Seman et al. 2018). These fungal morphologies may also impact how well Candida adheres to and invades host tissue.

Adherence and invasion of Candida is done through specific cell wall proteins including ALS3, HWP1, ECE1, SOD5, PHR1, PRA1, among others (Grubb et al. 2008; Losse et al. 2011; Manoharan et al. 2017; McKenzie et al. 2010). Once Candida adheres to the endothelium or epithelium, it is better able to breach host tissue (Gow et al. 2012; Grubb et al. 2008). This breach can occur through the damaging toxin, candidalysin, or through active hyphal penetration of the host to establish infection (Moyes et al. 2016). Additionally, the quorum sensing molecule farnesol represses the yeast-to-hypha transition, and may activate apoptosis of oral epithelial cells (Cheng et al. 2012; Moyes, Richardson, and Naglik 2015).

Lastly, Candida has a strong resistance to phagocyte killing. We have seen in a zebrafish model of infection, few instances of LC3-GFP, an autophagy reporter protein, localized with the phagosomal membrane, suggesting that this is not a useful method for the host in killing Candida (Brothers et al. 2013). To kill pathogens, the phagosome carrying the pathogen must fuse with lysosomes and *C. albicans* inhibits this process to avoid killing (Cheng et al. 2012). *C. albicans* can also inhibit ROS production by producing catalase and superoxide dismutase to counteract the respiratory burst (Cheng et al. 2012). Finally, vacuole formation may aid in resistance to stress brought on by host defense and aid in hyphal formation (Cheng et al. 2012; Rane et al. 2014).

1.1.3 The host's role in infection

In response to Candida's arsenal of evasion implements, the host combats fungal infection through its own surveillance mechanisms. Pattern recognition receptors (PRR) including Toll like

receptors and C-type lectin receptors, DC-SIGN and mincle, among others, work to recognize pathogen-associate molecular patters (PAMP) (Cheng et al. 2012). Each PRR recognizes a specific PAMP found on the pathogen's surface. Once recognized, an alarm is sent up and cytokines and chemokines are produced for recruitment of immune cells. Proinflammatory cytokines include tumor necrosis factor alpha, interleukin 1 beta, interleukin 6, interleukin 8, and interleukin 17 among many others (Cheng et al. 2012). Phagocytes, including neutrophils and macrophages, are specifically recruited to these signals and respond to the infection site. Upregulation of additional hematopoietic growth factors, G-CSF and GM-CSF, promote the myelopoiesis of additional immune cells to reinforce those already responding to infection and replace those lost (Karbassi et al. 1987; M. I. N. Wang, Friedman, and Djeu 1989).

Once at the site, neutrophils will engulf the pathogen and fusion of the lysosome with the phagolysosome results in the release of hydrolytic enzymes, antimicrobial peptides, and reactive oxygen species that are used against Candida. Additional mechanisms of killing include the candidacidal radical peroxynitrite and neutrophil extracellular trap formation (Cheng et al. 2012; Netea et al. 2015; Vázquez-Torres and Balish 1997). Macrophage killing of Candida occurs through fusion of lysosome with phagosomes (Cheng et al. 2012; Vázquez-Torres and Balish 1997); however, our zebrafish model of infection suggests that Candida and macrophages come to an impasses after engulfment. Here, macrophages were observed to have engulfed the yeast and prevented germination, but yeast were still able to replicate within the macrophage (Brothers, Newman, and Wheeler 2011b).

Finally, phagocytes must be cleared from the infection site. Dead or dying are cleared from the site via efferocytosis primarily by macrophages (Hosseini et al. 2016). In *M. marinum* infection, macrophages phagocytose dead cells that contain bacteria, and large aggregates of bacteria are expelled out of the tissue after death (Hosseini et al. 2016). Host cells that are necrotic are cleaned

up by neutrophils and other surrounding phagocytes which also pick up any remaining bacteria (Hosseini et al. 2016). A similar process is likely involved after clearance of fungal infection.

1.2 Models used to test host roles in disseminated candidiasis

1.2.1 *In vitro* models to test fungal shape on tissue to bloodstream spread

In vitro models of Candida infection are useful in that we can dissect the roles of specific host and pathogen characteristics that would influence infection outcomes in the host. Current cell culture models of interest include lines of macrophages, neutrophils, and endothelial cells. Cell culture models are well characterized like mouse J774 and RAW 264.7 cell lines which have numerous mutant strains available (Filler, 2014). Unfortunately, these lines are poor killers of *C. albicans*, but primary mouse macrophages from bone marrow or peritoneum can be a useful alternative. Because these macrophages are taken from the primary source, rather than being from an immortalized cell line, they may be more indicative of what occurs in the host (Filler, 2014). Care must be taken to choose appropriate cell lines for experimentation, as differences are present between mouse and human macrophages, notably, nitric oxide production for microbial killing (Filler, 2014). A fairly new development has been made in way of neutrophil cell lines. Studying neutrophils *in vitro* has been difficult as neutrophil isolation can be involved and the cells have a short life-span (Sykes et al. 2016). As an alternative to isolation from mice, a conditionally immortalized GMP cell line has been made to view neutrophil response *in vitro* (Sykes et al. 2016). These neutrophils can be modified and transplanted back into a mouse model to test molecular mechanisms of neutrophil response (Feldman, Vyas, and Mansour 2018; Sykes et al. 2016). Finally, endothelial cells line conditions can be modified so that blood flow can be simulated. Conditions of flow allow the endothelial cells to adhere to a surface and still have flow that would be present in the host. In this model, *C. albicans* yeast (Grubb et al. 2008) and hyphae (Sheppard and Filler 2014) were found to be more adherent under conditions of flow. Recently, an intestinal epithelial model

was used to test different *C. albicans* strains to disrupt barriers and translocate (Allert et al. 2018), simulating a "disseminated" type of infection in a dish.

While *in vitro* experiments using single or mixed cell types have been exploited to shed considerable insight into the interactions of *C. albicans* and the host, Candida is normally exposed to a variety of host cells, microbial flora, and different microenvironments in a living host during disseminated infection. It is unlikely a simple in vitro system will be able to recapitulate this complexity so, to gain a better understanding of how all these factors work together to influence the course of infection and Candida virulence, *in vivo* models must also be used. When used smartly, the reduced complexity found in *in vitro* systems can be leveraged to screen and identify candidate molecular pathways in host-pathogen interaction which can then be examined in animal models (Filler 2014).

1.2.2 Invertebrate *C. albicans* models demonstrate immune cell responsiveness

Several invertebrate models of *C. albicans* infection have been long established, including: *Drosophila melanogaster*, *Galleria mellonella,* and *Caenorhabditis elegans*. These invertebrate systems are a useful in-between model that often have relevant immune system components which are similar to mice and humans but are less complicated. *Drosophila melanogaster* has conserved Toll pathway which serves as a defense against pathogenic fungi, for example, but they do not have an adaptive immune system. *Drosophila* have been used to study fungal virulence factors and antifungal compounds in large-scale screens (Brunke et al. 2015; Chamilos et al. 2006). Additionally, flies have been used to dissect the roles of the host in systemic Candida infection by monitoring survival of flies infected with clinical isolates (Glittenberg et al. 2011). Results in the flies correlated with virulence of the strains in a murine model, suggesting Toll signaling in *Drosophila* might be required to predict virulence of Candida strains (Glittenberg et al. 2011).

Other invertebrate models, including *Galleria mellonella* and *Caenorhabditis elegans*, are similar in that they are frequently used for large scale screening and mortality experiments. *Galleria*

mellonella can be kept at 37°C equivalent to the temperature in mammalian hosts (Fuchs et al. 2010). Temperature effects Candida virulence traits, so this feature of the model is important to examine Candida specific traits. Additionally, the genome of *Galleria mellonella* is mostly known, so they can target and test specific host genes for infection. *Caenorhabditis elegans* has recently been used to study Candida virulence factors in which hyphal formation plays a large role. This model to has been used to test virulence between Candida strains *in vivo* and compare virulence in production of proteinases and phospholipases between strains easily (Ortega-Riveros et al. 2017). *Caenorhabditis elegans* can also be used as a model for intestinal epithelial infection. In this model, *C. albicans* pre-vacuolar protein sorting gene was found to contribute epithelial and mucosal pathogenesis (Rane et al. 2014). These invertebrate models can offer more complex systems in which to examine host-pathogen interactions than many *in vitro* dish experiments, while still offering the benefits of lower complexity and lower cost to enable molecular level screens of important infection pathways. As invertebrates however, many key factors known to be critical during human infection are missing, which diminishes the usefulness of these models and still necessitates that findings be confirmed in higher scale vertebrate systems to confirm relevance to human infection.

1.2.3 Vertebrate Models

1.2.3.1 Murine model of disseminated candidiasis

As a mammal, the mouse represents perhaps the most highly conserved model system when compared to humans that is widely used in science. The mouse model has been leveraged to provide innumerable insights into disease and immunity throughout the decades. In keeping with this, mouse models of fungal infection have long been a critical tool in studying the interactions of host immunity with fungal infections, including disseminated candidiasis. Mouse models of disseminated Candidiasis start with an immunosuppressed oral infection or Candida is injected directly into the bloodstream and mice die from progressive sepsis (Lionakis et al. 2011). The

mouse can also be used to look at infection in whole organs, such as the liver or kidney which are often most highly infected with Candida from the bloodstream (J. Bain, Gow, and Erwig 2014; Lionakis et al. 2011). Techniques for visualizing Candida in the mouse are developed for the ear and can be used to look at superficial infection sites (Doyle et al. 2006; de Wet et al. 1987). Due to the many points of conservation between mouse and humans, this model system allows for early stage development and evaluation of potential new therapeutics (J. Bain, Gow, and Erwig 2014). As a highly established genetically tractable model system, there are a variety of mouse strains available with specific deletions to examine the roles of key immune cells and systems, and manipulation of living conditions can establish germ free mice which can be used to ask specific questions about naïve immune response. All this contributes to making the mouse model a highly useful system for the study of host-pathogen interactions, including disseminated candidiasis. Despite its advantages, the mouse is not a perfect system for the study of disseminated candidiasis. *C. albicans* is not a natural colonizer of the mouse the way it is for humans, so they need to be made specially treat in some way before infection to allow colonization and dissemination (Naglik, Fidel, and Odds 2008). Because mice are not naturally colonized with Candida, the immune response in these animals represents a naive host, which will also differ from humans which are usually colonized and will therefore have some memory related immunity and other altered responses associated with long-term exposure to the pathogen. While it can be useful to have germ free or otherwise controlled microflora in mice, it is also difficult to draw conclusions from infections in germ free mice because a lack of normal microflora can alter infection dynamics (Naglik, Fidel, and Odds 2008). One significant disadvantage of the mouse model is that, beyond imaging of superficial infections, detailed host-pathogen interactions cannot be directly visualized during infection. This severely limits our ability to understand how the different components of the host immune system interact to fight infections and, in the case of disseminated candidiasis, frustrates efforts to understand how *C. albicans* is able to invade and spread throughout the host.

Rats are frequently used to imitate a vaginitis infection. To do this, they must be in a state of prolonged pseudooestus which is induced and maintained weekly (Naglik, Fidel, and Odds 2008). This model of vaginitis is particularly useful because the epithelium thickens into and squamous epithelium and allows for the growth of Candida (Naglik, Fidel, and Odds 2008). Rats are also used as an oral epithelial model with implants embedded in the mouth, or a gastrointestinal model of infection which is larger and easier to obtain prolonged blood samples from (Naglik, Fidel, and Odds 2008). The rat model is not a good gut translocation system, however, so it is not recommended for questions related to dissemination or organ fungal burdens. Other mammals used less frequently for fungal research and include the rabbit, guinea pig, and macaque for vaccine development (Naglik, Fidel, and Odds 2008).

1.2.3.2 Imaging in a live animal model

One of the most challenging tasks when using live animal models is imaging intact samples. There are number advantages imaging a live host during infection, including: 1) ability to examine host responses to infection in live or just-extracted tissue to retain most physiological conditions, 2) ability to look at specific microenvironments which may be difficult to simulate *in vitro*, 3) limiting alteration of normal response to infection due to experiment manipulation (Mitra et al. 2010). Several techniques have been developed to non-invasively image infected mouse tissue like bioluminescent Candida strains. These strains can be injected in surface tissue, like the ear, and observed for fungal morphogenesis and micro-abscess formation (Doyle et al. 2006; Mitra et al. 2010; de Wet et al. 1987). This technique has been tweaked to work with Aspergillus and two photon microscopy to observe infection in mouse lungs *in situ*, and on human patients with dermal fungal infections (J. Bain, Gow, and Erwig 2014) Although technology has come a long way for us to view these interactions in an intact host, these techniques still have significant limitations. Techniques like two photon microscopy are limited in the depth of tissue that they can penetrate to visualize events, requiring dermal infections or organ removal for imaging (Helmchen and Denk

2005). This leaves the technique unable to probe many important sites for deep-seated infections like disseminated Candidiasis. Furthermore, these complex techniques may not be readily available to most researchers. Other model organisms including invertebrates mentioned above and zebrafish offer an alternative method of asking host-pathogen questions and imaging in real time.

1.2.3.3 Zebrafish as an animal model to test both host and pathogen roles in disseminated disease

The zebrafish model has become a staple for examining host-pathogen interactions in an intact host. While zebrafish are not mammals, they are vertebrate animal with many similarities to the mouse and human in that there are conserved host process and immune system components (Sullivan and Kim 2008; Torraca et al. 2014). One key advantage that zebrafish have against other vertebrate systems is that larvae are optically transparent and many transgenic zebrafish lines are available, so we can follow fluorescently marked immune cells during infection (Tobin, May, and Wheeler 2012). Additionally, the fish can be easily manipulated via chemical or genetic means to alter cell populations or physiological processes (Ablain et al. 2015; Foley et al. 2009). Utilization of the larval zebrafish model allows scientists to examine the whole body, but because larvae are so small, infection size compared to what is found in mice and humans may not be comparable (Seman et al. 2018). Despite this, zebrafish larva have been used to test the host response to a variety of viral, bacterial, and fungal pathogens.

Candida albicans has been looked examined in several larval zebrafish studies. Candida infection was first established in fish in 2010 where they looked for a yeast-to-hypha transition during infection (Chao et al. 2010). Our lab has followed this work and examined NADPH oxidase during Candida infection, and phagocyte recruitment to infection (Brothers et al. 2013; Brothers, Newman, and Wheeler 2011b). Alternative infection sites in the zebrafish larvae have since emerged, and we can now test a mucosal model of infection in this versatile model organism (Y. Z. Chen et al. 2015; Gratacap et al. 2017; Gratacap, Rawls, and Wheeler 2013; Moyes et al. 2016; K.

Voelz, Gratacap, and Wheeler 2015). Other fungal pathogens have since been examined in the zebrafish model, including *C. neoformans, A. fumigatus, A. nidulans, C. albicans, C. parapsilosis,* and *Mucor* (Berthier et al., 2013; Knox et al., 2014; Rosowski et al., 2018; Torraca et al., 2014; Kerstin Voelz, Gratacap, & Wheeler, 2015).

Recently, we have utilized this model organism's yolk sac to examine Candida spread from a localized infection site (Seman et al. 2018). The yolk sac is surrounded by the yolk sac syncytial layer (Fishelson 1995), and has endothelial cells surrounding it on most sides during early development and epithelial cells on the surface comprising the skin (Kimmel et al. 1995). We have utilized the yolk sac here to ask questions related to host response spreading infection as done in previously (Saralahti and Ramet 2015; Seman et al. 2018). Drawing on the advantages offered by the zebrafish system, we can utilize fluorescently tagged Candida and host cells to visualize the interactions between the host and fungi in real-time (Seman et al. 2018; Tobin, May, and Wheeler 2012).

1.3 A hitchhiker's guide to phagocytes

We first investigated phagocytes as a means for Candida cell spread. Phagocytes have been proposed to be "Trojan Horse" in other viral and bacterial pathogens, and we propose that Candida uses host phagocytes to move throughout a host. The Trojan Horse mechanisms involves three distinct stages in which the pathogen is first engulfed by the phagocytes, the phagocyte then moves away from the site with the pathogen, and then finally the pathogen is released in another place leaving the phagocyte intact or dead. This process involves host cell signaling to recruit phagocytes to the infection site.

1.3.1 Role of inflammation in infection

Proinflammatory cytokines and chemokine production brings phagocytes into the infection site, and turns on hematopoietic stem cells to develop needed immune cell lineages (Griffith, Sokol, and Luster 2014; Hall, Crosier, and Crosier 2015). We focused on the inflammatory cytokines TNFα,

IL1β, and IL6 during our experiments because these cytokines have been shown to be important in other bacterial and fungal infections. Loss of TNFα during *Mycobacterium abscessus* infection in zebrafish lead to larval mortality and impaired neutrophil mobilization through IL-8 (Audrey Bernut et al. 2016). *Mycobacterium tuberculosis* infection in human macrophages has been shown to regulate IL1β maturation as a method of survival in the macrophage (Novikov et al. 2011). Similarly, IL6 is regulated by *Mycobacterium tuberculosis* to inhibit type I interferon in a murine macrophage line and persist in the macrophage (Martinez, Mehra, and Kaushal 2013). We have seen each of these proinflammatory cytokines upregulated in our zebrafish model with *C. albicans* (Bergeron et al. 2017; Gratacap, Rawls, and Wheeler 2013), and we can follow TNFα expression in transgenically marked zebrafish (Marjoram et al. 2015).

We can watch in real time as TNFα is expressed during the larval infection, and test if immune recruitment to the site of infection leads to weakened host barriers. As phagocytes move in and out of the infection site and produce proinflammatory cytokines, they leave holes in the infected tissues which may allow pathogen escape. Damage to the surrounding tissue will set off a stress response signal triggered by PAMPs or damage associated molecular patterns (DAMPs) (Soares, Teixeira, and Moita 2017). PRRs can contribute to tissue damage and disease tolerance control (Soares, Teixeira, and Moita 2017), and can signal the initiation of specific cell types to respond to the site (Rivera et al. 2016). If inflammation is left unchecked, it could lead to inflammation that is unnecessarily harmful to the host and potentially allow pathogen escape.

1.3.2 A "Trojan Horse" mechanism of pathogen spread

Once phagocytes have arrived at the infection site, they engulf the pathogen and work to kill it. Unfortunately for the host, these attempts are not always successful and, if phagocytes containing live pathogens move away from the infection site, can act as a "Trojan horse" that helps microbes spread to distant sites. During *Mycobacterium marinum* infection, a model of tuberculosis, the mycobacterium resist killing in the macrophage and begin to replicate within the phagosome. From

there, they escape into the cytosol and responding macrophages form a granuloma (Clay et al. 2007; Torraca et al. 2014). *Staphylococcus aureus* once engulfed by macrophages will resist intracellular killing and incomplete killing by neutrophils results in an "immunological bottleneck" wherein persistent bacteria are selected for (Prajsnar et al. 2012; Thwaites and Gant 2011; Torraca et al. 2014; Yoshida, Frickel, and Mostowy 2017). In *Cryptococcus neoformans* infection, macrophages are required for containment of cryptococcal cells. Loss of macrophages is detrimental to the host and leads to uncontrolled pathogen replication. That said, the capsule of *C. neoformans* can prevent phagocytosis and may also play a role in getting it released from some macrophages (Charlier et al. 2009; Vu et al. 2014; Yoshida, Frickel, and Mostowy 2017). Finally, macrophages that take up Candida have intracellular replication of yeast which leads to an impasse in the clearance or release of the pathogen (Brothers, Newman, and Wheeler 2011a; Torraca et al. 2014).

Once phagocytes have been recruited to the infection site and engulfed the pathogen, they may undergo reverse migration and move away from the infection site. This process is brought on by cues passed between macrophages and neutrophils, such as those given at a wound site (Nourshargh, Renshaw, and Imhof 2016), or towards inflammation resolution (de Oliveira, Rosowski, and Huttenlocher 2016). Reverse migration has been well characterized for neutrophils in a zebrafish model where the process was first visualized (de Oliveira, Rosowski, and Huttenlocher 2016). It has been proposed that neutrophils undergo reverse migration if they sense decreased levels of chemoattractants at the site or if they receive new chemoattractant cues from another source (Q. Deng and Huttenlocher 2012; de Oliveira, Rosowski, and Huttenlocher 2016). Reverse migration also occurs in other cell types, like monocytes and dendritic cells, which can leave the site via drainage by the lymphatic system (Burn and Alvarez 2017). Together, this suggests that both neutrophils and macrophages can receive cues and undergo migration from the site of infection, supporting the second step of the Trojan Horse mechanism.

1.3.3 Pathogen release from phagocytes

Pathogens are often released from phagocytes through pyroptosis, pyronecrosis, or necroptosis. Each of these mechanisms results in lytic cell death of the phagocyte. Pyroptosis culminates in cell swelling, lysis, and proinflammatory cytokine and cell content release (Krysan, Sutterwala, and Wellington 2014; Meara et al. 2018a). Macrophages may undergo pyroptosis in order to deny safe-harbor and intracellular nutrients for engulfed pathogens (Krysan, Sutterwala, and Wellington 2014; Meara et al. 2018b). *C. albicans* has been shown to induce macrophage lysis by pyroptosis, but it's still being investigated if this is an active process chosen by the host or a deviant act by the pathogen. Host programmed pyroptosis releases proinflammatory cytokines which may be beneficial to overall outcomes, or Candida could force pyroptosis of the phagocyte to enable its escape (Krysan, Sutterwala, and Wellington 2014; Meara et al. 2018b). Recent work has shown fungal morphology and glycosolated proteins in the cell wall of Candida help macrophage-induced pyroptosis (Erwig and Gow 2016; Meara et al. 2018b).

Non-lytic exocytosis (NLE) or vomocytosis is a similar event in which Candida is released from the phagocyte, but this release allows both host cell and pathogen to remain intact. NLE was first described in *C. neoformans* infection following cryptococcal engulfment by macrophages; (J. M. Bain et al. 2012; Gilbert et al. 2017). This type of pathogen release may be more beneficial to both host phagocyte which avoids cell lysis and the pathogen which avoids antimicrobial responses. In the cryptococcal infection, they propose that the fungus hitches a ride in macrophages across the blood brain barrier, and then facilitates NLE to leave the phagocyte and gain direct access to the brain (Erwig and Gow 2016). Candida has been shown to be non-lytically expelled from macrophages *in vitro* (J. M. Bain et al. 2012). Here, a yeast cell was engulfed by a macrophages, it began to germinate, and then was released from the macrophage hyphal-tip first (J. M. Bain et al. 2012). These lytic and non-lytic expulsion events make up the last stage of the Trojan Horse mechanism and allow the pathogen access to host tissues.

1.4 Traversing the endothelium through endocytosis or paracellular invasion

Other mechanisms of Candida dissemination involve the spread of yeast through the endothelium via host cell endocytosis or paracellular invasion. Host endocytosis involves the adherence of either yeast or hyphal forms of Candida to the endothelium and subsequent uptake by these cells. Theories for endocytosis include 1) conversion to a hyphal form which adhere and damage the endothelium, and 2) adherence of yeast to the endothelium without morphogenetic change and endocytosis into the endothelium (Gow et al. 2012; Grubb et al. 2008). More recent evidence suggests that this morphogenetic conversion to hyphal form is not required for dissemination to occur *in vivo* (Seman et al. 2018). The role of paracellular invasion involves the spread of yeast between junctions or fenestrations in the endothelium (Grubb et al. 2008) which are likely caused by disruption of the host tissue during infection similar to what is seen during *Cryptococcus neoformans* infection (Charlier et al. 2009). These mechanisms support passage of yeast directly into the bloodstream and understanding pathogen interactions with the endothelium will help identify areas with therapeutic potential. This section will discuss endothelial cell interactions with pathogens during infection and consequences of these interactions for the host.

1.4.1 Endothelial response to infection

The endothelial cell layer is the last line of defense before pathogens gain access to the bloodstream where they may disseminate throughout the host. As such, the endothelium has developed unique strategies to combat infection. Under normal physiological conditions, the luminal side of the endothelium is anti-coagulent and anti-thrombogenic, preventing the adherence of host platelets and neutrophils; however, upon infection, the endothelial cells are activated to modulate thrombosis, inflammation, and immune recruitment (Roumenina et al. 2016). This activation results in increased vasodilation, thrombus formation, and tissue damage (Roumenina et al. 2016). Endothelial cells are classified in two ways: macrovascular which includes veins and arteries, and the microvasculature which includes capillaries and arterioles. Depending on the

vasculature bed, the endothelium will differ in vessel size and cell junction composition. For instance, the macrovascular is non-fenestrated while the microvascular capillaries have more open pores to allow cell trafficking (Roumenina et al. 2016). During inflammation, these vasculature beds will respond to leakiness, increased neutrophil adherence, and thrombosis, resulting in activation of key pathways for immune regulation including nuclear factor kappa B (Roumenina et al. 2016). During Candida infection, fungi will adhere to the endothelium through a variety of adherence mechanisms, including: the ALS3 gene family, complement protein regulator C4b, and outer cell wall component like N- or O- linked mannosyl residues, among others (Grubb et al., 2008; Sheppard & Filler, 2014). After adhering, Candida can penetrate the endothelium into the bloodstream by damaging the cell layer, hyphal penetration or direct uptake of yeast.

1.4.2 Vascularization in the presence of pathogens

Angiogenesis is the process by which new blood vessels are formed from existing vasculature. It is a physiologic response to tissue inflammation and ischemia, which can be brought on with pathogen invasion (Otrock et al. 2007). In response to infection, this process is often invoked by the host to enhance immune response and limit pathogen spread. Pathogens can evade this process by producing anti-angiogenic agents like the gliotoxin produced by *Aspergillus fumigatus* (Ben-Ami et al. 2009), or use the angiogenesis program to support their own growth like *Mycobacterium marinum* granuloma formation (Torraca et al. 2017). In *Cryptococcus neoformans* infection, cryptococcal cells become trapped in the vasculature and damage blood vessels through increased blood pressure (Gibson et al. 2017). Here, they found that dissemination of cryptococcal cells could occur both in areas where blood vessels were damaged and where they were intact (Gibson et al. 2017). Infection with *Candida albicans* results in a similar pattern of infection, where fungal growth damages tissue and endothelial cells respond by expressing genes that inhibit apoptosis and stimulate angiogenesis (Chin et al. 2016). Mice infected with *Candida albicans* had growth of microabscesses in the kidney and brain which resulted in endothelial cell proliferation to

the combat yeast cells adhering to the endothelium (Ashman and Papadimitriou 1994; Chin et al. 2016). Yeast also interact closely with the vasculature endothelium during disseminated infection and influence the inflammatory response (Barker et al. 2008; Chin et al. 2016). Together, this data suggests that endothelial cells are critical for the recognition of pathogens, enhancement of the immune system to clear the infection, and upregulation of inflammation to combat infection.

1.4.3 Endocarditis and cardiotoxicity

Cardiotoxicity during candidiasis is associated normally associated with antifungal treatment, such as echindocandins, rather than toxins produced by Candida (Ben-Ami 2018). However, Candida can in rare cases cause endocarditis when the patient has indwelling central venous catheters or other devices (Ben-Ami 2018; Kara et al. 2018). Fungal endocarditis is less common than bacterial endocarditis in humans, but is a serious infection that presents with prolonged fever and changing heart murmur as a result of fungal masses in the heart or vasculature (Kara et al. 2018).

Cardiotoxicity is more likely to be caused by toxins produced by the infecting bacteria. During *Clostridium difficile* infection in a zebrafish model infection, *C. difficile* toxin B was found localized in the pericardia region of the larvae following 24 hours of infection. Here, they found that bacterial toxin caused cardiotoxic effects in the form of heart damage and deformation, loss of blood flow, and loss of function in cardiomycetes ability to pump blood (Hamm, Voth, and Ballard 2006). Similarly, bacterial infection with *Streptococcus pneumoniae* results in circulating pneumolysin, a toxin that creates cardiac complications during invasive disease (Alhamdi et al. 2015). Here, they found that pneumolysin, produced by pneumococci in the bloodstream, increase cardiac proteins that mark cardiac injury and cause inflammation (Alhamdi et al. 2015).

Previous work in our zebrafish model suggests that dissemination of Candida passes into the heart tissue before continuing in the blood stream to cause disseminated infection (unpublished data). Often, as the disseminated Candida grows in the fish, masses of Candida are found in the

heart and vasculature (Seman et al., 2018; this study). Our study tested the idea that reduced heart rate would eliminate bloodflow and allow us to visualize areas of yeast escape and potentially limit overall dissemination. To do this, we used chemicals to reduce heart rate including valproic acid and terfenadine (Li et al. 2016; Milan et al. 2003) which allowed us to examine the role of heart beat and blood flow on systemic disease.

CHAPTER 2

HOST MEDIATED MECHANISMS OF FUNGAL CELL SPREAD IN A TRANSPARENT ZEBRAFISH INFECTION MODEL

2.1 Introduction

Candida albicans is a small non-motile fungus that can cause disseminated candidiasis in immunocompromised populations. This dimorphic pathogen is a normal commensal organism of the mouth, gastrointestinal track, and vagina that causes life-threatening invasive candidiasis in immunocompromised patients. *C. albicans* is able to spread from mucosal sites to internal organs in immunocompromised mouse disease models and this is believed to be a primary infection route for this fungus in humans as well (Koh et al. 2008; Koh 2013; Naglik et al. 2011). Recent work using a tissue-to-bloodstream *C. albicans* dissemination model in zebrafish has established that the yeast form is specialized for promoting infection spread (Seman et al. 2018). Although we still do not understand how yeast orchestrate this movement, it has been proposed that *C. albicans* spreads via phagocyte-dependent or –independent mechanisms (Gow et al. 2012; Grubb et al. 2008).

Bacterial and fungal pathogens utilize the host's immune cells in a "Trojan Horse" mechanism to spread to outlying tissues, stimulating engulfment, surviving within the phagocyte for sufficient time to allow migration away from the infection, then provoking release from the phagocyte. Both *in vitro* and zebrafish disease models have been used to demonstrate how neutrophils (Prajsnar et al. 2012) and macrophages (Bojarczuk et al. 2016; Clay et al. 2007; Harvie et al. 2013; Santiago-Tirado et al. 2017) can be vehicles for dissemination of Mycobacteria, Cryptococci and Streptococci. Although *C. albicans* was previously suspected of being an extracellular pathogen, intravital imaging in the zebrafish model suggests that it can establish an impasse with macrophages that enables migration from the infection site (Brothers, Newman, and Wheeler 2011b).

Independently of phagocyte-driven spread, *C. albicans* may be moved directly into the bloodstream from tissues via endocytosis by endothelial cells or paracellular invasion. Candida can cause endothelial cell damage and stimulate endocytosis *in vitro*, suggesting one strategy for invasion through this barrier (Filler 2014; Grubb et al. 2008; Moyes and Naglik 2011; Naglik et al. 2011). Once fungi get into the bloodstream, they can be carried by blood flow throughout the host, a process that results in rapid and universal dispersion (MacCallum and Odds 2005). Movement of *C. albicans* yeast through the endothelial barrier has not yet been studied *in vivo*, largely due to technical limitations in murine models.

To systematically test the importance of these host-mediated mechanisms of yeast spread, we used a recently described yolk infection model (Saralahti and Ramet 2015; Seman et al. 2018). The yolk sac is a syncytium that nourishes larvae and is directly in contact with endothelial cells of the vasculature, the liver and the intestinal tract (D'Amico and Cooper 2001; Fishelson 1995; Kimmel et al. 1995; Kondakova and Efremov 2014). This anatomical structure represents a simplified system where translocation through the endothelium and spread throughout the bloodstream can be monitored through longitudinal imaging of both fluorescent fungi and phagocytes.

High-resolution intravital imaging established that both macrophages and neutrophils engulf yeast, while *C. albicans* survives within macrophages and can be released far from the site of infection through non-lytic exocytosis. Systematic elimination of both macrophage and neutrophil function, however, resulted in no loss in dissemination frequency. Similarly, elimination of blood flow did not in and of itself result in a reduction in dissemination. When both phagocytes and blood flow were disabled, however, there appeared to be a reduction in the distance they spread. Thus, phagocyte-dependent and –independent modes are redundant and the versatility of *C. albicans* in using different strategies ensures robust spread of infection.

2.2 Materials and Methods

2.2.1 Animal care and maintenance

Adult zebrafish used for breeding were housed at the University of Maine Zebrafish Facility in recirculating systems (Aquatic Habitats, Apopka, FL). Zebrafish care protocols and experimental procedures were conducted in accordance with NIH guidelines under Institutional Animal Care and Use Committee (IACUC) protocol A2015-11-03. Following collection, embryos were kept 150 mm petri dishes with E3 media (5 mM sodium chloride, 0.174 mM potassium chloride, 0.33 mM calcium chloride, 0.332 mM magnesium sulfate, 2 mM HEPES in Nanopure water, pH 7) plus 0.3 mg/liter methylene blue (VWR, Radnor, PA) to prevent microbial growth for the first 6 hours. Larvae were then moved to fresh E3 media supplemented with 0.02 mg/ml of 1-phenyl-2-thiourea (PTU) (Sigma-Aldrich, St. Louis, MO) to prevent pigmentation. Larvae were reared at 28°C at a density of 150 larvae per 150 mm petri dish. Transgenic lines used are provided in Table 2.1.

Table 2.1 Transgenic and mutation zebrafish lines

Transgenic line	Fluorescent cells	Mutation	Reference
Tg(mpx:EGFP)	Green neutrophils	-	(Renshaw et al. 2006)
Tg(Mpeg1:GAL4)/(UAS:nfsB-mCherry)	Red macrophages	-	(Ellett et al. 2011; Pisharath and Parsons 2009)
Tg(Mpeg1:GAL4)/(UAS:Kaede)	Photoconvertible Green to Red macrophages	-	(Davison et al. 2007; Ellett et al. 2011)
Tg(tnf:EGFP)	Green cells with *tnf* expression	-	(Marjoram et al. 2015)
Tg(LysC:dsRed)	Red neutrophils	-	(Hall et al. 2007; Marjoram et al. 2015)
Tg(fli1:EGFP)	Green endothelium and early macrophages	-	(Lawson and Weinstein 2002)
Rac2-D57N	Red neutrophils	Dominant negative Rac2	(Rosowski et al. 2016)
AB (wild type)	-	-	Zebrafish International Resource Center

2.2.2 Zebrafish larvae infection

Larvae at ~32 hours post fertilization were manually dechorionated and anesthetized in fresh E3 media plus 0.02 mg/ml PTU and Tris-buffered tricaine methane sulfonate (160 _g/ml;

Tricaine; Western Chemicals, Inc., Ferndale, WA). Larvae were injected in the yolk sac with 5 nl volume PBS control or *C. albicans* at $5x10^6$ CFU/ml in PBS. Larvae were microinjected as described previously (Seman et al., 2018) and screened on a Zeiss Axio Observer Z1 microscope to ensure the correct injection and starting inoculum of *C. albicans* in the yolk (Carl Zeiss Microimaging, Thornwood, NJ). Scored larvae were then moved to fresh E3 media plus PTU which was changed every other day. Where indicated, media was supplemented with metronidazole, terfenadine, or valproic acid following infection. Larvae were kept at 28°C for $NRG1^{OEX}$ yeast locked infections (Peters et al. 2014) or 21°C for wild type Caf2 infections (Seman et al. 2018). These temperatures were chosen as they are safest for zebrafish and allow for yeast and hyphal growth of *C. albicans* (Ellett et al. 2018; Seman et al. 2018). Following 42 hours post infection or 5 days post infection for mortality experiments, larvae were euthanized by Tricaine overdose.

A movie of the yolk sac infection was taken on an Olympus SZ61 stereomicroscope system (Olympus, Waltham, MA) connected to an Excelis HDS microscopy camera and monitor system (World Precision Instruments, Sarasota, FL). CaptaVision software was used to record the video and Fiji-ImageJ was used to compile the file.

2.2.3 *C. albicans* strains and growth conditions

C. albicans strains used for larval infection were grown for 24 hours at 37°C on yeast-peptone-dextrose (YPD) agar (20 g/L glucose, 20 g/L peptone, 10 g/L yeast extract, 20 g/L agar, Difco, Livonia, MI). Single colonies were picked to 2 x 5mL liquid YPD and grown overnight at 30°C on a wheel. Prior to microinjection, liquid cultures were washed twice in phosphate buffered saline (5 mM sodium chloride, 0.174 mM potassium chloride, 0.33 mM calcium chloride, 0.332 mM magnesium sulfate, 2 mM HEPES in Nanopure water, pH = 7) and the concentration of yeast adjusted to $5x10^6$ CFU/ml in PBS for larval zebrafish infections. Wild type *Caf2-iRFP C. albicans* was used for heat killing and UV inactivating experiments. Overnight cultures were washed twice and resuspended in PBS at $2.5x10^7$ cells/ml, then boiled for 10 minutes or placed in an uncovered

polystyrene petri dish (60 mm x 15 mm, VWR, Radnor, PA) for exposure. A CL-1000 UV cross-linker was used for UV inactivation of Candida (Bergeron, et al., 2017) (UVP, Vernon Hills, IL) and yeast were exposed four times to 100,000 μJ/cm^2 with swirling between each exposure. Following boiling or UV-inactivation, cells were stained with AlexaFluor 555 by co-incubation of cells in PBS with sodium bicarbonate (0.037 M final concentration, pH 8.2) in the dark for 40 minutes with periodic vortexing. Cultures were then washed four times in PBS and brought to 2x10^7 CFU/ml for injection into the yolk sac. Proper heat killing and UV inactivation was confirmed by plating 50 μl of the prepared 2x10^7 CFU/ml killed yeast and 50 μl of the prepared 5x10^6 CFU/ml live yeast used for larval injection on YPD plates and incubated overnight at 30°C.

For CFU quantification, groups of 6 larvae were taken after injection of Candida and screening and homogenized at 0 hpi in 600 ul of PBS. 100 μl of the homogenate was plated on YPD agar supplemented with gentamicin (30 μg/ml, BioWhittaker, Lonza), penicillin-streptomycin (250 μg/ml, Lonza), and vancomycin hydrochloride (3 μg/ml, Amresco, Solon, OH). Individual larvae were homogenized for CFUs in 600 μl PBS after the 40 hpi time point, and 100 μl of the 1:6 dilution or 1:60 dilution was plated on YPD for countable colonies. Plates were labeled by plate wells so that the larvae CFU count could be paired with dissemination scores and larval images. YPD plates were incubated overnight at 30°C and colonies counted the following day so CFUs/fish could be calculated.

2.2.4 Macrophage ablation

Where indicated, macrophages were ablated by injection of clodronate liposomes (Clodronateliposomes, Amsterdam, The Netherlands) in the caudal vein, larvae were bathed in metronidazole, or embryos were injected with *pu.1* morpholino oligonucleotides (MO, Genetools). Liposomes were injected in the caudal vein at a 3:1:1:1 ratio of 5mg/ml liposomes:PBS:phenol red:10 kDa Cascade blue dextran (8% w/v) in a total volume of 8-10 nl per larvae (Bojarczuk et al., 2016; others?) at ~28 hpf. Larvae recovered in E3 media for 4 hours and then infected with *C.*

albicans. *Tg(Mpeg:GAL4)/(UAS:nfsB-mCherry)* larvae were bathed in 20 mM metronidazole for 4 hours after injection with *C. albicans* yeast and kept in E3 media plus PTU and 10 mM metronidazole for the remainder of the experiment (Tobin, May, & Wheeler, 2012; other Mpeg-mCh refs for fish line?). Translational blocking (CCTCCATTCTGTACGGATGCAGCAT) and splice blocking (GGTCTTTCTCCTTACCATGCTCTCC) MOs were co-injected into 1-2 cell stage embryos (A. Bernut et al. 2014; Clay et al. 2007). The MOs were combined (2.5 ng translation blocking and 0.4 ng splice blocking) with 10 kDa Cascade blue dextran (8% w/v) and phenol red for visualization of injection with total volume injected at 2 nl. Ablation of macrophages with MO technology was observed by loss of red fluorescence in *Tg(Mpeg:GAL4)/(UAS:nfsB-mCherry)* larvae.

2.2.5 Chemical blockade of blood flow

For chemical inhibition of blood flow, larvae were reared and infected with *C. albicans* as described and then placed in petri dishes containing 0.1 mg/ml valproic acid in E3 media plus PTU or 2 uM terfenadine in E3 media plus PTU and corresponding vehicle controls (water and DMSO, respectively). Larvae were observed for reduced heartbeat and loss of blood flow in the trunk and tail by 24 hours post treatment (or 24 hpi). An Olympus SZ61 stereomicroscope system (Olympus, Waltham, MA) connected to an Excelis HDS microscopy camera and monitor system (World Precision Instruments, Sarasota, FL) was used to record 60 s movies with CaptaVision software. Loss of blood flow was otherwise characterized under a dissection scope and scored as reduced or loss of heartbeat.

2.2.6 RNA isolation and qPCR analysis

Larvae were pooled into groups based on phagocyte recruitment to the yolk sac and dissemination of yeast (non-recruited/non-disseminated, non-recruited/disseminated, recruited/non-disseminated, and recruited/disseminated). Larvae were euthanized by overdose in tricaine and immediately homogenized in TRIzol (Invitrogen, Carlsbad, CA) for RNA isolation. Larval groups ranged from 2-15 fish in 3 independent experiments. RNA was isolated using the

Direct-zol RNA miniprep kit (Zymo Research, Irvine, CA) using the manufacturers recommended protocol. Final RNA was eluted in 20 ul nuclease free water and stored at -80°C until cDNA synthesis. Using the iScript reverse transcriptase supermix (Bio-Rad, Hercules, CA), cDNA was synthesized from 500 ng RNA per sample. RT-qPCR was done on a CFX96 thermocycler (Bio-Rad, Hercules, CA) using the cycles: 95°C for 30 s, 95°C for 5 s followed by 60°C for 20 s for 39 cycles, then 95°C for 10 s followed by 65°C for 5 s (Bergeron et al. 2017). The Bio-Rad CFX Manager software was used to analyze threshold cycles and dissociation curves. Larval gene expression was normalized to the gapdh control gene (ΔCT), as done previously (Bergeron et al. 2017; Gratacap, Rawls, and Wheeler 2013), and compared to the mock infected PBS controls (ΔΔCT).

Table 2.2 Primers used for qPCR

Gene	Sequence (5'-3')	Reference
IL1β	Forward: GTCACACTGAGAGCCGGAAG	(Gratacap, Rawls, and Wheeler 2013)
	Reverse: TGGAGATTCCCAAACACACA	
IL6	Forward: GGACGTGAAGACACTCAGAGACG	(Bergeron et al. 2017)
	Reverse: AAGGTTTGAGGAGAGGAGTGCTG	
TNFα	Forward: CGCATTTCACAAGGCAATTT	(Bergeron et al. 2017; Gratacap, Rawls, and Wheeler 2013)
	Reverse: CTGGTCCTGGTCATCTCTCC	
gapdh	Forward: TGGGCCCATGAAAGGAAT	(Bergeron et al. 2017; Gratacap, Rawls, and Wheeler 2013; Mattingly et al. 2009)
	Reverse: ACCAGCGTCAAAGATGGATG	

2.2.7 Histology

Larvae were euthanized after 42 hpi in tricaine overdose and shipped overnight in PBS for histology. Larval samples underwent saggital cryosectioning and stained with DAPI and Phalloiding-568. Slides were then shipped back and sections were imaged on the Olympus IX-81 inverted confocal microscope.

2.2.8 Fluorescence microscopy

Tg(mpeg1:GAL4) adults were crossed with *Tg(UAS:Kaede)* (yeast locked experiments) or *Tg(mpeg1:GAL4)/ Tg(UAS:Kaede)* adults were incrossed (wild type Candida experiments) for larvae with photoconvertible green to red macrophages (Ellett et al. 2011). Larvae were reared and

infected with *C. albicans* as described, and at 24 hpi larvae were embedded in 0.5% low melting point agarose (LMA) in E3 media plus Tris buffered tricaine methane sulfonate (200 mg/ml) in glass-bottom 24-well imaging dishes. Larvae were scored for recruitment of macrophages and yeast dissemination prior to photoswitching. Photoswitching was done as described previously using a 405 nm laser at 10% power on a Olympus IX-81 inverted microscope with an FV-1000 confocal system for 10 minutes on Fluoview XY repeat with a 20X (0.75 NA) objective (Brothers et al. 2013; T.M. Tucey et al. 2018). After photoswitching, 10X (0.40 NA) images were taken of the yolk sac area immediately following photoswitching and of the whole fish at 30 and 40 hpi. Imaging was done at room temperature and larvae were kept at 28°C (yeast-locked infections) or 21°C (wild type infections) between imaging sessions. To keep the fish from drying out, 2 mL of E3 media plus PTU was layered over each larva following the first imaging session.

Time lapse imaging for all experiments was done between 32 and 40 hpi unless noted otherwise. For photoswitching experiments, one larva was chosen for time lapse imaging between 32-40 hpi, and between 46-54 hpi and 56-64 hpi. Larvae were removed from the initial 24-well plate and re-embedded in an 8-well μ-slide insert for the ibidi heating system K-frame (ibidi, Deutschland) for temperature control. The heating system was set up at least one-half hour before the start of the time lapse for the system to come to temperature. Larvae were kept at the temperature of their counterparts kept in the incubator at that time. Time lapses were run on "FreeRun" and images were acquired in succession. Time lapse imaging was done with a 20X (0.75 NA) objective unless noted otherwise (Figure 3A time lapse of Xmas fish; 10X (0.40 NA). Individual fluorescent channels were compiled on Fluoview software before being transferred for compilation and analysis in Fiji-ImageJ (Schindelin et al. 2012).

Fluorescent channels were acquired with optical filters for 635 nm excitation/668 nm emission, 543 nm excitation/572 nm emission, and 488 nm excitation/520 nm emission, for far red fluorescent cells, red fluorescent cells, or green fluorescent cells, respectively. Phalloidin-568 was

captured with the optical filter for 543 nm excitation/668 nm emission for histology microscopy. Cascade blue was captured using the optical filter 405 nm excitation/422 nm emission for larvae treated with clodronate liposomes.

2.2.9 Fiji-ImageJ and MatLab image analysis

2.2.9.1 Quantification of photo-switched macrophages

To measure whether macrophages stayed at the site of infection or moved to other sites of the zebrafish, we counted the number of photo-switched macrophages in the head, yolk, or tail from images. We used Maximum Intensity Z stack projections to quantify the total number of macrophages in the fish over time. We normalized the photo-switched macrophages counted at 32 and 40 hpi (or 6 and 16 hours post switch (hps)) to the original number of photo-converted macrophages at the site of infection at 24 hpi (0 hps).

2.2.9.2 Quantification of fluorescent phagocytes in the yolk sac

To measure the efficiency of our clodronate and metronidazole methods of macrophages ablation, images were processed primarily in Fiji-ImageJ (Schindelin et al. 2012). Z stack projections (Maximum Intensity Projection) were used to count the number of red fluorescence macrophages or green fluorescent neutrophils in a 6-somite region of the trunk or in the yolk sac during infection.

2.2.9.3 Measuring phagocytosed versus extracellular yeast

To score and quantify disseminated yeast in Rac2-D57N fish treated with clodronate (Figure 2.13), 20X images were taken on the Olympus confocal at 40 hpi. Fiji-ImageJ was used to score the larvae for yeast that was intra- and extracellular while Photoshop (version CS5 12.1 x64, Adobe Systems Incorporated) was used to trace over yeast scored as intra- and extracellular (Brothers, Newman, and Wheeler 2011; Seman et al. 2018). PhotoShop layers were annotated and the area calculated in ImageJ.

2.2.9.4 Measuring fluorescent pixels in the area of infection

To quantify the amount of TNFα expressing cells or neutrophils in the area of *C. albicans* cells, masks were made of each fluorescent channel (TNFα, neutrophils, and *C. albicans*) in Fiji-ImageJ. Each mask was composed using the same threshold per individual experiment to measure a fluorescent channel. Masks were made as 25 Z slices to examine the overlap between Candida and neutrophils or *tnfα* expression in each Z slice. This allows us to distinguish between bystander neutrophils and neutrophils that were recruited to Candida. Similarly, this also distinguishes between background TNFα expression in the larva and TNFα expressing cells interacting with Candida. The three-dimensional landscape of the channel masks is a more accurate depiction of the infection site and should capture host cells at the site and ignore those on a different plane.

Images of mock infected larvae were used to quantify the background fluorescence of neutrophils and *tnfα* expression in a healthy state. To determine how much area to measure in these larvae, we took the average area of Candida from all 25 Z slices in our infected larvae and divided this by 25. A box of this computed size was made as a region of interest (ROI) in ImageJ and made into a mask to be read as the "Candida" in our Matlab script. The neutrophil and TNFα pixels in this region through all 25 Z slices was used to compare background fluorescence in the fish.

A MatLab script quantified the number of TNFα or neutrophil pixels in the area of *C. albicans* pixels (Fig 2.13, 2.14, 2.18, and 2.20) (The MathWorks, Inc., R2017b, Natick, MA). The script also measured the number of fluorescent pixels in the image, so *C. albicans* growth could be measured. The sum of neutrophil or TNFα pixels was quantified for each fish and the median with 95% confidence interval graphed using GraphPad Prism. Statistical analysis was done using a non-parametric one-way ANOVA with Kruskal Wallis posttest.

2.2.9.5 Measuring distance yeast travel in whole fish

To measure how far yeast moved from the yolk sac edge, additional masks were made for each fish using the DIC channel to outline the yolk sac and body of the fish. The *C. albicans* mask was subtracted from yolk mask and fluorescent pixels found outside the body mask were omitted. A distance map was made for each Candida pixel away from the yolk mask. These distances were binned in the MatLab program (1 bin for every pixel away from the yolk) and bins were pooled and normalized to the number of fish per group before plotting on a histogram.

2.2.10 Statistical analysis

Statistical analysis was performed in Graphpad Prism 6 (Graphpad software, Inc., La Jolla, CA). All analysis was completed with non-parametric tests unless noted otherwise. P-values are indicated as: * $p \leq 0.05$, ** $p \leq 0.01$, *** $p \leq 0.001$, **** $p \leq 0.0001$. n.s. = not significant. Mortality experiments were assessed with Kaplan-Meier survival curves and the Bonferroni correction was used to assess significant differences. Mortality was observed as loss of heartbeat in all experiments where bloodflow was not altered. In experiments utilizing valproic acid or terfenadine to reduce heart rate and blood flow, mortality was scored as larval putrification demonstrated by loss of tissue integrity, graying of tissue, and sloughing of dermis layer. Histograms and yeast travel distances were compiled and analyzed in Matlab and Graphpad software.

2.3 Results

Pathogen spread within a host is crucial for the pathogenesis of severe disease like sepsis, but understanding possible roles of the host in this process has been particularly difficult to quantify in mammalian infection models. Fungal pathogens can disseminate as yeast or hyphae, and recent work using a larval model of zebrafish infection suggests that *C. albicans* yeast are specialized for spread from tissue to bloodstream (Seman et al. 2018). We sought to use this uniquely tractable model to probe the host's role in yeast dissemination, postulating that yeast may spread through phagocyte-dependent or –independent strategies.

2.3.1 *C. albicans* yeast dissemination and larval death is preceded by innate immune cell recruitment to a localized infection site

To understand if host innate immune responses are associated with *C. albicans* spread, we infected transgenic zebrafish larvae in the yolk with yeast-locked fungi and intravitally imaged both host immune cells and fungi. Larvae were infected with yeast-locked *NRG1*^{OEX} (*NRG1*^{OEX}*-iRFP*; Figure 2.1A, Movie 2.1) and scored for recruitment of phagocytes to the infection and yeast cell spread from the infection site. Larvae in which one or more phagocytes were in contact with *C. albicans* in the initial infection site were scored as "Recruited", and larvae with one or more *C. albicans* yeast outside of the yolk sac were scored as "Disseminated". To better understand if immune cell involvement was associated with yeast dissemination or infection resolution, larvae were longitudinally imaged over a 16-hour time course. Fish were almost exclusively found to be in only three of the expected four classes, with about 50% in the "No Recruitment/No Dissemination" (NR/ND) class, almost none in the "No Recruitment/Dissemination" (NR/D) class, and 25% each in the other two classes (Recruited/No Dissemination and Recruited/Disseminated) (Fig 2.1B and C). Larvae that had recruited macrophages at 24 hpi stayed the same or progressed to a recruited state with *NRG1*^{OEX}*-iRFP* dissemination at 40 hpi. Larvae that began with recruited macrophages and disseminated *NRG1*^{OEX}*-iRFP* did not revert to a non-recruited or non-disseminated state. In limited cases, dissemination occurred without the response of phagocytes to the yolk sac, and only in one case did it lead to later phagocyte recruitment to the yolk sac. These experiments demonstrated that recruitment of phagocytes tends to precede dissemination (Fig 2.1B and C), suggesting a role for phagocytes in the dissemination of yeast, either directly through the Trojan Horse mechanism, or indirectly through inflammation-mediated weakening of host barriers that would normally block access to the vasculature.

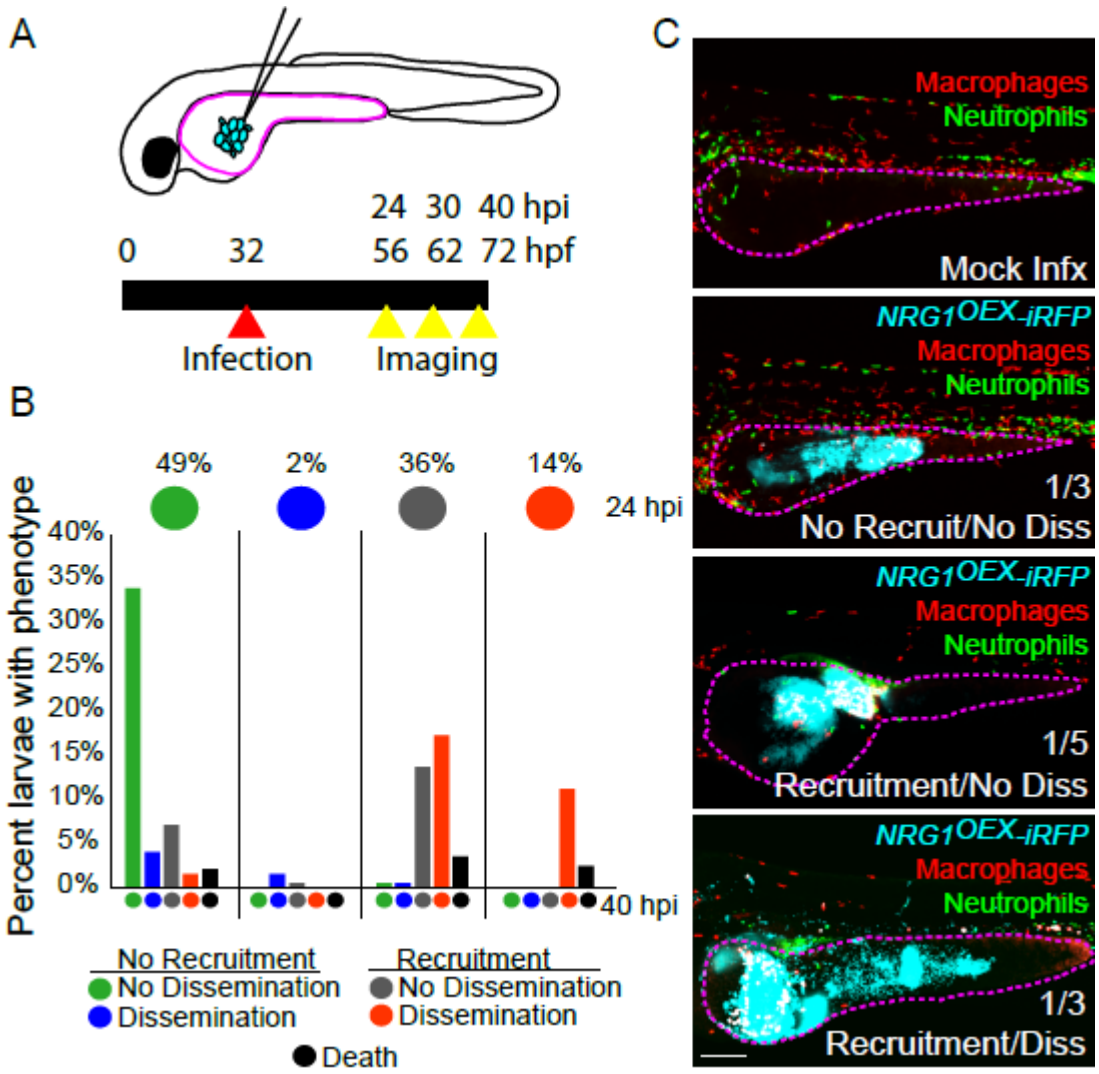

Figure 2.1. Macrophage and neutrophil recruitment to the site of infection is positively associated with dissemination Larvae with fluorescent macrophages were infected with a far-red fluorescent yeast-locked *C. albicans* (*NRG1*^{OEX}*-iRFP*) in the yolk sac at ~32 hpf. (A) Schematic of the yolk sac injection and timeline of infection with larvae screened for recruitment of fluorescent phagocytes to the yolk and dissemination of yeast at 24, 30, and 40 hpi. (B) Progression of infection in which larvae with early recruitment of macrophages go on to develop disseminated infection and larvae rarely revert back to a non-disseminated state. Scores were pooled from larvae with fluorescent macrophages from a total of 12 experiments: 5 experiments

in *Tg(mpeg:GAL4)/(UAS:Kaede)*, 4 experiments in *Tg(mpeg:GAL4)/(UAS:nfsb-mCherry)*, and 3 experiments in *Tg(fli1:EGFP)* x *Tg(mpeg:GAL4)/(UAS:nfsb-mCherry)*. A total of 197 fish were followed from 24 to 40 hpi. (C) Examples of each score in *Tg(mpeg:GAL4.)/(UAS:nfsb-mCherry)/Tg(mpx:EGFP)* larvae with green fluorescent neutrophils and red fluorescent macrophages. The yolk sac is outlined in magenta and the fluorescent macrophage positive larvae with this score at 40 hpi is indicated in the lower right of the image. Scale bar = 150 μm.

2.3.2 Dissemination is an active process whereby yeast drive their own spread

We first sought to determine if yeast dissemination is passive or driven by fungal-specific determinants for dissemination in this model. We reasoned that if dissemination were passive it might be triggered by a given level of fungal burden, enhanced by proximity to the vasculature, or even occur with dead yeast. Previous work has shown that different starting inoculums of yeast don't influence dissemination rate (Seman et al. 2018), which suggested that dissemination frequency is relatively insensitive to inoculum size. We also found no difference in fungal burden among groups of recruited and disseminated larvae (Fig 2.2A-C), suggesting that neither dissemination nor phagocyte responses are driven by the presence of a threshold of *NRG1*^{OEX}. Comparing the location of yeast in the yolk with distance to fluorescent vascular endothelium, we found that proximity of the infection site to blood vessels is not associated with spread of infection (Fig 2.3A and B). Finally, we found that dissemination is significantly reduced with killed yeast, suggesting that yeast provide essential cues to mediate their own spread (Fig 2.4A and B). Together, these data suggest that dissemination and immune recruitment are driven by active rather than passive processes. Because these dissemination events occurred with live yeast, we focused on host mediated processes of yeast spread without concern for inadvertent yeast spread related to experiment technique.

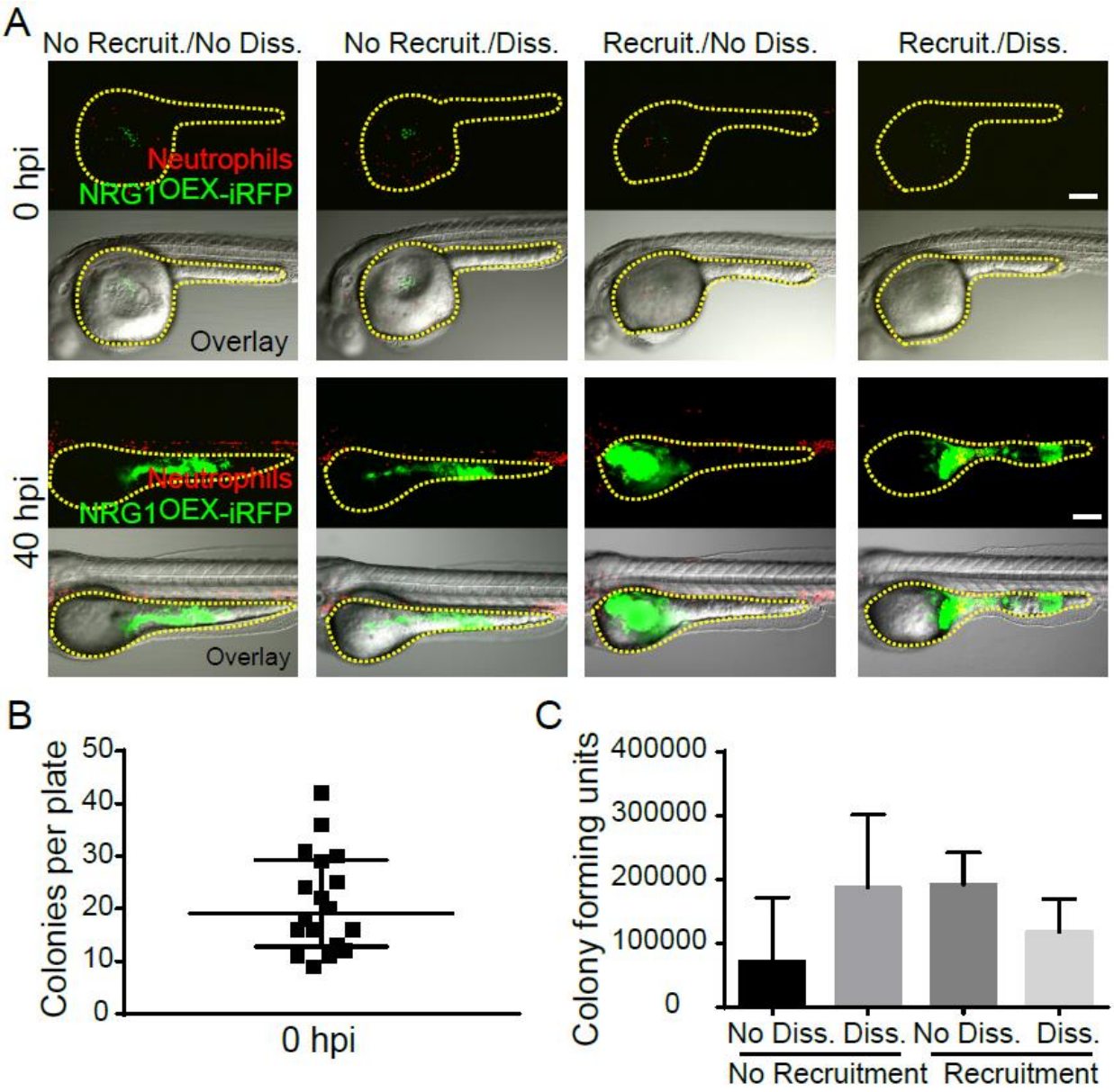

Figure 2.2. Initial Candida inoculum does not indicate whether neutrophils will be recruited to the yolk sac or result in dissemination events *Tg(mpx:EGFP)* larvae were infected with *NRG1*^{OEX} as described previously and immediately imaged on the confocal for starting inoculum. (A) Example images of larvae just infected (top) and at 40 hpi (bottom), 10X objective, scale bar = 150 μm. Images demonstrate little difference in starting inoculum resulting in different infection results. (B) CFUs of screened larvae at 0 hpi. Bars show median and interquartile range of yeast per fish. Pooled from three experiments, n = 18 infected fish,

median colonies per plate is 19. (C) CFUs from each type of recruitment/dissemination score. Bars indicate median and interquartile range. Pooled from three experiments, left to right n = 20, 8, 6, 20. Tested with a one-way ANOVA with Dunn's post test, n.s.

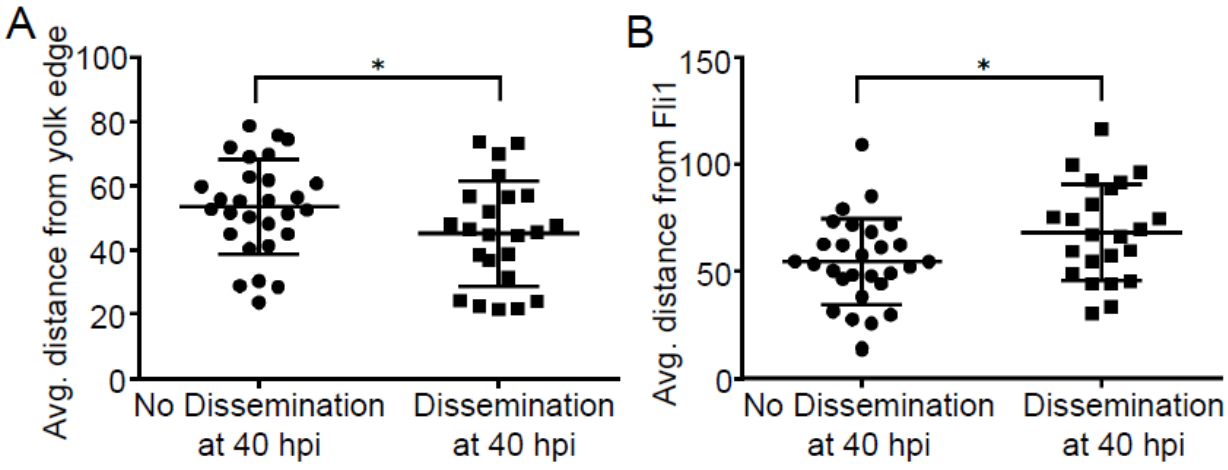

Figure 2.3. Location of *C. albicans* affects dissemination. *Tg(mpeg:GAL4)/(UAS:nfsb-mCherry)* fish were crossed with *Tg(fli1:EGFP)* fish and infected with *NRG1^{OEX}-iRFP* as described. Images taken at 24 hpi with a 10X objective were used to quantify the pixel distance of fluorescent Candida away from the (A) edge of the sac outlined by the DIC image, or (B) GFP positive endothelial cells lining the vasculature around the yolk sac. Represented are the average distances for each larvae (each point represents a single fish). Candida in fish that developed dissemination by 40 hpi was significantly closer to the edge of the yolk than in fish that did not develop dissemination ($p = 0.0312$, Student's t-test), but was further away from GFP positive endothelium than in fish that did not have dissemination by 40 hpi ($p=0.0134$, Student's t-test). Pooled from 3 experiments, n = 28 non-disseminated larvae and 23 disseminated larvae.

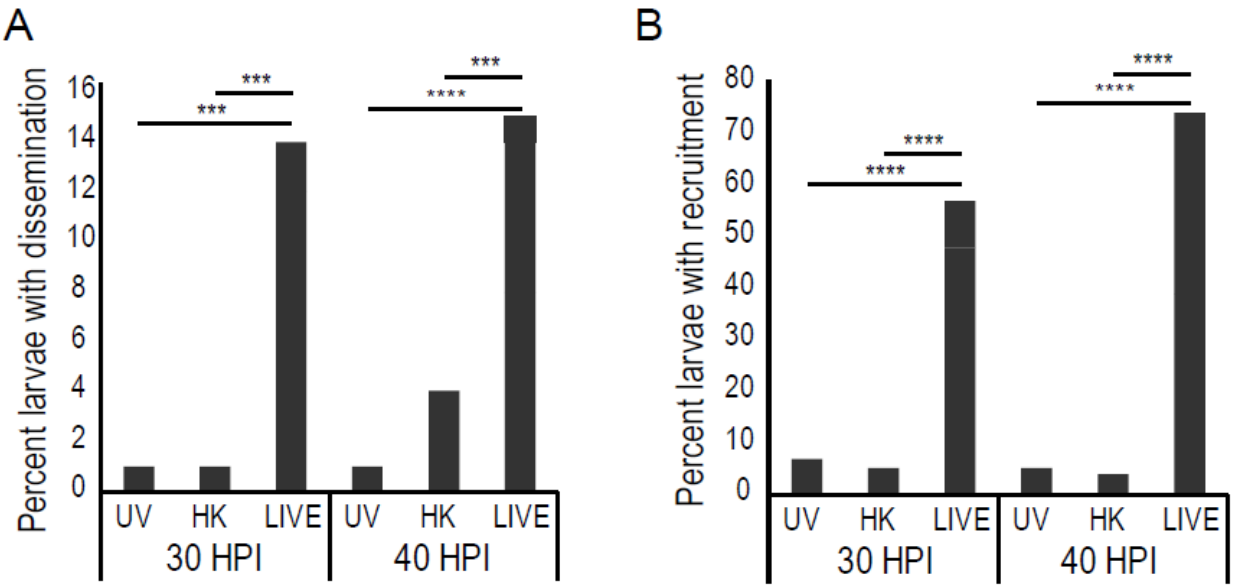

Figure 2.4. Killed yeast do not readily disseminate from the yolk sac or elicit immune cell response. *Tg(mpx:EGFP)* larvae were infected with a wild type *C. albicans* and kept at 21°C for the course of infection. Candida was prepared by heat or UV killing and stained with AlexaFluor555 prior to injection in the yolk. Larvae were followed for neutrophil recruitment and fungal dissemination at 24, 30, and 40 hpi. Care was taken to remove larvae with dissemination events at 24 hpi to ensure later dissemination events were a result of normal infection processes rather than researcher manipulation. (A) Percent larvae with dissemination of UV inactivated, heat killed, or live wild type *C. albicans* at 30 and 40 hpi. Pooled from 4 experiments, left to right n = 96, 77, 85. Fisher's exact test used to measure differences between non-disseminated and disseminated scores, *** $p \leq 0.001$, **** $p \leq 0.0001$. (B) Percent larvae with neutrophil recruitment to UV inactivated, heat killed, or live fungi. Same larvae as followed in panel A. Fisher's exact test used to measure differences between larvae with non-recruited and recruited scores, **** $p \leq 0.0001$.

2.3.3 Phagocyte recruitment correlates with pro-inflammatory gene upregulation and local expression of TNFα

Because we found phagocyte recruitment to the site of infection tended to precede yeast dissemination, we sought to test if this dissemination was related to physical movement of yeast within phagocytes or from yeast passage through weakened host tissues. Phagocytes can indirectly facilitate pathogen dissemination by proteolysis of epithelial cell junctions and by producing pro-inflammatory cytokines that increase local vascular permeability (Basset et al. 2003; Dejana, Orsenigo, and Lampugnani 2008; Marjoram et al. 2015; F. Wang et al. 2005). We therefore examined if dissemination events were associated with increases in inflammatory cytokine production. We scored for infection spread and recruitment of macrophages and measured cytokine mRNA levels in pooled larvae from each infection category. Larvae that had recruitment of macrophages to the site of infection had significant increases for tumor necrosis factor α (TNF α), interleukin-1-beta (IL1β), and interleukin-6 (IL-6), and this increase in expression in recruited larvae was independent of dissemination (Fig. 2.5A). We found similar results for infected larvae with both fluorescent neutrophils and macrophages, where increases in TNFα, IL1β, and IL-6 were also independent of dissemination (data not shown). These data suggest that inflammatory gene expression is associated with phagocyte recruitment, and that cytokine expression at the infection site might precede dissemination.

As TNFα was found to be upregulated in all larvae with phagocyte recruitment scores, we were interested in determining where TNFα was being expressed in relation to the location of yeast. A transgenic reporter zebrafish line of *tnfa* transcriptional activity was used to visualize the expression of TNFα in *Candida* infected fish (Marjoram et al. 2015). We found *tnfa:EGFP* expression localized primarily at the site of infection and occasionally in phagocytes interacting with disseminated fungi far from the infection site (Fig 2.5B and C). Parallel to the qPCR results, *tnfa:EGFP* expression at the site of infection appeared to correlate with phagocyte recruitment

(data not shown). Taken together, these data suggest that phagocytes recruited to the site of infection produce locally high levels of proinflammatory cytokines that may alter the infection environment, but elevated cytokine levels are not sufficient to drive dissemination events. We then sought to test physical transport of yeast within phagocytes.

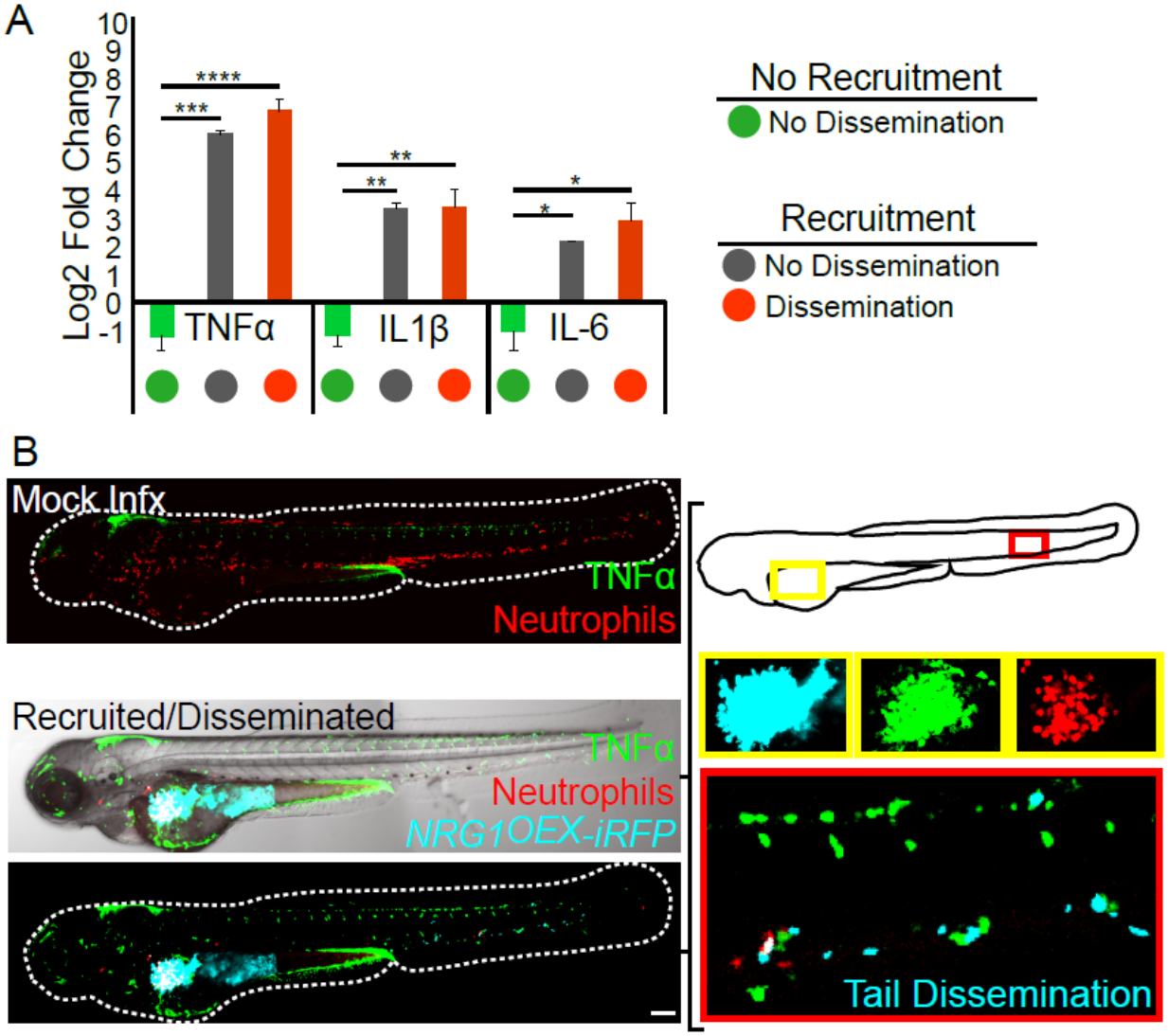

Figure 2.5. Innate immune cell recruitment is positively associated with the upregulation of *tnfα* at the site of infection. (A) *Tg(mpeg:GAL4)/(UAS:nfsb-mCherry)* larvae were scored for macrophage recruitment to the site of infection and yeast dissemination at 24 hpi, then homogenized for isolation of total RNA followed by cDNA synthesis for qPCR. Gene expression for TNFα, IL1β, and IL-6 were normalized to *gapdh* and PBS mock infected larvae were used for

reference (ΔΔCT). qPCR for all genes was run in triplicate and represented is the fold induction (2ΔΔCT) for each gene tested. Total RNA was extracted from 3 independent experiments with 97 PBS larvae, 50 no recruitment/no dissemination, 32 recruited/no dissemination, and 18 recruited/disseminated total larvae used for analysis. An ordinary one- way ANOVA with Tukey's multiple-comparisons posttest demonstrates significantly higher gene expression in larvae with recruited macrophages at the site of infection which is independent of dissemination scores (* $p \leq 0.05$, ** $p \leq 0.01$, *** $p \leq 0.001$, **** $p < 0.0001$). (B-C) Example *Tg(LysC:Ds-Red)/Tg(tnfα:GFP)* larvae with red fluorescent neutrophils and green fluorescence with *tnfα* expression in either a mock infected larvae (B) or a yeast-locked *C. albicans* infected fish (C). Scale bar = 100 μm.

2.3.4 Innate immune cells transport yeast into and throughout the bloodstream

Phagocytes can unwittingly spread viruses, intracellular bacteria and intracellular fungi in a host (J. M. Bain et al. 2012; Charlier et al. 2009; Nolan et al. 2017; Santiago-Tirado et al. 2017; Seider et al. 2010; Thwaites and Gant 2011). Until recent intravital imaging experiments, it was not appreciated that *C. albicans* can survive inside phagocytes and create an impasse that could potentially abet its spread into new host tissues through a Trojan Horse mechanism (Brothers et al., 2011). This "Trojan Horse" mechanism has three distinct stages: first, phagocytes respond to the infection and engulf the pathogen, then phagocytes move out of the infection site, and finally the pathogen exits the phagocyte in distant tissues. Time lapse imaging demonstrated phagocytosis of yeast by both neutrophils and macrophages (Fig. 2.6A and B, data not shown) in and near the infection site. We also documented macrophages carrying yeast away from the site of infection and into the yolk sac circulation valley (Fig. 2.6A and B, Movie 2.3) establishing the first step of the Trojan Horse mechanism. To look at overall phagocyte-fungi interaction dynamics in yolk infection, we quantified the number of neutrophils and macrophages at the initial infection site over time. We found that there was an increase in the number of phagocytes at the site of infection by 30 hpi, and this decreased by 40 hpi (data not shown). This decrease in phagocyte number at the later time

point was either because immune cells were leaving the site or dying as a result of infection (Tucey et al., 2018), but time-course images couldn't distinguish between these possibilities.

To test this idea, we used a transgenic fish with photo-switchable Kaede-expressing macrophages to track macrophages recruited to the infection site. The area photo-switched in each fish is indicated in the schematic of Fig 2.7A, and the timeline of infection, photo-switch, and post photo-switch imaging is indicated in Fig 2.7B. Larvae were classified into three groups: mock infected used for photo-converted baseline levels of macrophages near the site, no recruitment whose photo-converted macrophages did not interact with Candida, and recruited larvae that had macrophages recruited to Candida by 0 hours post switch (hps) (Fig 2.7C-D). There is a significant loss in macrophages only in fish that recruited macrophages to the infection site (Fig 2.8A). Once macrophages are recruited to the infection site and interact with *C. albicans,* macrophages tend to remain in the infection microenvironment and die (Fig 2.8B). Despite the low frequency of this event, we wanted to use this transgenic line to test if the pathogen can escape from the macrophages that do leave the infection site.

From the time lapse movie of Fig 2.6, it's clear that phagocytes respond to the infection, phagocytose yeast and carry them away from the infection site, but this movie does not answer if or how the pathogen escapes from the phagocyte. We found that a minority of photo-switched macrophages with phagocytosed yeast remained viable and migrated from the infection site (Fig. 2.9A-C). We followed photo-switched macrophages and imaged *C. albicans*-macrophage dynamics at 40 hpi in distant infection foci. We found instances of *C. albicans* being released from macrophages in two fish from one independent experiment. In the first larvae, one photo-converted macrophage was brought by the bloodstream to the tail where it released a yeast (Fig. 2.9B, Movie 2.2) and in the second larvae two photo-converted macrophages exocytosed three yeast (Fig. 2.9C, Movie 2.4). These time-lapses include clear instances of yeast escaping from macrophages far from

the infection site, providing evidence that the third step of the process of phagocyte-aided dissemination does occur *in vivo*.

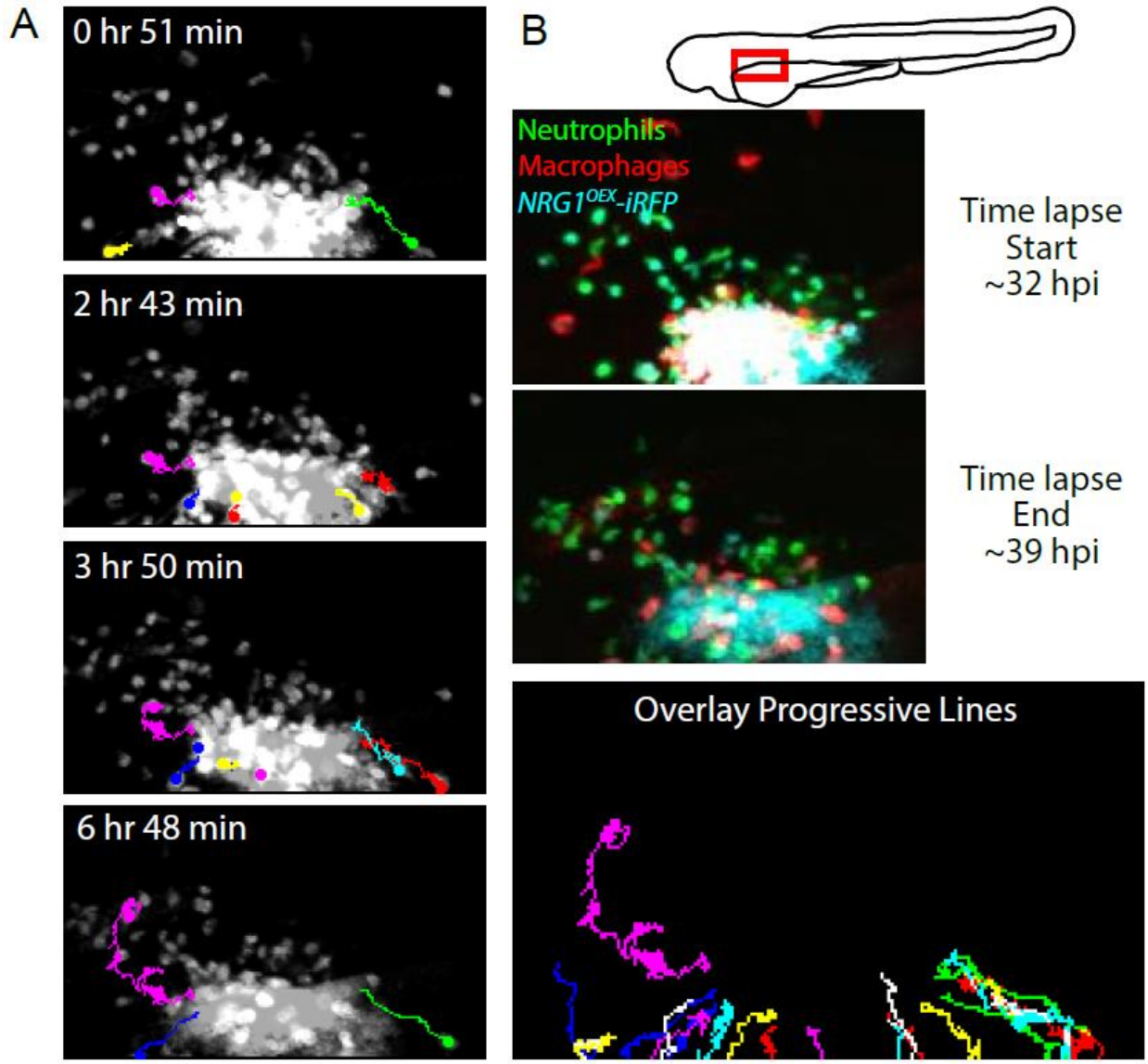

Figure 2.6. Phagocytes actively participate in the transport of yeast within the bloodstream

Tg(mpeg1:GAL4/UAS:nfsb-mCherry)/Tg(mpx:EGFP) were infected with *NRG1^{OEX}-iRFP* as described and scored for recruitment of phagocytes and dissemination of yeast. (A) Time lapse taken over the course of 7 hours starting at ~32 hpi. The schematic above illustrates the area imaged, 10X objective. Neutrophils and macrophages were observed moving within and away from the infection site carrying yeast. Dots and lines indicate tracks taken by phagocytes during the time lapse.

Phagocytes were observed taking yeast from the site of infection in these cases. (B) Compilation of tracks from individual phagocytes during the time lapse in a single overlay image.

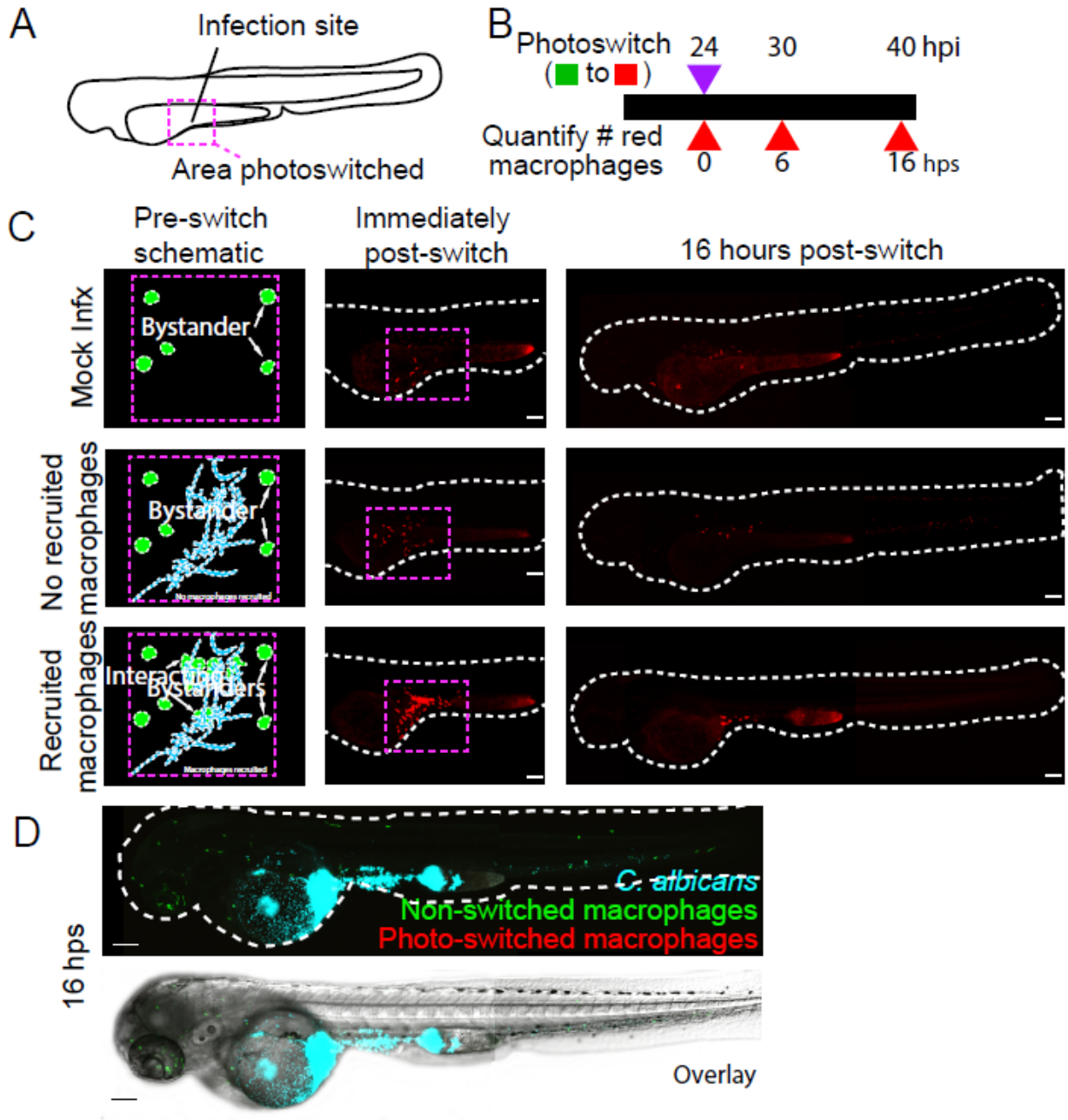

Figure 2.7. A photo-convertible zebrafish larvae demonstrates macrophages interact with fungi at the site of infection *Tg(mpeg1GAL4/UAS:Kaede)* larvae were infected with *NRG1*^{OEX}*-iRFP* and scored for recruitment of macrophages at 24 hpi. Macrophages near the infection site were

photo-switched at 24 hpi, and confocal images of each photo-switched larvae were taken at 24, 30, and 40 hpi (0, 6, and 16 hr post switch [hps]) to track macrophages. (A) Schematic indicating the region where macrophages were photo-switched. (B) Timeline of photo-switching and macrophage imaging post switch. (C) Representative z projections of photo-switched macrophages in representative single larvae with median number of photo-switched macrophages for each category. Schematics to the left show the photo-switched area for fish in each category: Mock infection (only bystander macrophages photo- switched), No macrophages recruited (no macrophages interacting directly with fungi; only bystander macrophages photo-switched), Macrophages recruited (macrophages interacting directly with fungi; interacting and bystander macrophages photo-switched). Scale bar, 100 μm. (D) The whole fish, stitched from three 10X objective images, of the of the Recruited macrophage scored larvae from panel C. The top image demonstrates the maximum z projection with all fluorescent channels, and the bottom image includes a single slice of the DIC. Scale bar, 100 μm.

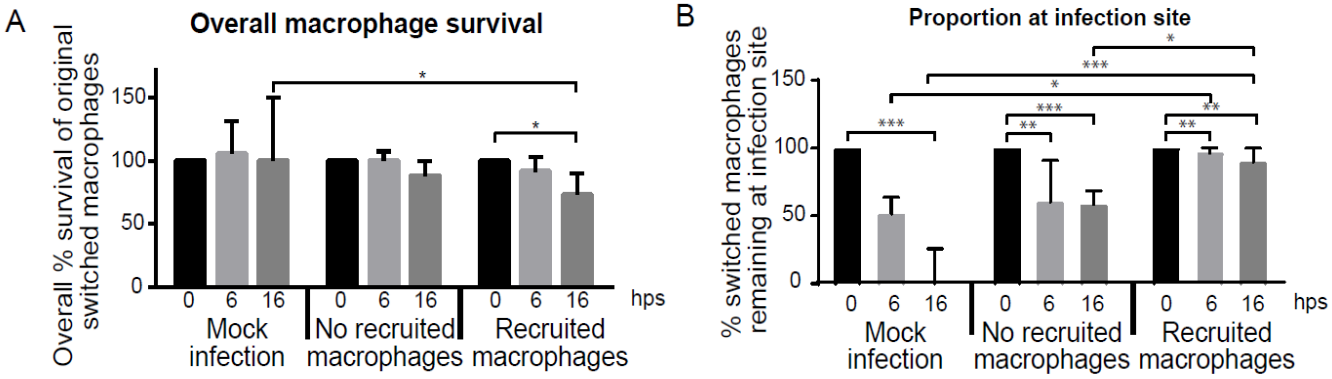

Figure 2.8. Macrophages die in the infection microenvironment (A) There is a significant loss in macrophages only in fish that recruited macrophages to the infection site. Bars indicate the median percentage of photo-switched macrophages that persisted in each group at 6 and 16 hps. Macrophage numbers for each fish were normalized to the number photos-witched at 24 hpi, equal to 0 hps. Pooled from five experiments, groups from left to right contain the following number of

larvae: n = 6, n = 9, and n = 18. Medians and interquartile range are shown and were compared using Kruskal-Wallis statistics with Dunn's correction for multiple comparisons. *p < 0.05. (B)

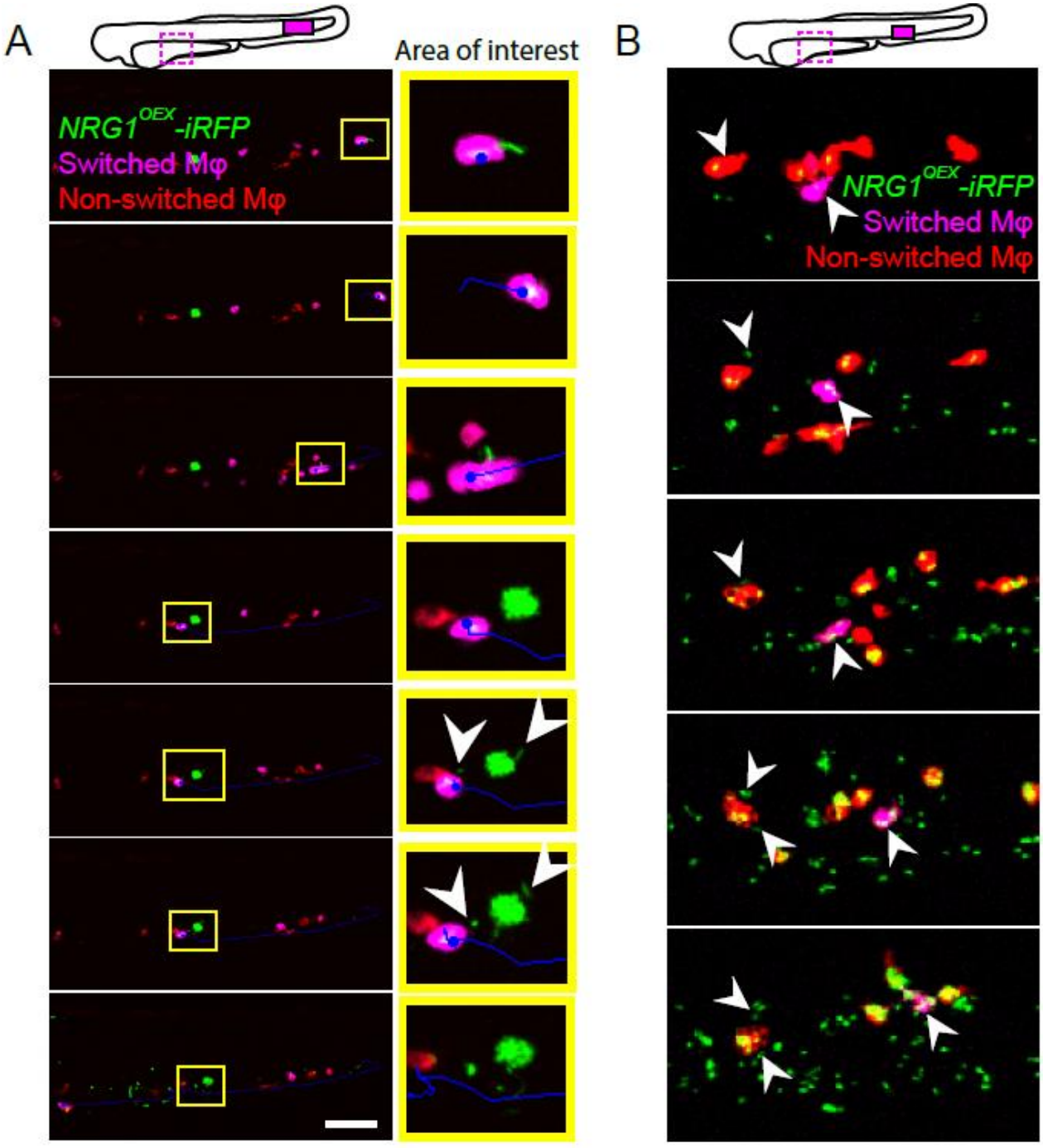

Figure 2.9. Macrophages actively participate in the transport of yeast within the bloodstream. *Tg(mpeg:GAL4)x(UAS:Kaede)* macrophages near the infection site were photoswitched at 24 hpi, and confocal images of each photoswitched larva were taken at 24, 30, and

40 hpi to track macrophage movement. (A) Time lapse panel of a *Tg(mpeg:GAL4)x(UAS:Kaede)* larva with a photoconverted macrophage moving out of the blood stream into tail tissue. The top fish schematic shows the regions used for photoswitching (magenta dashed box) at 24 hpi and the region selected for time lapse (magenta solid box) from ~32 hpi to ~40 hpi. The yellow highlighted area demonstrates a photo-converted macrophage stopping in the bloodstream, rolling down the tail, and then releasing yeast. White arrows in the image demonstrate non-lytic expulsion events. (B) Panel demonstrating yeast growth within a photo-converted macrophage and a "new" macrophage and subsequent release of yeast cells from both macrophages in the tail. White arrows in the image demonstrate non-converted macrophages releasing yeast and a photo-converted macrophage releasing yeast. 20X objective.

2.3.5 Neutrophil inactivation coupled with macrophage ablation does not alter infection outcomes

While these time-lapse experiments documented the occurrence of Trojan Horse-mediated spread, they are anecdotal, and the high-content nature of the experiments prevented quantification of these events in large numbers of infected fish of all cohorts to determine the relative contribution of infected macrophages to overall dissemination. To define the importance of phagocyte-mediated dissemination, we took advantage of the ability to ablate macrophages and disable neutrophils in the zebrafish larva.

We first investigated if the ablation of macrophages alters yeast spread by eliminating macrophages either by injection of liposomal clodronate (Bernut et al. 2014; Bojarczuk et al. 2016; Carrillo et al. 2016; Charlier et al. 2009) or by addition of metronidazole pro-toxin to larvae with nitroreductase-expressing macrophages (Davison et al. 2007; Gray et al. 2011; Pisharath and Parsons 2009). We first confirmed that both methods are effective. Larvae treated with clodronate liposomes or metronidazole had an almost complete loss of macrophages and no change in recruited neutrophils (Fig 2.10A-D).

Using these ablation methods, we imaged larvae and counted the number of neutrophils or macrophages in the yolks of infected fish to determine if there were differences in phagocyte recruitment. Macrophages were successfully eliminated from the infection site, and neutrophils appeared to be unhindered in their response to *C. albicans* with either treatment (Fig 2.11A-C). Additionally, ablation of macrophages by either method did not result in any alteration in dissemination frequencies at any time point (Fig. 2.11D). Ablated larvae also had a similar progression of events where phagocyte recruitment (neutrophils) preceded fungal dissemination (data not shown). We complemented these chemical ablation experiments with additional experiments using *pu.1* morpholinos to block macrophage development. This method also yielded similar dissemination frequencies of yeast with and without macrophage development (Fig. 2.12A and B). Taken together, these experiments, using three different ways of eliminating macrophages, clearly show that macrophages are unexpectedly not required for efficient dissemination.

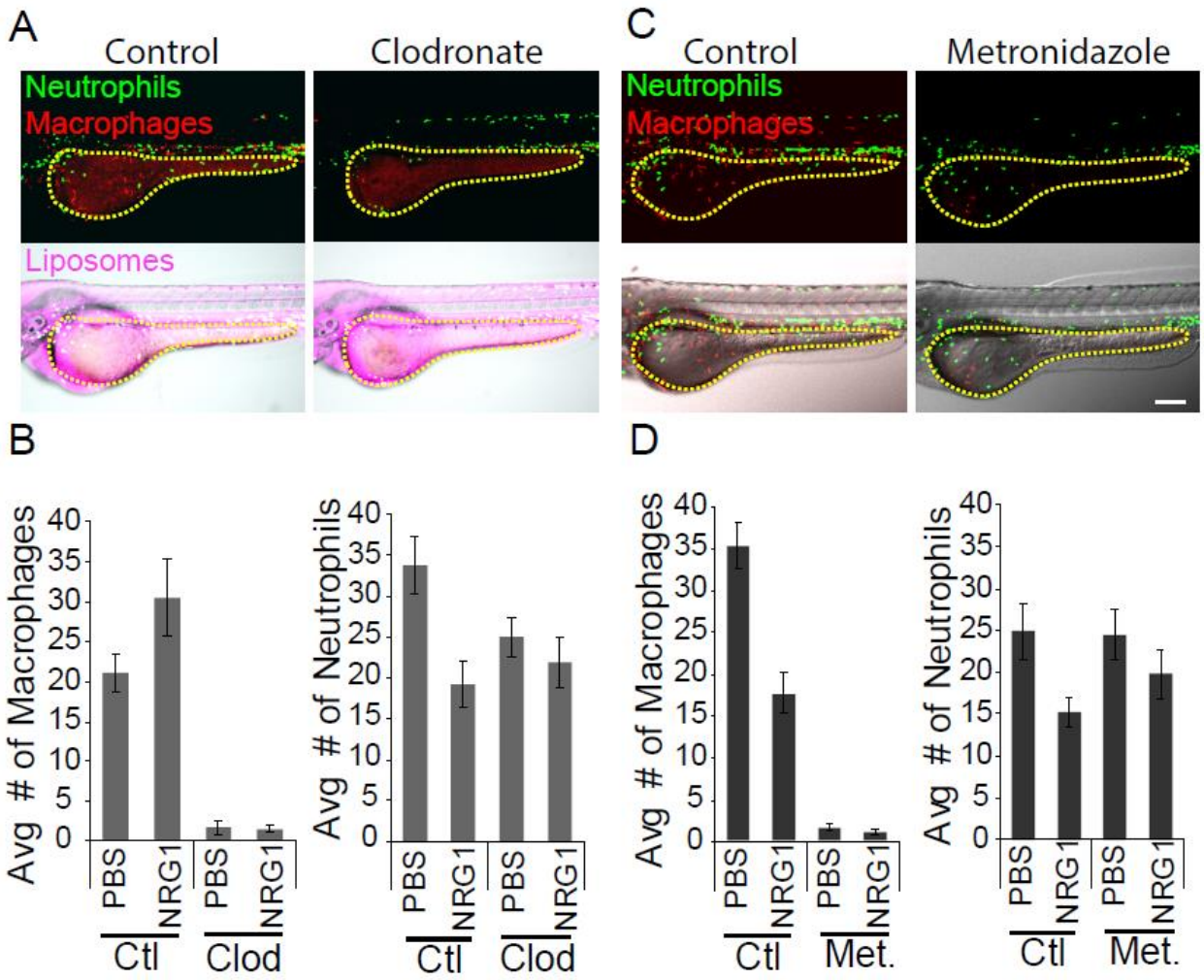

Figure 2.10. Clodronate liposomes and metronidazole treatment are effective methods for macrophage ablation. *Tg(mpeg:GAL4/UAS:nfsb-mCherry)/Tg(mpx:EGFP)* larvae with green fluorescent neutrophils and red fluorescent macrophages were used to check efficiency of ablation methods. Larvae were either injected at 28 hpf with 8-10 nl of control or clodronate liposomes (3:1:1 lipsomes:phenol red:10kDa dextran) in the caudal vein or bathed in 20 mM metronidazole for 4 hours following infection and 10 mM metronidazole thereafter. (A) Images of control and clodronate liposome treated larva, 10X objective, scale bar = 150 μm. (B) Number of macrophages or neutrophils counted in a 6-somite region in the trunk at 40 hpi. Bars indicate the median and interquartile range. Liposome treated larvae pooled from 4 experiments, left to right, n = 8, 18, 8, and 18. (C) Images of control and metronidazole treated larvae. (D) Number of macrophages or

neutrophils counted in the same region as B. Bars indicate the median and interquartile range. Pooled from 4 experiments, left to right, n = 8, 30, 11, and 19. A one-way ANOVA with Kruskall-Wallis post-test was used to test groups, * ≤ 0.05, ** p ≤ 0.01, *** p ≤ 0.001, **** p ≤ 0.0001, n.s. = not significant.

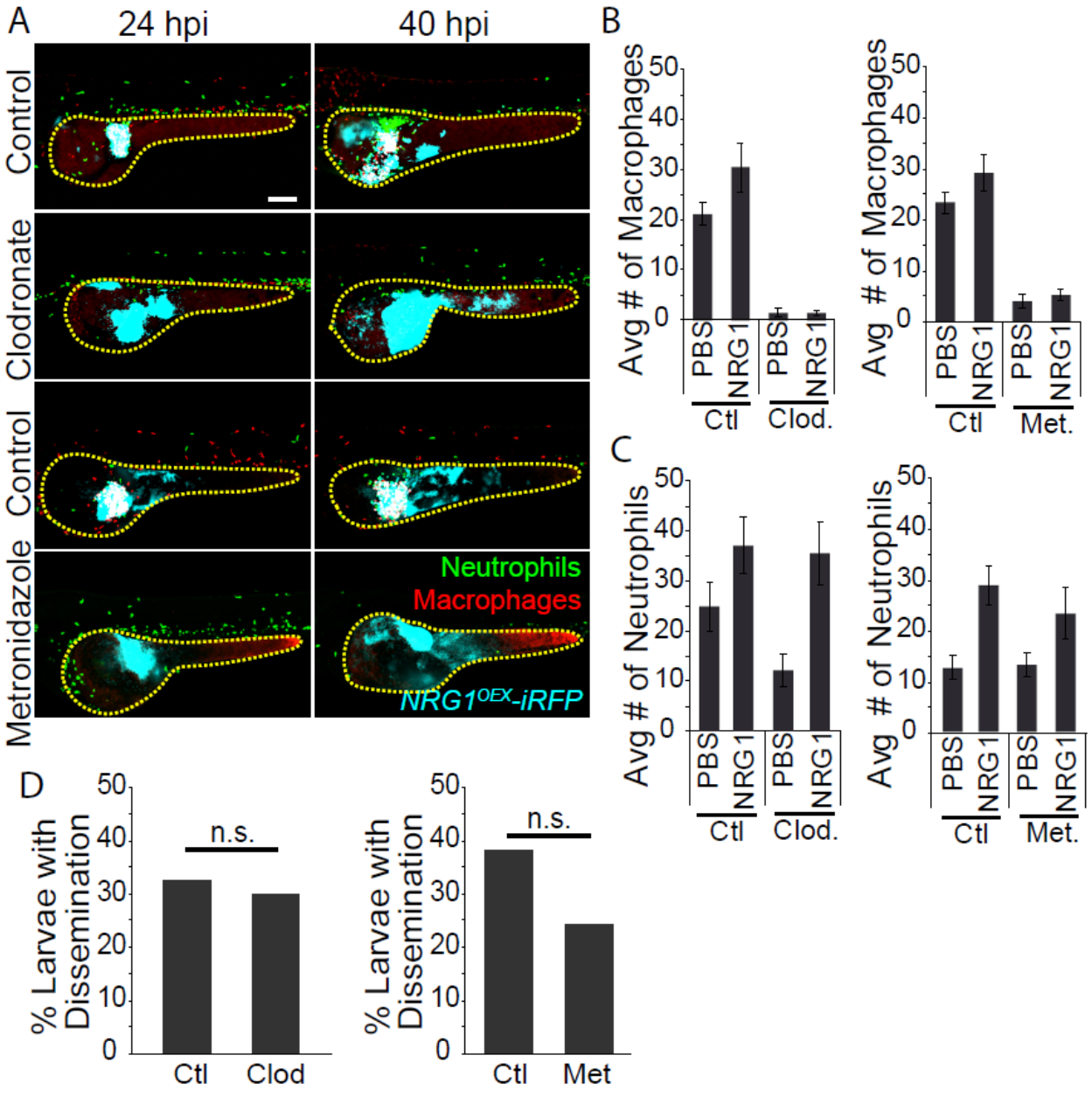

Figure 2.11. Macrophage ablation does not alter dissemination rates. *Tg(mpeg:GAL4/UAS:nfsb-mCherry)/Tg(mpx:EGFP)* larvae were also used to examine phagocyte recruitment to the infection

site. (A) Representative images of infected larvae with each treatment, 10X objective, scale bar = 150 μm. (B) Number of macrophages and (C) neutrophils counted in the yolk between clodronate (left) and metronidazole (right) treated larvae. Same larvae as quantified in Figure 2.10. Bars indicate the median and interquartile range. A one-way ANOVA with Kruskall-Wallis post-test was used to test groups, * ≤ 0.05, ** p ≤ 0.01, *** p ≤ 0.001, **** p ≤ 0.0001, n.s. = not significant. (D) Percent larvae with dissemination between clodronate (left) and metronidazole (right) treated larvae. Fisher's exact test, n.s.

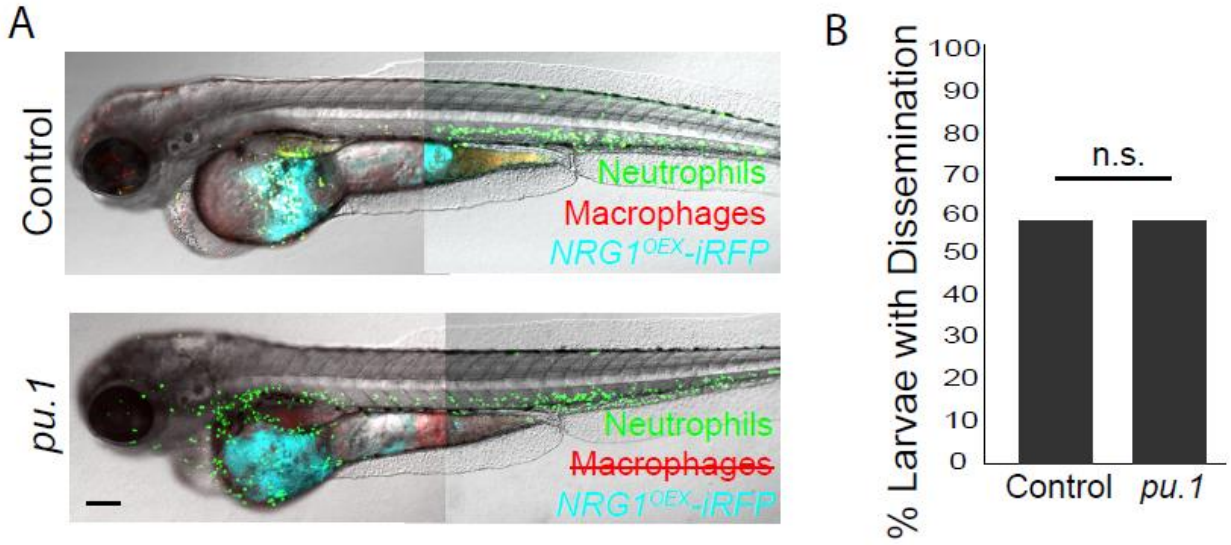

Figure 2.12. Ablation of macrophages by morpholino oligonucleotide does not alter dissemination frequencies *Tg(mpeg:GAL4)/(UAS:nfsb-mCherry)/Tg(mpx:EGFP)* embryos were injected at the one-cell stage with a combination of splice blocking and translational blocking *pu.1* morpholino oligonucleotides to inhibit macrophage development. A Cascade blue fluorescent 10kDa dextran was injected with the morpholino mix, and larvae were screened for correct injection of the morpholino mix following infection with *NRG1^{OEX}-iRFP*. (A) Representative images of control and ablated larvae at 40 hpi. Two 10X objective images stitched together, scale bar = 150 μm. (B) Percent larvae with dissemination at 40 hpi. Pooled from 3 independent experiments (n=54 control larvae and n=54 morphant larvae) a Fisher's exact test was used for analysis, n.s.

2.3.6 Phagocyte ablation is associated with increases in extracellular yeast in the bloodstream

Because we observed neutrophils at the infection site and also interacting with disseminated yeast in areas near the yolk (Fig 2.5 and 2.6), we sought to determine if neutrophils could substitute for macrophages in transporting yeast. We used Rac2-D57N larvae, with defective neutrophils which are unable to extravasate from the bloodstream (Qing Deng et al. 2011), and eliminated macrophages with clodronate. To our surprise, there was again no difference in dissemination rates in the context of impaired neutrophils, ablated macrophages, or both (Fig 2.13A). The fact that elimination of both major phagocyte types does not alter dissemination infection dynamics suggests that infection spread by a Trojan Horse mechanism is redundant and that other mechanisms play important roles.

We reasoned that elimination of both major professional immune cell types might alter infection dynamics significantly, limiting the ability of the host to contain bloodstream pathogens and thereby enhancing the ability of yeast to survive and proliferate once gaining access to the bloodstream. We quantified whether disseminated yeast were found intracellularly or extracellularly, as shown in Fig. 2.13B. While larvae without functional macrophages had more extracellular yeast, neutrophil perturbation did not affect the ratio (Fig. 2.13C). The total quantified pixels for each group was calculated and groups were found to have similar amounts of total disseminated yeast, so differences between extracellular and phagocytosed scores is not affected by the amount of dissemination (Fig 2.13D). Together, these results suggest that although phagocytes, particularly macrophages, participate as Trojan Horses, and macrophages are required to contain disseminated yeast intracellularly, they are not required for dissemination to occur.

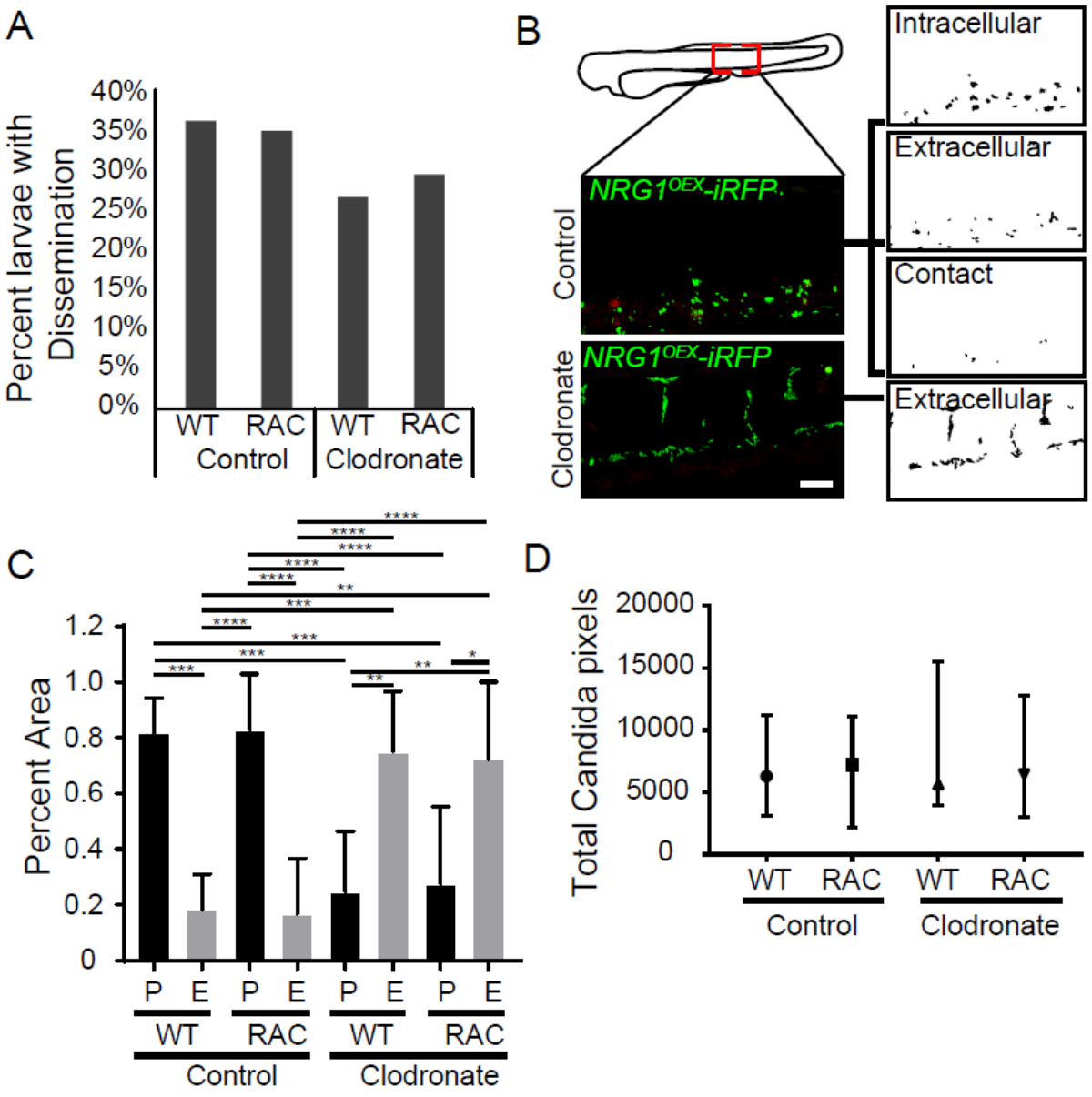

Figure 2.13. Phagocytes as Trojan Horses are not the primary source of yeast dissemination. Rac2-D57N zebrafish were outcrossed to AB fish for a mix of progeny with wildtype (WT) and neutrophil deficient (RAC) larvae. Larvae were injected with control or clodronate liposomes and infected with *NRG1^{OEX}-iRFP* as previously described. (A) Percent infected larvae with dissemination at 40 hpi; results are pooled from 6 experiments; Ctl/WT n=179, Ctl/RAC n=163, Clod/WT n=184, and Clod/RAC n=156. A Fisher's Exact test was used to measure differences between WT/RAC and Non-Disseminated/Disseminated scores, n.s.

(B) Schematic of the area used to quantify disseminated yeast. Images were used to score yeast as Phagocytosed (P; inside or in contact with phagocytes) or Extracellular (E; not contained), 20X objective, scale bar = 50 μm. (C) Percent area of Phagocytosed or Extracellular yeast for each group. Comparisons were done with a non-parametric ordinary one-way ANOVA and Dunn's posttest (* p≤ 0.05, ** p ≤ 0.01, *** p ≤ 0.001, **** p < 0.0001), and bars indicate the median with interquartile range. Pooled from 6 experiments, Ctl/WT n=16, Ctl/RAC n=21, Clod/WT n=15, and Clod/RAC n=18. (D) Total pixel counts for disseminated yeast are shown with the median and interquartile range. Same larvae as used in C, n.s.

2.3.7 TNFα production is dependent on macrophages but not neutrophils

These phagocyte ablation data suggested that neither phagocyte type is required for dissemination but did not address if phagocyte ablation affects local inflammatory gene expression at the site of infection. To determine if *tnfa* expression was altered in response to macrophage ablation, *Tg(LysC:dsRed)/TgBAC(tnfa:GFP*) larvae were infected and imaged for *tnfa* expression in presence or absence of macrophages. Representative images of control liposome- and clodronate liposome-treated larvae are shown in Figure 2.14A, where the yellow outline depicts the infected area used for analysis. Neutrophils were found at the site of infection in both control and clodronate-treated larvae, but control larvae had slightly more neutrophil recruitment than their clodronate treated counterparts (Figure 2.14B). TNFα expression was essentially absent in clodronate-treated infected larvae (Figure 2.14C), correlating with a slight reduction in neutrophil recruitment to the infection site. We sought to determine if there was a relationship between TNFα and neutrophil levels in the clodronate-treated fish, which would indicate if neutrophils drive *tnfα* expression in the absence of macrophages. In control fish, we found a positive correlation between *tnfa:EGFP* expression and neutrophil levels, but in the absence of macrophages, this relationship was lost and there was even a slight negative correlation (Figure 2.14D). These experiments suggest that macrophages are the primary drivers of *tnfa* expression at the fungal infection site.

To complement these macrophage experiments, we sought to examine the effects of macrophage ablation in the context of neutrophil inactivation. Rac2-D57N and *TgBAC(tnfa:GFP*) fish were crossed to create larvae with functionally deficient neutrophils and TNFα-controlled green fluorescence. Representative images (median *tnfa:GFP* levels) of control and clodronate-treated fish at 40 hpi have no *tnfa:GFP* expressed in macrophage ablated fish (Fig. 2.15A). Quantification of images of these fish demonstrate a trend toward higher *tnfa* expression in larvae with functional macrophages as compared to the clodronate-treated larvae, regardless of neutrophil status (Fig. 2.15B). Similar to what was found previously (Fig. 2.12A), there was no change in dissemination rates with loss of one or both phagocytes types in our Rac2-D57N cross with *TgBAC(tnfa:GFP*) (Fig. 2.15C). This data suggests that macrophages are vital for *tnfa* expression either because they are the primary producers of TNFα or because their presence is required so that other host cells are cued to produce TNFα.

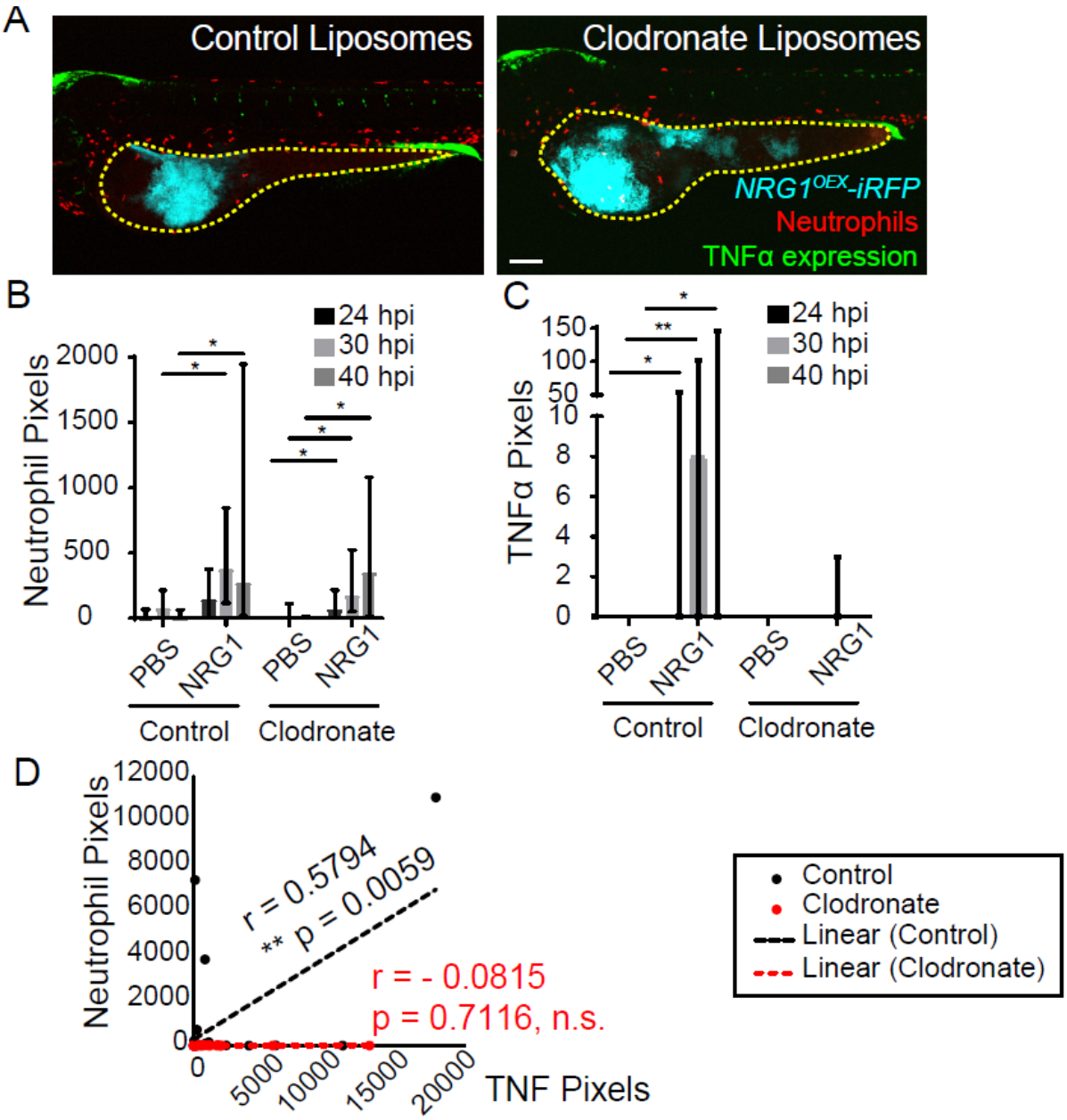

Figure 2.14. Macrophage ablation limits TNFα production. *Tg(LysC:Ds-Red)/Tg(tnfα:GFP)* larvae with red fluorescent neutrophils and green fluorescence with *tnfα* expression were treated with liposomes and infected with *NRG1*^{OEX}*-iRFP*. (A) Representative images of control and clodronate treated *Tg(LysC:Ds-Red)/Tg(tnfα:GFP)* larvae at 40 hpi. Area in yellow outlines the yolk sac, 10X objective, scale bar = 100 μm. (B) Fiji-ImageJ was used to make masks of the fluorescent channel. The number of neutrophil pixels in the area of yeast was measured from these masks in MatLab

software. Data pooled from 5 experiments, total fish used for quantification, left to right: n= 10, 21, 9, 23. Bars are the median with 95% confidence interval, tested by an ordinary one-way ANOVA with Kruskal-Wallis posttest. * p ≤ 0.05. (C) Using the same images as in panel B, *tnfα* expression in the area of *NRG1^{OEX}-iRFP* fluorescence was quantified in pixels. Bars are the median with 95% confidence interval, tested by an ordinary one-way ANOVA with Kruskal-Wallis posttest. * p ≤ 0.05, **p ≤ 0.01. (D) Correlation graph between recruited neutrophils (B) and *tnfα* expression (C) overlapping areas of *NRG1^{OEX}-iRFP* fluorescence.

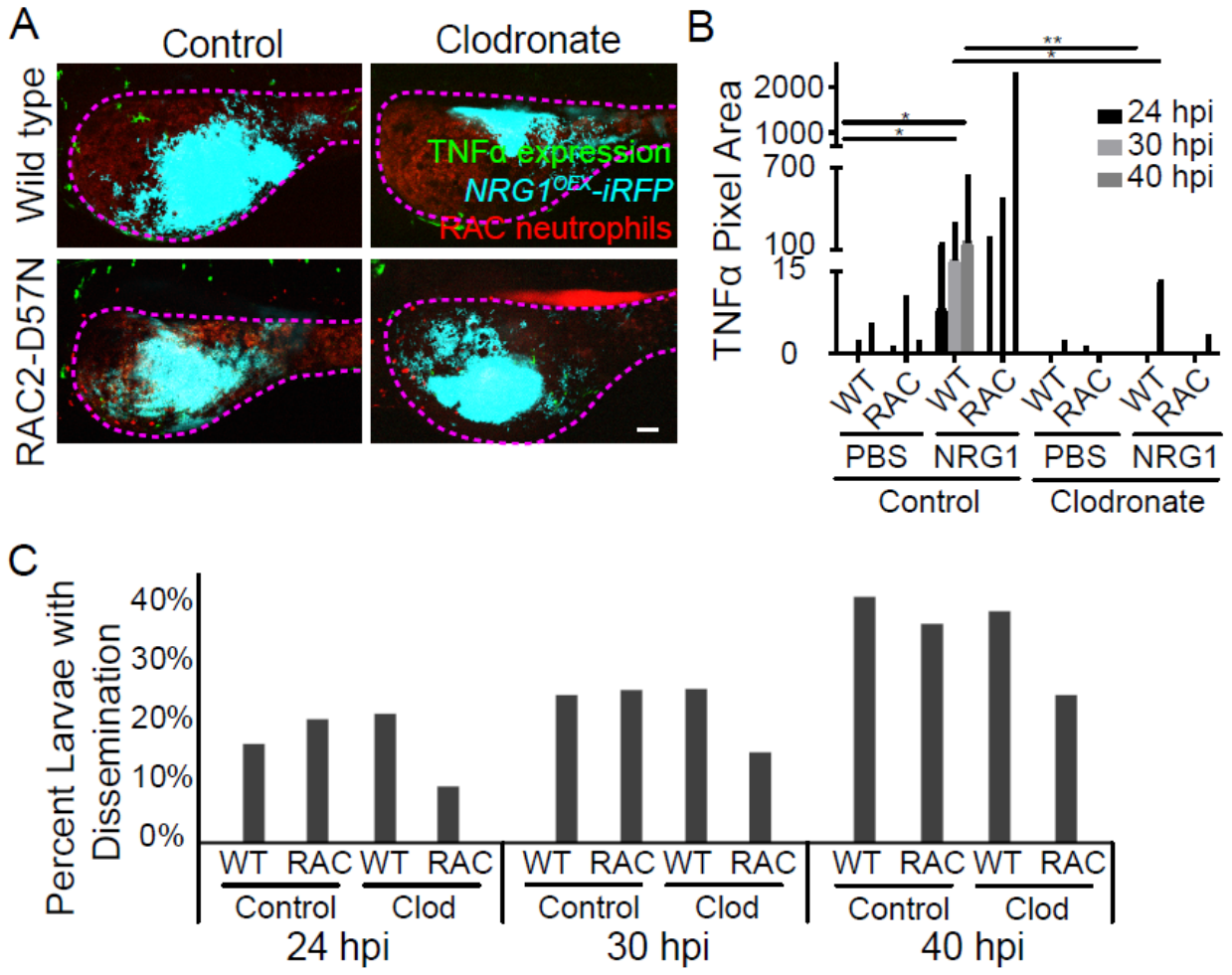

Figure 2.15. Macrophages are primarily responsible for *tnfα* production RAC2-D57N zebrafish were crossed with *Tg(tnfα:GFP)* fish for progeny with wildtype or neutrophil deficient larvae (RAC) with green fluorescence with *tnfα* expression. Larvae were also treated with liposomes and infected

with *NRG1^{OEX}-iRFP*. (A) Representative images of each larval group at 40 hpi. Area in magenta shows the yolk sac outline. 20X objective, scale bar = 50 μm. (B) To determine which cells were expressing *tnfα,* 20X images were used to measure *tnfα* expression in the area of *C. albicans*. Pooled from 5 experiments, left to right n = 10, 12, 28, 31, 9, 12, 27, & 30. An ordinary one-way ANOVA with a Kruskal-Wallis posttest was used, * $p \leq 0.05$, ** $p \leq 0.01$, and bars are the median with 95% confidence interval. (C) Percent Rac2-D57N x *Tg(tnfα:GFP)* larvae with dissemination, pooled from the same 5 experiments with the addition of larvae not imaged, left to right, n = 36, 62, 46, 52. Fisher's Exact Test, n.s. within timepoints.

2.3.8 Loss of blood flow reduces level of dissemination events but not rates of dissemination

While many pathogens use phagocytes to traverse epithelial and endothelial barriers, regulated endo- and exocytosis and paracellular movement represent alternative possible pathways of yeast dissemination into the bloodstream. Extracellular yeast that enter the bloodstream may be then transported away from the infection site by blood flow to distant tissues. To determine the role of blood flow in spreading infection, we took advantage of the ability of zebrafish larvae to grow and develop for the first seven days without a heartbeat, exchanging gases directly with the surrounding water (J. N. Chen et al. 1996; Kimmel et al. 1995; Stainier, Lee, and Fishman 1993).

We allowed for development until the time of infection to avoid disrupting normal hematopoiesis, then blocked blood flow using non-toxic doses of one of two previously characterized inhibitors of heart beat, terfenadine (Hassel et al. 2008; Milan et al. 2003) or valproic acid (Li et al. 2016; Rubinstein 2006). Successful blood flow blockade with 2 μM terfendadine can be seen in Movie 2.5 where the treated larva has reduced heart beat and loss of blood movement in the trunk and tail. Time-course and time-lapse imaging of treated larvae showed that neither drug altered phagocyte responses to *C. albicans* challenge (Fig. 2.16A-B, data not shown), demonstrating that phagocyte recruitment is independent of blood flow. Overall dissemination rates (non-

disseminated vs. disseminated) were unchanged between larvae with and without blood flow, but the level of yeast dissemination (low vs. medium + high) was lower when larvae were treated with terfenadine (Fig. 2.16C). This qualitative alteration in the pattern of dissemination suggested that blood flow plays a specific role in spreading the infection.

We repeated this experiment using a transgenic zebrafish line with green endothelial cells, *Tg(fli1:EGFP)* (Lawson and Weinstein 2002), to determine the roles of the endothelium during infection without blood flow. In this zebrafish line, we also saw that the overall dissemination rates were unchanged with loss of blood flow, but the level of yeast dissemination (low vs. medium + high) was lower in larvae without blood flow (Fig 2.17A). To understand how yeast penetrate host tissue, we used time lapse imaging to observe yeast near the endothelium. This time lapse imaging demonstrates that the endothelial cells take up yeast directly from the yolk sac and into the surrounding tissue in DMSO vehicle control treated larva (Fig 2.17B and C, Movie 2.6). Because of the poor resolution on this image, we are unable to deduce whether this was host micropinocytosis or paracellular invasion; however, this time lapse suggests that host cells, including endothelial cells and phagocytes, do have a direct role in the passage of yeast from a localized infection site.

Histology sectioning of terfenadine-treated *Tg(fli1:EGFP)* larvae shows yeast are found in tissues near the heart and the trunk next to the yolk sac extension (Fig. 2.18A). There are several thin layers of DAPI stained cells, including endothelial cells, in which disseminated yeast are caught. The location of the yeast in these layers suggests that yeast are able to enter host tissue, potentially increasing their chances of making it to the bloodstream where they are carried to distant sites.

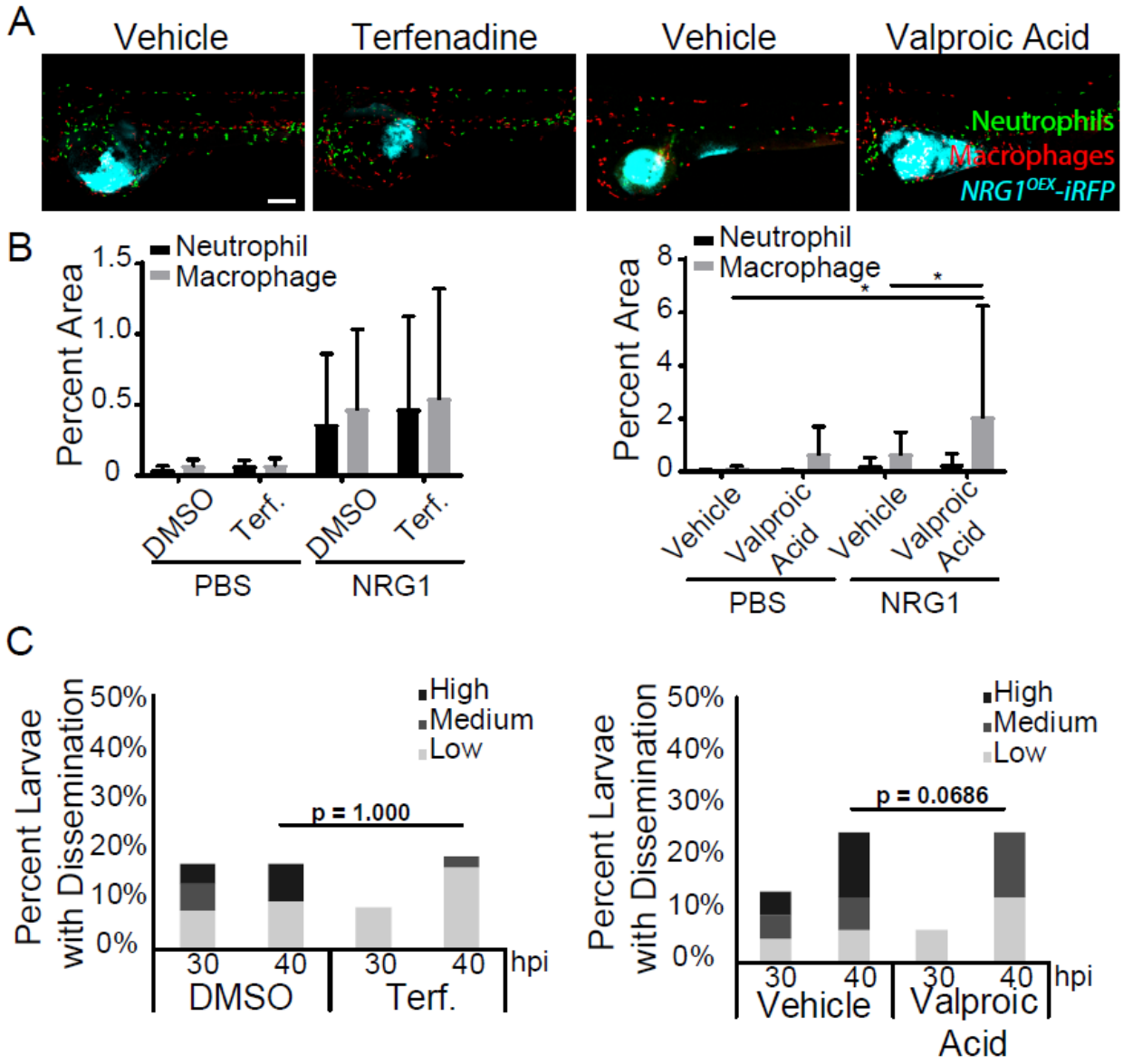

Figure 2.16. Chemical inhibitors of heart beat reduced blood flow, but not phagocyte recruitment or overall yeast dissemination. *Tg(Mpeg:GAL4/UAS:nfsb-mCherry)/Tg(mpo:EGFP)* larvae were bathed with 2 μM terfenadine in DMSO or in 0.1 mg/ml valproic acid in E3 media following infection with *NRG1^{OEX}-iRFP*. (A) Representative images of infected larvae at 40 hpi treated with control or chemical blood flow blockers. (B) Percent area of the infection site with recruited macrophages and neutrophils. Pooled from 3 experiments with terfenadine, left to right, n = 11, 9, 25, and 23. Pooled from 3 experiments with valproic acid, left to right, n = 9, 7, 26, and 15. Statistical analysis done using a two-way ANOVA and Sidak's multiple comparison's test, * ≤ 0.05.

(C) Dissemination scores of terfenadine treated larvae (pooled from 3 experiments, left to right, n = 52 and 48) and valproic acid treated larvae (pooled from 3 experiments, left to right, n = 22 and 16). Statistical analysis done using a Fisher's exact test, n.s.

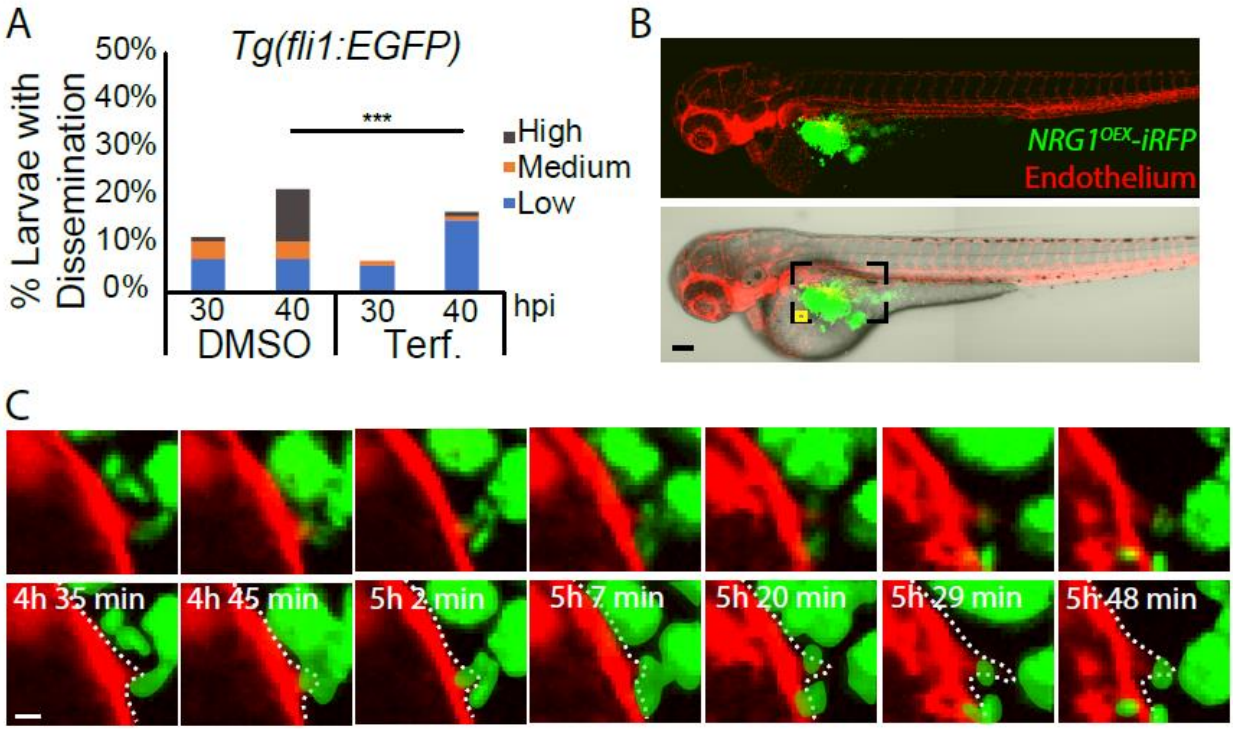

Figure 2.17. Host endothelial cells actively move yeast cells. *Tg(fli1:EGFP)* larvae were infected with *NRG1^{OEX}-iRFP* and bathed in DMSO control or terfenadine in E3 media to block blood flow. (A) Percent larvae with dissemination at 30 and 40 hpi scored as having "low", "medium", and "high" disseminated yeast. Pooled from 7 experiments, DMSO n = 110, terfenadine n = 118. A Fisher's Exact test was used to measure differences between "low" vs. "medium" plus "high" scores, p *** p ≤ 0.001. (B) A *Tg(fli1:EGFP)* larvae with blood flow was taken for time lapse between 32 and 40 hpi. Two 10X images were stitched using Fiji-ImageJ, scale bar = 150 μm. Area outlined in black is the area taken for time lapse and the area in yellow is the region shown in the panel D. (D) Panel from a cropped area of the time lapse. Panels were taken from a single Z slice over the course of one hour, 20X objective, scale bar = 10 μm.

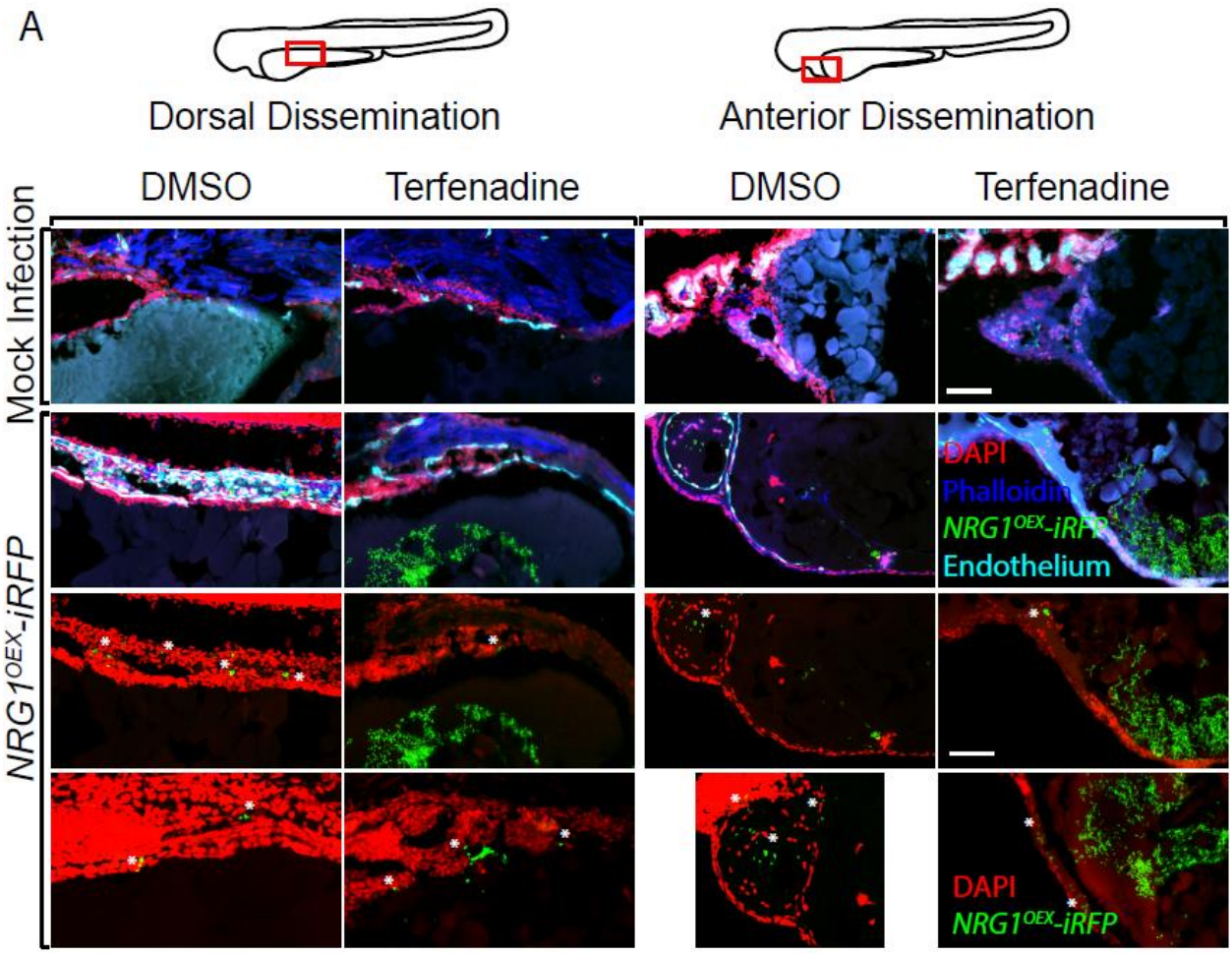

Figure 2.18. Yeast breach the yolk syncytial layer to surrounding tissue and endothelium. *Tg(fli1:EGFP)* larvae, which have fluorescent endothelial cells, were used to identify areas of yeast cell breach into surrounding host tissue in the presence (DMSO) and absence (terfendadine) of blood flow. Larvae were infected as previously described and, following 40 hpi, sections of the yolk were taken for histology. (A) Sections of *Tg(fli1:EGFP)* mock infected and infected larvae examining dorsal dissemination (left) and anterior dissemination (right) events. Sections were stained with DAPI (illustrated in red) to indicate surrounding cells and phalloidin (illustrated in blue) to indicate muscles or F-actin in host structures. *NRG1^{OEX}-iRFP* (illustrated in green) and *Tg(fli1:EGFP)* (shown as cyan) retained fluorescence during sectioning and staining. White asterisks indicate areas of

disseminated yeast which appear to be embedded in the yolk syncytial layer and heart. 40X objective, scale bar 100 = μm.

2.3.9 Loss of both phagocytes and blood flow may limit yeast spread.

Blockade of blood flow reduced the number of fungi that left the infection area, but it did not affect the percent of fish with some tissue-to-blood dissemination. Because phagocyte responses and *tnfα* expression were unaltered by blocking heartbeat, we reasoned that phagocytes might account for basal rates of dissemination. To test the combined activity of blood flow and phagocyte-mediated spread, we quantified dissemination in larvae lacking phagocytes and heartbeat. Utilizing the Rac2-D57N outcross to *Tg(tnfα:GFP)* larvae or Rac2-D57N outcross to AB, we injected all of the fish with clodronate liposomes and bathed in terfenadine. Larvae lost *tnfα* expression with macrophage ablation and had limited neutrophil response to the infection site (data not shown) as seen in our previous experiments (Fig 2.14 and 2.15). While following larvae through the course of the infection, we observed Rac2-D57N larvae treated with clodronate and terfenadine appeared to have disseminated of yeast nearer the heart and trunk adjacent to the yolk, while control larvae had disseminated yeast in more distant places (Fig 2.19A). This was a potentially interesting observation because blocking blood flow should not inhibit the host's endothelial cells' ability to endocytose yeast. We also a noted a significant difference in the rates of disseminated *C. albicans* between immunosuppressed larvae with and without heartbeat (Fig 2.19B) which suggests that neutrophils in the absence of bloodflow may play a role in limiting yeast proliferation after dissemination.

To test if our experimental methods altered overall yeast growth in the fish, images of whole larvae were taken at 40 hpi to measure all Candida pixels in the fish. ImageJ was used to stitch three 10X images together to make a unified fish image, and MatLab software was used to measure overall Candida in the larvae. There was no difference in the total number of Candida pixels in the whole fish (Fig 2.19C) suggesting Candida growth was not inhibited by treatment with

clodronate or terfenadine. Similarly, there was no difference in the total number of Candida pixels found outside the yolk sac (Fig 219D). Together, this data suggests that our treatment of the larvae does not influence yeast growth during larval infection and that the differences between dissemination rate are not due to an overall difference in Candida growth.

Using these same larval images used to measure Candida pixels, we measured the distance yeast travel from the edge of the yolk sac to the rest of the body. The distance yeast traveled was thresholded into "near" (≤25 pixels from the yolk edge) and "far" (≥55 pixels from the yolk edge) where there are more "far" pixels in immunosuppressed larvae with bloodflow than those without (Fig 2.19E-G). By blocking blood flow, the "far" scored disseminated yeast are lost ("near" and "far" scores illustrated by the schematic in Fig 2.19E) where yeast are no longer near the yolk. We found that larvae with deficient neutrophil response tended to have greater yeast distance traveled suggesting neutrophils play a key role in limiting the spread of yeast in the bloodstream (Fig 2.19F). This data suggests that the overall disseminated Candida is not different between larval groups, but the distance the yeast travels or the areas they are found in are different. Here, the host aids in dissemination events through phagocyte mediated mechanisms or by direct uptake through the endothelium where yeast are then dispersed by blood flow.

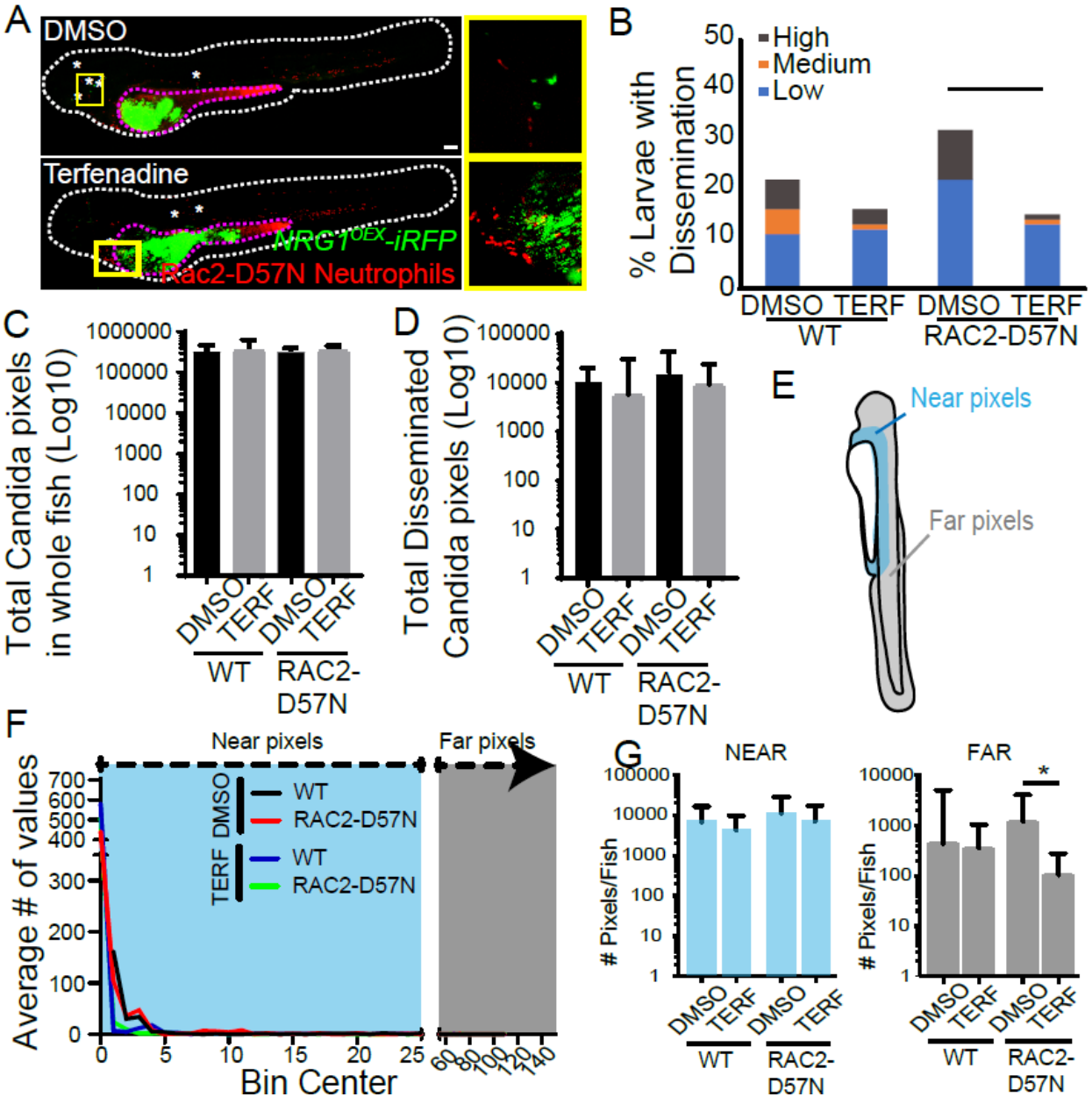

Figure 2.19. Loss of phagocytes and blood flow may limit yeast spread Rac2-D57N zebrafish were crossed to *Tg(tnfα:GFP)* or wildtype AB fish for neutrophil deficient offspring. All larvae were injected as described previously with clodronate liposomes for macrophage ablation, and control or terfenadine for blood flow blockade. Larvae were then infected with *NRG1^{OEX}-iRFP*. (A) Representative images of Rac2-D57NxAB larvae at 40 hpi. Three 10X objective images stitched together in ImageJ, scale bar = 100 μm. White dotted line indicates the whole fish body, the dotted

magenta outlines the yolk sac, and the yellow boxes indicate areas of the fish with disseminated yeast which is accompanied with a zoomed image. Disseminated yeast are also indicated by white asterisks. (B) Percent larvae with dissemination pooled from experiments done with Rac2-D57NxAB and Rac2-D57Nx*Tg(tnfα:GFP)* larvae. Pooled from 10 experiments, left to right n = 146, 140, 136, 150. A Fisher's exact test was used to differences between Low and High dissemination rates, * $p \leq 0.05$. (C) Quantified Candida pixels in the whole fish (yolk plus body) and (D) in the body of the fish. Pooled from 6 experiments, left to right n = 15, 21, 8, and 10. A one-way ANOVA with Kruskal Wallis post-test used to test significance, n.s. (E) Schematic of the scoring system for disseminated yeast. Yeast that were ≤25 pixels from the yolk sac edge were scored as "near" and yeast that were ≥55 pixels from the yolk sac edge were scored as "far". (F) A frequency distribution histogram of the distance in pixels that yeast travel from the yolk sac edge sorted into single bins. Distances less than 5 pixels was omitted from analysis. Same fish quantified as in C and D. (G) Larvae were re-scored with the number of pixels near or far from the yolk sac edge, a one-way ANOVA with Kruskal Wallis post-test used to test significance, * $p \leq 0.05$.

2.3.10 Dissemination of a wildtype *C. albicans* follows similar infection patterns as yeast-locked *C. albicans*

These data, taken together, suggest that yeast spread to distant tissues by a combination of phagocyte-mediated dissemination and extracellular dispersal through the endothelial layers followed by circulation-mediated movement. While use of the yeast-locked *NRG1*^{OEX} strain enabled these detailed analyses of dissemination in the absence of extensive tissue damage and early death, we felt it was important to determine if key aspects of yeast dissemination are mirrored during infections with wildtype *C. albicans* that produce a mix of filaments and yeast. Infections with wildtype *C. albicans* resulted in the expected high levels of mortality due to invasive filaments (Seman 2018). Nevertheless, we were able to confirm that phagocyte recruitment precedes dissemination (Fig. 2.20A), dissemination frequency is unaffected by loss of phagocyte function

(Fig. 2.20B-C), and phagocyte recruitment to the site of infection is accompanied by a macrophage-dependent local upregulation of *tnfα* (Fig. 2.21A-B). Many interactions of phagocytes with *C. albicans* were captured in these experiments, so it is perhaps not unexpected that loss of macrophages, neutrophils, or both phagocyte types allows significant levels of fungal growth in the yolk, in contrast to fully immunocompetent fish (Fig. 2.21C). Consistent with previous work that showed no association of fungal burden with dissemination (Seman et al 2018), we also found no difference in fungal burden between fish with and without dissemination (Fig. 2.21D). Taken together, our data suggest that the processes of yeast dissemination are similar for both yeast-locked and wildtype yeast.

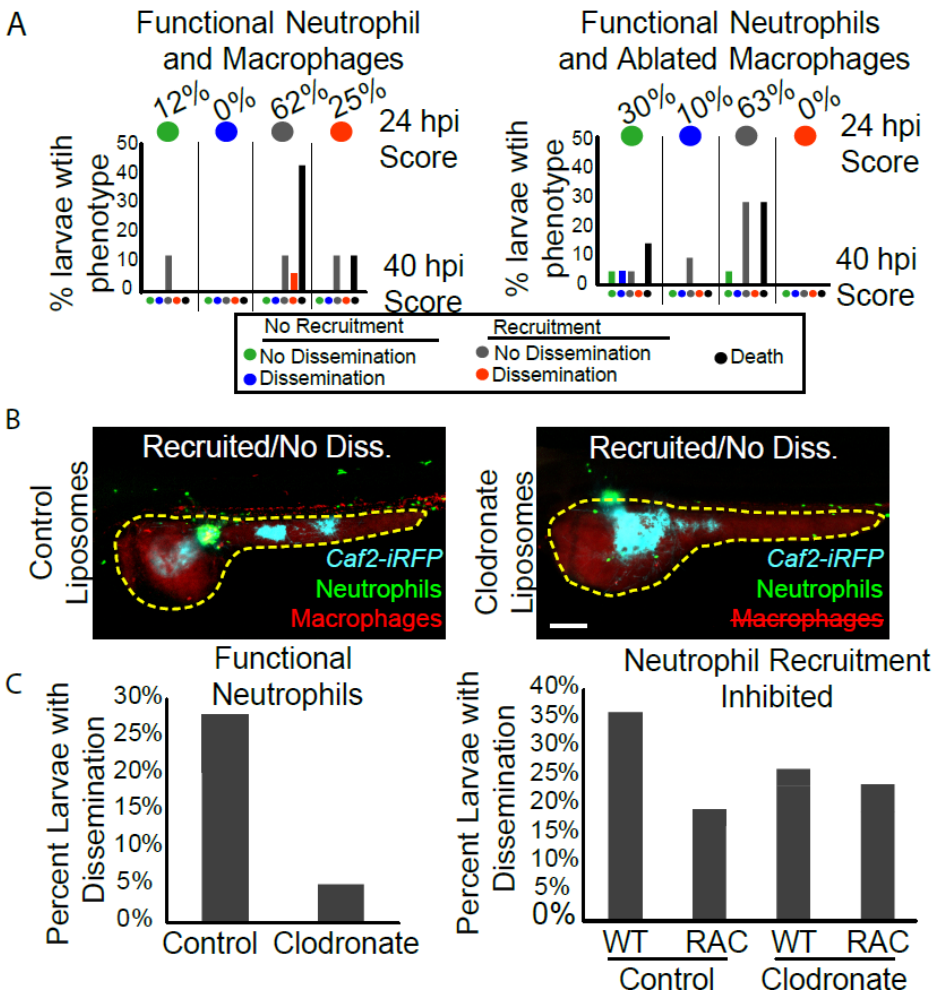

Figure 2.20. Infection with a wild type *C. albicans* demonstrates similar infection patterns as a yeast-locked strain *Tg(Mpeg:GAL4)/(UAS:nfsB-mCherry)/Tg(mpx:EGFP)* or RAC2-

D57Nx*Tg(tnfα:GFP)* larvae were injected with control or clodronate liposomes and infected with the wild type *Caf2-iRFP C. albicans* as described for the yeast-locked infections. (A) *Tg(Mpeg:GAL4)/(UAS:nfsB-mCherry)/Tg(mpx:EGFP)* were scored for immune recruitment and dissemination of yeast between 24 and 40 hpi. Scores for phagocyte recruitment and yeast dissemination were used to calculate the percent larvae with that phenotype as in Figure 2.1B. Pooled from 2 experiments, control larvae n = 16, clodronate larvae n = 21. (B) Images of Recruited/Non-disseminated *Tg(Mpeg:GAL4)/(UAS:nfsB-mCherry)/Tg(mpx:EGFP)* larvae treated with control or clodronate liposomes at 40 hpi. Area in yellow shows the yolk sac outline. 10X objective, scale bar = 150 μm. (C) Percent dissemination of *Tg(Mpeg:GAL4)/(UAS:nfsB-mCherry)/Tg(mpx:EGFP)* larvae (left) and RAC2-D57N/*Tg(tnfα:GFP)* larvae (right) at 40 hpi. Left: Same as panel A. Right: Pooled from 3 experiments, left to right n = 11, 36, 34, and 21. Fisher's exact test, n.s.

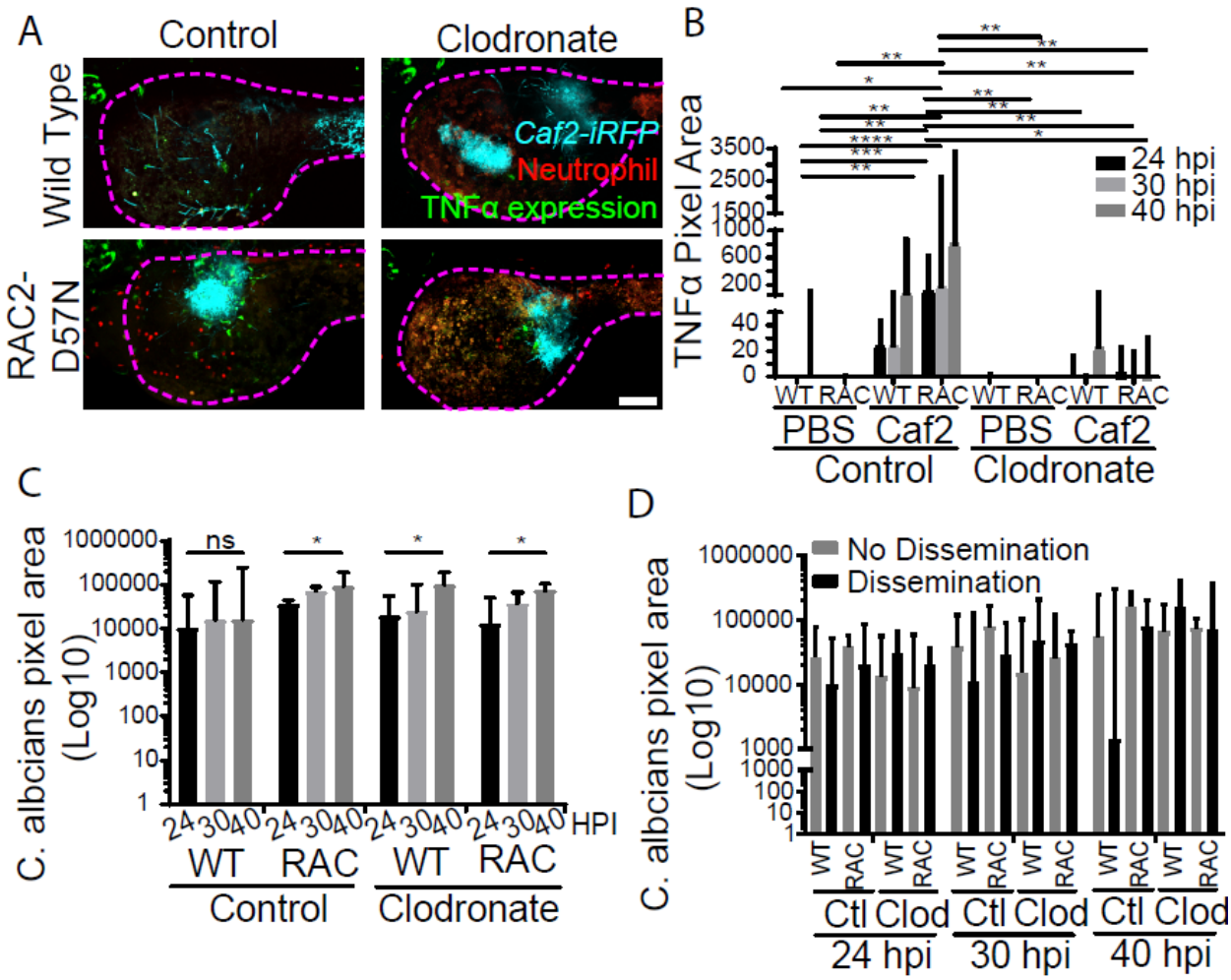

Figure 2.21. Phagocytes are not the primary source of wild type yeast spread RAC2-D57Nx*Tg(tnfα:GFP)* larvae were injected with control or clodronate liposomes and infected with the wild type *Caf2-iRFP C. albicans* as described for the yeast-locked infections. (A) Representative images of control (left) and clodronate (right) treated larvae. Area in magenta shows the yolk sac outline. 20X objective, scale bar = 100 μm. (B) Pixel area of cells expressing *tnfα* during wild type *C. albicans* infection. Pooled from 3 experiments, left to right n = 5, 7, 11, 15, 7, 5, 16, 16. An ordinary one-way ANOVA with a Kruskal-Wallis post-test, * $p \leq 0.05$, ** $p \leq 0.01$, *** $p \leq 0.001$., **** $p \leq 0.0001$. (C) Level of wild type *C. albicans* growth over time in each type of fish quantified in pixels from images. Same larvae used to quantify *tnfα* pixel area in Panel B. An ordinary one-way ANOVA with a Kruskal-Wallis posttest, * $p \leq 0.05$. (D) Level of *C. albicans* growth tested between non-

disseminated and disseminated larvae. Same larvae used to quantify *tnfα* pixel area in Panel B tested by one-way ANOVA with a Kruskal-Wallis posttest, n.s. All bars indicate the median with 95% confidence interval.

2.4 Discussion

Although invasive candidiasis poses a significant clinical risk, we still understand little about how this small non-motile fungus spreads throughout a host and what roles the host itself plays in limiting or enabling its movement. Using longitudinal intravital imaging of *C. albicans* and the host, we found that phagocyte-dependent and -independent mechanisms provide redundant pathways from tissue to bloodstream and throughout the host. On one hand, we find phagocytes can traffic yeast far from the infection site even in the absence of blood flow, releasing them in distant tissues. On the other hand, we show that even when phagocytes are disabled the yeast are able to efficiently get into the bloodstream and use blood flow to reach far tissues. These multiple strategies emphasize the versatility of *C. albicans* and suggest that we need to understand fungal interactions with both endothelial cells and phagocytes to understand the mechanics of tissue-to-bloodstream dissemination.

Phagocyte recruitment correlates with pro-inflammatory gene upregulation and local *tnfα* expression. Cytokine upregulation is a key step in innate immune response to an infectious threat, and this is the case in our infection model (Hall, Crosier, and Crosier 2015). Imaging by time-lapse at the single cell level revealed that *tnfα*-expressing cells are motile and are absent when macrophages are depleted, suggesting that only macrophages express *tnfα* in this infection model. Although imaging of *tnfα* levels in macrophage transgenics was not performed here, nearly all *tnfα*-GFP+ cells were found to also be mpeg1:dTomato+ in a similar swimbladder infection model (L. S. Archambault and R. T. Wheeler, unpublished observations). Proinflammatory cytokines at the infection site likely promote vascular permeability that may enhance fungal spread to the

bloodstream by endocytic, paracellular and/or Trojan-Horse pathways (Grubb et al. 2008; Marjoram et al. 2015; Orozco, Zhou, and Filler 2000; F. Wang et al. 2005).

We documented all of the key steps of Trojan Horse-mediated spread of *C. albicans in vivo*: recruitment, phagocytosis, reverse migration and fungal escape. The hijacking of phagocytes by *C. albicans* raises important questions about how and why innate immune cells transport yeast into the bloodstream and release them far from the infection site. While neutrophil reverse migration is now well-documented (Henry et al. 2013; Holmes et al. 2012; Nourshargh, Renshaw, and Imhof 2016; de Oliveira, Rosowski, and Huttenlocher 2016; Shelef, Tauzin, and Huttenlocher 2013), we still do not know what host and fungal signals regulate yeast-laden macrophages to leave the infection site. Further, although non-lytic exocytosis (NLE) is utilized by many pathogens, its regulation is poorly understood and likely involves both host and pathogen cues (J. M. Bain et al. 2012; Gilbert et al. 2017). Further work focused on NLE *in vivo* may reveal more about how *C. albicans* and other pathogens escape macrophage containment during vertebrate infection.

Neutrophils and macrophages were found to be dispensable for efficient dissemination. This was unexpected because we documented Trojan Horse dissemination, we found that phagocytes are sufficient to spread *C. albicans* in the absence of blood flow, and we know that macrophages are key for spread of other fungal and bacterial pathogens (Bojarczuk et al. 2016; Charlier et al. 2009; Clay et al. 2007). *C. albicans* may be able to efficiently spread without hitchhiking on phagocytes because it grows relatively well extracellularly compared to other phagocyte hitchhikers and/or because it has effective alternative means of entering and exiting the bloodstream without phagocytes. Further, as phagocytes both limit infection and spread yeast, there may be a counterbalancing effect of phagocyte elimination, where extracellular yeast are able to survive and proliferate in the blood in their absence. In this scenario, a decrease in phagocyte-mediated spread could be made up for by an increase in survival and proliferation in the bloodstream in the absence of attacking immune cells.

How do *C. albicans* yeast get through the epithelium and endothelium without phagocytes? Hyphae are known to translocate through epithelial and endothelial cell barriers *in vitro*, but yeast translocation has not yet been analyzed in these systems. Yeast passage through epithelial layers is infrequent in most epithelial *in vitro* models of barrier passage, which could be due to the loss of normal tissue architecture *in vitro* and/or to the altered expression of ligands and receptors that mediate internalization. There are a number of candidate host receptors, fungal adhesins and proteolytic enzymes that could participate in yeast translocation, including cadherins, EphA2, EGFR, ErbB2, secreted aspartyl proteases (SAPs), candidalysin, Als3p (Allert et al. 2018; Grubb et al. 2008; Wächtler et al. 2012).

Loss of blood flow reduces the amount of disseminated yeast but not rates of dissemination into the bloodstream. Dissemination is similarly diminished in the absence of blood flow and phagocyte function, and dissemination appears to be limited to tissues adjacent to the yolk (diffusion isn't enough, probably because of adherence to the vascular lumen). This suggests that dissemination can occur efficiently through phagocytes alone when they are active, or through extracellular spread and blood flow when phagocytes are disabled. These appear to be redundant mechanisms used for yeast spread (phagocytes and blood flow), which might actually be somewhat antagonistic. Phagocytes directly lead to spread but limit extracellular yeast in the blood.

While the larval zebrafish model has unique advantages in imaging and manipulation, these come with some limitations as well. The small size of the fish allows one to image the whole fish on the confocal, but the related limitation of the model is that dissemination distances are quite small, compared to what you would have in a mouse or human. Therefore, in translating our findings to the human host, we may find a differential time frame for extracellular spread by rapid blood flow as compared to phagocytes moving more slowly through tissue and lymph. Furthermore, although the overall anatomy is similar between fish and man, the tissue architecture of yolk, epithelium and endothelium is not representative of all potential sites of tissue-to-bloodstream dissemination in

mammals. Based on our findings in the zebrafish and the known conservation of cell types and molecules among vertebrates, we predict that both phagocyte-mediated and extracellular mechanisms of spread are important in mammalian tissue-to-blood dissemination. Unfortunately, although large groups of fungi can be tracked non-invasively in the mouse, testing of these ideas in a mammal will have to wait for new methods that will allow tracking of individual yeast and phagocytes to distant tissues (J. Bain, Gow, and Erwig 2014; Doyle et al. 2006; Mitra et al. 2010).

Leveraging the advantages of the zebrafish model system, we have identified some host roles in the spread of *C. albicans* yeast from tissue to blood. We documented Trojan Horse spread of *C. albicans* and showed that it is redundant with phagocyte-independent dissemination. Conservation of adhesion molecules, cell types and anatomy among all vertebrates suggests that both mechanisms are likely to also be important in mammalian infection. Clinical observations are consistent with our findings that *C. albicans* moves in the blood both inside and outside of phagocytes (Chandra et al. 2007; Duggan et al. 2015; Woth et al. 2012; D. Zhao et al. 2015). From a therapeutic standpoint, our results suggest that prevention of *C. albicans* dissemination will require tools that block both endothelial and phagocyte-driven movement of the yeast.

CHAPTER 3

THROMBOCYTES AND *CANDIDA ALBICANS* INFECTION

3.1 Introduction

Although platelets comprise only a small fraction of circulating cells in the blood, they play essential roles in both hemostasis and host defense (Yeaman 2014). Disseminated candidiasis involves the translocation of yeast or hyphae across the endothelium and into the bloodstream (Gow et al. 2012; Grubb et al. 2008). Once there, *Candida* encounters platelets which initiate an antimicrobial response. As *C. albicans* is moved through the body via the bloodstream, it may be sequestered in organs where platelets form clots to stop bleeding and limit further infection (Davis, Miller-Dorey, and Jenne 2016). Additionally, platelets may encourage dissemination of yeast as the platelets are proposed to endocytose yeast cells and transport them through the host (Speth et al. 2013; Speth, Rambach, and Lass-Florl 2014). We were interested in observing the host platelet interactions with *C. albicans in vivo*.

Platelets coat *C. albicans* in the blood and can recognize and interact with yeast and hyphal cell surfaces (Robert et al. 2000). This recognition can lead to some antimicrobial activity through the release of soluble mediators like cytokines and chemokines and activation of the innate and adaptive immune system (Bruserud 2013). Platelets are an understudied component of the immune response which may be important for neutrophil recruitment. The formation of platelet-neutrophil complexes (PNCs) have been well characterized in animal models (Page and Pitchford 2013), and infections with *Streptococcus pyogenes* and *Escherichia coli* demonstrate that these complexes are beneficial for limiting organ damage during sepsis (Hurley et al. 2016) and promoting the entrapment of bacteria by neutrophil extracellular traps (McDonald et al. 2012). Recently, zebrafish thrombocytes have also been shown to interact conversely with macrophages during *Mycobacterium marinum* infection where loss of platelet activation led to a reduction in

mycobacterial burden (Hortle et al. 2018). Together, these studies demonstrate the diverse roles platelets play with the innate immune system during sepsis.

To examine these questions *in vivo*, we utilized a transgenic zebrafish line in which thrombocytes fluoresce green or red (Lin et al. 2005). Our lab has utilized the zebrafish yolk sac as a model of disseminated candidiasis as we can observe host-pathogen interactions with *C. albicans* in real time in this space. The zebrafish yolk sac model of infection has become the principal method of investigating disseminated disease because of the 1) location of the yolk sac infection to the endothelium, 2) accessibility of immune cells to the site of infection, and 3) visualization of fluorescently labeled neutrophil and thrombocyte transgenic lines. These fluorescently marked thrombocytes, which are similar to megakaryocytes found in humans (Lin et al. 2005), were observed specifically for recruitment to *C. albicans*. We used confocal microscopy to examine the interactions between platelets and *C. albicans* in a live host model.

Contradicting information has been found between *in vivo* and *in vitro* experiments examining platelets interactions with *Candida*. The zebrafish offers a unique advantage to follow thrombocyte interactions with *Candida* in real time and how this affects infection outcomes. We have found that zebrafish thrombocytes interact closely with hyphae in a localized yolk sac infection model. Neutrophils and thrombocytes are recruited to the yolk sac where both cell types react to fungal hyphae. Interactions between neutrophils and thrombocytes at the site appear to be infrequent but may be of interest for future study. As humans and mice die of multiple organ failure and sepsis like symptoms that include platelet-associated phenotypes, the outcomes of this work will provide needed insight into the roles of platelets during disseminated fungal disease and highlight areas of therapeutic potential. Currently, platelet numbers are used to identify patients with sepsis (Woth et al. 2012), and this work may also indicate potential markers of candidiasis to test for in patient blood samples to diagnose and treat candidiasis at early onset.

3.2 Materials and Methods

Tg(cd41:GFP) zebrafish were incrossed for experiments examining green fluorescent thrombocyte interactions with a red fluorescent *C. albicans*. Larvae were collected, cleaned, and prepared for infection as described in Chapter 2. Larvae were infected with $5x10^6$ CFU/ml in PBS of wild type *Caf2-dTomato C. albicans*. Larvae were kept at 21°C after infection in order to have a range of morphology during the infection without killing the fish (Seman et al. 2018). Larvae were scored for initial inoculum on a Zeiss Axio Observer Z1 microscope (Carl Zeiss Microimaging, Thornwood, NJ), and then scored for dissemination and imaged 24, 30 and 40 hpi on an Olympus IX-81 inverted microscope with an FV-1000 confocal system as described in Chapter 2.3.

To examine thrombocyte-neutrophil interactions, *Tg(cd41:mCherry)* zebrafish were outcrossed to *Tg(mpo:EGFP)* zebrafish for larvae with red fluorescent thrombocytes and green fluorescent neutrophils, respectively. Larvae were collected as described but allowed to develop at 33°C until 2 dpf before being infected with *Caf2-dTomato* and moved to 21°C. This change in experiment protocol was to observe better development of thrombocyte fluorescence before infection. Larvae were scored for dissemination of yeast and recruitment of neutrophils at 20 and 32 hpi.

For imaging, larvae were anesthetized in Tricaine and embedded in 0.4% low melting point agarose (Lonza, Switzerland) in 24-well glass bottom dishes. Larvae were scored for dissemination and imaged at the timepoints given above. Fluorescent channels were acquired with optical filters for far red fluorescence at 635 nm excitation/668 nm emission, red fluorescence at 543 nm excitation/572 nm emission, and green fluorescence at 488 nm excitation/520 nm emission. A 10X objective (0.4 NA) was used to take images of the yolk of *Tg(cd41:GFP)* larvae at 24, 30, and 40 hpi. A single larva from each experiment was gently removed from the 24-well dish and re-plated on an 8-well μ-slide insert for the ibidi heating system K-frame (ibidi, Deutschland) for time lapse imaging. Images were acquired with a 20X (0.75 NA) objective and the Fluoview software was set

on “FreeRun” to acquire images in succession. Fluorescent channels were compiled on the Fluoview software individually and further compilation and analysis was complete with Fiji-ImageJ software (Schindelin et al. 2012).

3.3 Results and Discussion

We utilized the transgenic zebrafish *Tg(cd41:GFP)* to visualize the response of larval thrombocytes to *C. albicans* infection. Thrombocytes are actively recruited to wild type *C. albicans* in the yolk sac with significantly more thrombocytes recruited by 40 hpi in infected fish than their mock infected counterparts (Fig 1A). Confocal imaging of infected larvae revealed thrombocytes interacting closely with invading hyphal filaments on the side of the yolk sac (Fig 1B and C) and near the trunk of the fish (Fig 1B and D). This demonstrates that thrombocytes are actively recruited to the site of infection like other innate immune cells to a wild type *C. albicans* and is likely reacting to damage caused by hyphal filaments.

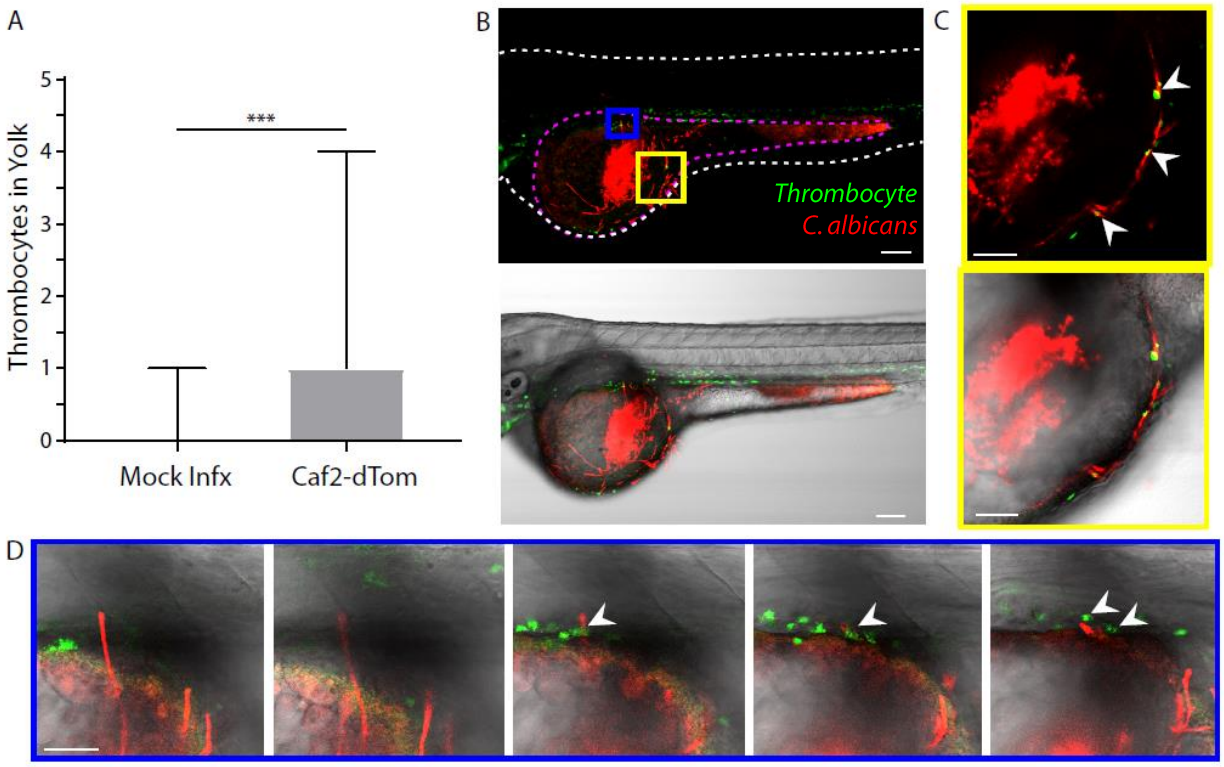

Figure 3.1. Thrombocytes move into the site of infection and interact directly with fungal filaments. *Tg(cd41-GFP)* larvae were infected with a red fluorescent *C. albicans* and kept at 21C for the duration of the experiment. (A) The number of thrombocytes counted within the yolk sac via epifluorescence at 40 hpi. Pooled from two experiments, PBS mock infected larvae n = 28, *Caf2-dTomato* infected larvae n = 49. Bars indicate the median and 95% confidence interval. Mann-Whitney test, *** $p \leq 0.001$. (B) Non-representative example of larvae with thrombocytes at the site of infection, 10X objective, scale bar = 100 μm. (C) Selected region of the fish in panel B which demonstrates thrombocytes interacting directly with fungal filaments. Single Z stack, scale bar = 50 μm. (D) Selected region of the fish in panel B demonstrating a series of the Z stack where hyphae are breaching the yolk barrier, scale bar = 50 μm. White arrowheads indicate areas of thrombocyte-filament interactions. Thrombocytes may be forming a clot near the area of yolk sac breach.

Time lapse microscopy was also utilized during these experiments to visualize in real time what role thrombocytes play during infection. Fig 2A demonstrates thrombocytes interacting with hyphae in the yolk at the start of the time lapse started roughly at 32 hpi and ending about four hours into the time lapse. Areas where thrombocytes are attached or related closely to filaments are indicated by white arrows. The panel below highlights a close interaction between a green positive thrombocyte and *C. albicans* growth. A maximum projection of 6 Z slices was taken to observe multiple thrombocytes in the field chosen. In this panel, it appears that the thrombocyte has attached to the filament and is wrapping around the filament like a responding neutrophil or macrophage might. This time lapse suggests that thrombocytes may behave as a significant source as an innate immune cell, potentially releasing antimicrobial peptides or initiating the response of other innate immune cells (Hortle et al. 2018).

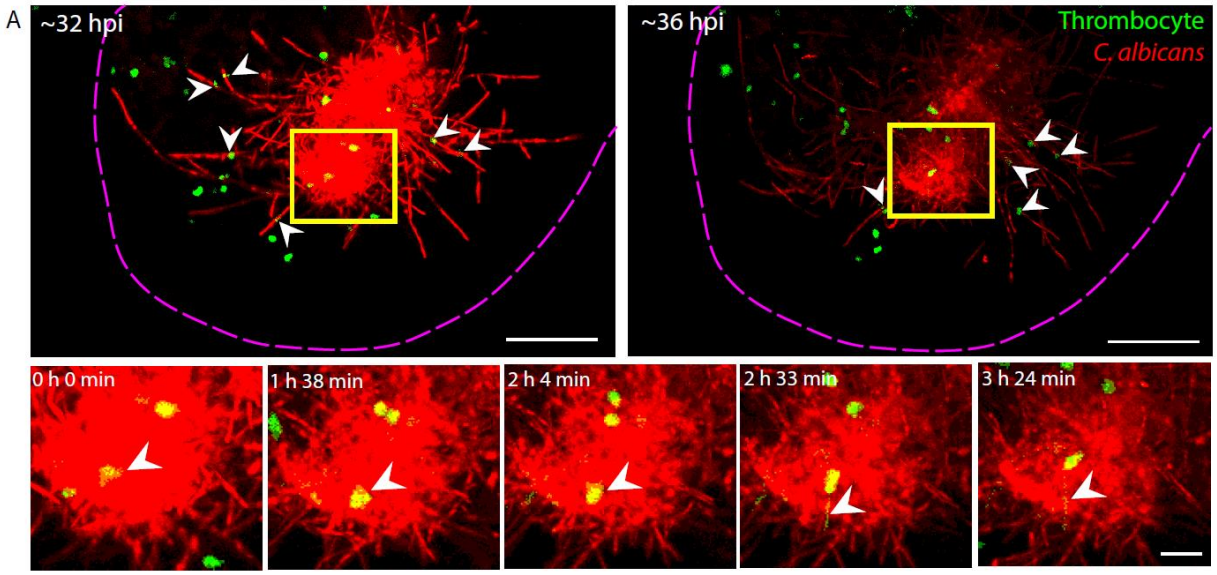

Figure 3.2. Thrombocytes attach to fungal filaments like other phagocytes *Tg(cd41-GFP)* larvae were infected with a red fluorescent *C. albicans* and kept at 21C for the duration of the experiment. (A) Single larvae observed for interactions between thrombocytes and fungal filaments during time lapse. Top row: Region selected for time lapse, maximum Z projection for all 25 slices taken, 20X objective, scale bar = 100 um. Magenta outlines the yolk sac and yellow box indicates

region highlighted below. Bottom row: Region highlighted from the time lapse. Maximum Z projection for 6 slices (at 6.6 um/slice), scale bar = 20 um. Thrombocytes were observed between 3 hours of the 8 hour time lapse. White arrows indicated thrombocytes interacting with fungal filaments

Platelet-neutrophil complexes (PNCs) have been well described in humans and animal models of infection. These PNCs are essential for neutrophil recruitment to inflamed tissues, and platelets prime neutrophils for adhesion to the vascular endothelium as well as other processes including phagocytosis and increased respiratory burst (Page and Pitchford 2013). We were interested in understanding the relationship of neutrophils and thrombocytes during a wild type *C. albicans* in our zebrafish model. This time lapse from a single larva in a single experiment is promising preliminary data to describe the interactions between thrombocytes and neutrophils. During the course of this roughly 8 hour time lapse, neutrophils and thrombocytes respond to *C. albicans* in the yolk sac as demonstrated previously. Here, however, we do not see neutrophils and thrombocytes interacting prior to reaching the infection and they do not appear to be forming intimate or long-lasting complexes. One potential instance of thrombocyte-neutrophil interaction with a *C. albicans* filament occurs at roughly 35 hpi when a thrombocyte investigates a neutrophil sitting on a hyphal cell before moving away (Figure 3A). A second instance of thrombocyte-neutrophil interaction occurs at roughly 41 hpi at the bottom of the yolk near the yolk sac circulation valley. Here, a neutrophil carrying a yeast cell contacts a thrombocyte briefly, the yeast is exchanged, and the yeast is released (Figure 3B). This time lapse indicates that neutrophils and thrombocytes interact during infection, however, it may not occur as frequently. The time lapse focused on the site of infection specifically, but it may be worth noting areas of thrombocyte-neutrophil complexes elsewhere in the fish during the course of infection.

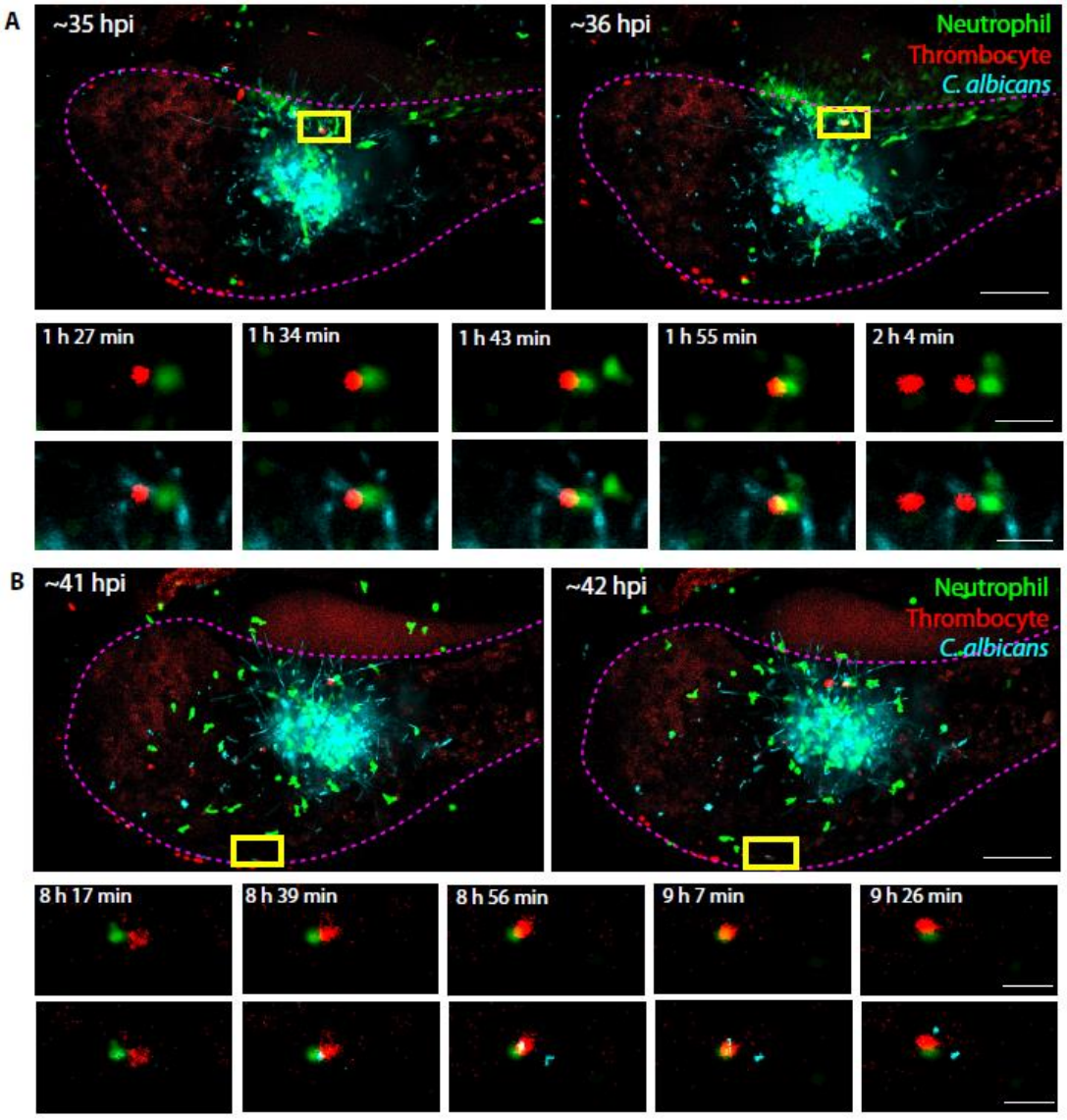

Figure 3.3. Thrombocytes and neutrophils interact at the site of infection *Tg(mpx:EGFP)* zebrafish were crossed with *Tg(cd41-mCherry)* zebrafish for larvae with green fluorescent neutrophils and red fluorescent thrombocytes. Larvae were infected with a far-red fluorescent wild type *C. albicans* strain at ~32 hpf and kept at 21°C. A single larva was followed via time lapse between 35 and 44 hpi. (A-B) Top row: A maximum Z projection of the larvae the beginning and end of the timeframe in question, scale bar = 100 μm. Area in magenta outlines the yolk, area in yellow indicate the region selected for viewing. Bottom row: same single z slice image of the area of interest, scale bar = 20 μm. Single Z slices are 10.45 μm thick.

CHAPTER 4

DISCUSSION AND FUTURE DIRECTIONS

We have tested several mechanisms of host mediated fungal cell spread including dissemination through phagocyte carriage, leakage through weakened host tissue, and potential endothelial cell uptake. We found that although macrophages actively remove yeast from the infection site and release it in distant tissues, phagocytes are not required for dissemination to occur. Similarly, macrophages appear to be the primary producers of TNFα in this model of infection, but loss of macrophages results in loss of *tnfα* expression did not alter dissemination patterns. Endothelial cells are actively seen taking up yeast cells, and loss of blood flow appears to limit yeast spread. Although these methods of testing the host's role in dissemination encompass many of the interactions between the host and pathogen, there are still potential mechanisms that we have not addressed in this study. Other untested host mediated mechanisms for future study include both other tissue mediated mechanisms like non-lytic expulsion events, thrombocytes and the lymph system, and more specific molecular mechanisms from the host and pathogen.

It seems counterproductive for the host immune system to expel pathogens without first killing it; however, we have clearly shown that this is a process that occurs with macrophages during Candida infection in zebrafish (Fig 2.8). Non-lytic expulsion (NLE) events may help the host phagocyte avoid lysis, but the release of the fungal pathogen may aid its survival and spread (Erwig and Gow 2016). Actin, the Wiskott-Aldrich syndrome protein (WASP), and the actin-related protein 2/3 nucleating complex together prevent NLE from occurring by making actin cages around phagosomes (Erwig and Gow 2016). During Candida infection of macrophages in a murine model, actin recruitment to phagosomes containing *C. albicans* is dependent on intraphagosomal hyphal growth rates, suggesting actin is thwarted by the fungus to escape the phagosome (J. M. Bain et al. 2012; Erwig and Gow 2016). In order to understand how these NLE events influence host outcomes, it will be important to learn what cues macrophages receive that support NLE. Moving

forward, we can continue to leverage the zebrafish to appreciate this process by following macrophages during larval infection and counting the number of non-lytic and lytic expulsion events that occur. We would also determine whether macrophages with non-lytic expulsion events go on to live or die following yeast expulsion, and how these events influence larval mortality. As this experiment would be technically challenging, we could use a mutant zebrafish lacking WASP, involved in the prevention of NLE (Erwig and Gow 2016), as an alternative method to test host response to loss of NLE. This mutant zebrafish line has delayed neutrophil recruitment to *Staphylococcus aureus* infections and limited phagocytosis and clearance events (Jones et al. 2013). We would be interested in testing if *C. albicans* elicits a similar host response in these fish and determine what the loss of NLE does for dissemination rates.

Another host mediated mechanism of yeast cell dissemination that we are beginning to explore includes the utilization of platelets as a means of escape. Platelets respond to yeast and hyphal forms of Candida (Robert et al. 2000; Vancraeyneste et al. 2016; Woth et al. 2012), and in our zebrafish model thrombocytes interact directly with both forms of Candida in the yolk sac (Figs 3.1-3). Platelets allows viruses like HIV to disseminate throughout the body and because the thrombocytes can carry Candida yeast, we suspect that they are an as yet uncharacterized source of fungal spread (Speth et al. 2013; Speth, Rambach, and Lass-Florl 2014). Additionally, platelets that form platelet-neutrophil complexes prime neutrophils to respond to infection (Page and Pitchford 2013) and these primed neutrophils are better able to from neutrophil extracellular traps which can be used to trap systemic bacterial infection (McDonald et al. 2012). Our zebrafish model of Candida infection can be leveraged to ask if these platelet-neutrophil complexes are formed during infection, and if neutrophils are better able to respond to disseminated yeast after priming. Primed neutrophils are likely to use the vasculature or lymphatic system then to reach the infection site.

We found that blocking blood flow via chemical treatment with terfenadine limited the level of dissemination events (“low” vs “medium” plus “high” scores) (Fig 2.16). Here, we focused on

disseminated yeasts within the bloodstream, but did not account for disseminated yeast in the surrounding lymph system. The lymphatic system is essential for tissue fluid homeostasis and immune trafficking (Jung et al. 2017; Yaniv et al. 2006). Zebrafish begin to develop the lymph system at roughly 1 dpf in the posterior cardinal vein (Jung et al. 2017), so our zebrafish model of infection has functional lymph and vasculature systems when Candida is injected. To build upon our understanding of Candida dissemination, we can therefore test how much of the disseminated Candida travels via the lymph system rather than the closely associated vasculature system. We can utilize transgenic zebrafish models in which the lymph expresses green fluorescence (*Tg(mrc1a:egfp)*) crossed with a transgenic with a red fluorescent vasculature system (*Tg(kdrl:mCherry)* (Jung et al. 2017). In this line, we will be able to determine where the yeast are located more clearly. Treatment with terfenadine to reduce heart rate and eliminate blood flow would allow us to identify yeast movement in the lymph. We hypothesize that treatment with terfenadine would do little to disrupt the lymph system itself as we still see uninhibited phagocyte recruitment with terfenadine treatment (Fig 2.15). These experiments would demonstrate another plausible route of travel for yeast in mice and humans.

Our study has focused on tissue specific mechanisms of dissemination, and established effective methods for eliminating some host responses. To gain a more refined understanding of these processes, we can to utilize these tools to ask questions at the molecular level, including some about Candida invasion into host tissue. *C. albicans* secretes candidalysin, a toxin that causes epithelial cell damage, and allows invasion into host tissue (Swidergall and Filler 2017). Previous work in our lab has shown that neutrophil recruitment and tissue damage are reduced during an candidalysin mutant strain of Candida (ece1Δ/Δ) in a zebrafish swim bladder infection model (Moyes et al. 2016). Here, they found that candidalysin was important for fungal pathogenesis and activation of the immune response (Moyes et al. 2016). This ece1Δ/Δ deletion mutant was also defective in damaging and stimulating oral epithelial cells *in vitro* and was greatly attenuated in a

mouse model infection, suggesting that candidalysin plays key roles in fungal pathogenesis (Moyes et al. 2016; Swidergall and Filler 2017). We are interested in testing this strain of Candida in our zebrafish yolk sac model with terfenadine treatment. We hypothesize that the ece1Δ/Δ Candida strain will be greatly inhibited in its ability to disseminate as it is less likely to damage host tissue. Additionally, the loss of blood flow would help indicate areas where fungi are able to breach and disseminate.

Similarly, we are interested in how Candida is able to cross the endothelium or epithelium even without the presence of phagocytes. We have utilized fluorescently labeled dextran to visualize leaky tissues that may allow fungal cells to pass through, a technique used previously to test Inflammatory Bowel Disease in zebrafish and during bacterial infection in mice (Bolcome et al. 2008; Marjoram et al. 2015; Sutton et al. 2003); unpublished data, B. Seman, S. Manandhar, A. Scherer). These leakage experiments would be best suited for hyphal infection, where we can note hyphal penetration of host tissue. In conjunction with this, we have done some preliminary work to examine the adherens junctions between epithelial cells in a yolk sac model using the plakoglobin-citrine protein-fusion transgenic zebrafish (Trinh et al. 2011). This zebrafish line allows us to visualize when hyphae breach the epithelial barrier, especially in a hindbrain model of infection (unpublished data, L. Walker). Together, the combination of plakoglobin fluorescence and dextran might give clues to how much dissemination is a result of fungal damage to host tissues.

Finally, Candida specific molecular markers like Als3 and Ssa1 which are invasins that aid in receptor mediated endocytosis could be potentially important fungal molecules to test in our system. Normally, these invasins interact with E-cadherin and EGFR/HER2 on host cells which activates clathrin endocytosis and directs the uptake of fungus into host tissue (Liu et al. 2015; Swidergall and Filler 2017; Wächtler et al. 2012; Zhu and Filler 2010). A mutant *als3/als3* Candida strain is unable to attach to host cell surfaces (Liu and Filler 2011; X. Zhao et al. 2004), so we plan utilize this, and similar, Candida strains to test the loss of adhesion and its impact on yeast spread.

By testing this and similar molecular markers, we can more clearly understand which are important for fungal invasion.

The study performed here informs us on specific methods yeast utilize to move through a host. We plan to continue to use this versatile infection model and the tools developed in this study to look at specific molecular mechanisms of yeast spread. Together, this information will provide useful information for identifying therapeutic targets specific for reducing the risk of disseminated candidiasis.

APPENDIX

Movie 2.1 Macrophage move from the site of infection. The movie depicts a single larva being injected with 4 nl of phenol red at ~32 hpf in the yolk sac. The movie was taken as described and was compiled at 5 frames per second (fps) in Fiji-ImageJ.

Movie 2.2 Macrophages move away from the site of infection. *Tg(mpeg:GAL4)/(UAS:nfsb-mCherry)/Tg(mpx:EGFP)* larva infected with *NRG1^{OEX}-iRFP* in the yolk sac. Images were taken with a 10X objective between 32-40 hpi and the images were compiled in ImageJ at 5 fps. Images were cropped to limit field of view to the site of infection. Macrophages are depicted in red, neutrophils in green, and yeast in cyan.

Movie 2.3 A photo-switched macrophage releases yeast far from the site of infection. *Tg(mpeg:GAL4)/(UAS:Kaede)* larva were infected with *NRG1^{OEX}-iRFP* and macrophages were photo-converted at 24 hpi. A larva was taken for time lapse imaging between 44 hpi and 52 hpi. Images were taken with a 20X objective and the images were compiled in ImageJ at 5 fps. Images were cropped to limit field of view to the site of disseminated infection, and the time lapse shows 40 minutes of the total 8 hour movie (near roughly 50 hpi). Non-photo-converted macrophages are depicted in red, photo-converted macrophages in magenta, and yeast in green.

Movie 2.4 Photo-switched and non-photoswitched macrophages release yeast. *Tg(mpeg:GAL4)/(UAS:Kaede)* larva were infected with *NRG1^{OEX}-iRFP* and macrophages were photo-converted at 24 hpi. A larva was taken for time lapse imaging between 32 hpi and 40 hpi. Images were taken with a 20X objective and the images were compiled in ImageJ at 5 fps. Images were cropped to limit field of view to the site of disseminated infection. Non-photo-converted macrophages are depicted in red, photo-converted macrophages in magenta, and yeast in green.

Movie 2.5 Terfenadine treatment effectively blocks bloodflow in zebrafish larvae. Healthy larvae taken were treated with DMSO vehicle control or 2 μM terfenadine at ~32 hpf. The larvae

were imaged on the Olympus SZ61 stereomicroscope system at the mock 40 hpi mark. The DMSO larvae is on the top and the terfenadine treated larvae is on the bottom of the movie. The movie was taken as described and was compiled at 5 frames per second (fps) in Fiji-ImageJ.

Movie 2.6 Endothelial cells actively move yeast. *Tg(fli1:EGFP)* larvae were infected with *NRG1^{OEX}-iRFP* and a larva was taken for time lapse imaging between 32 and 40 hpi. Images were taken with a 20X objective and compiled in ImageJ at 5 fps. Images were cropped to limit field of view to the site of possible endothelial interaction with Candida. Endothelial cells are depicted in red and Candida in green.

REFERENCES

Ablain, Julien et al. 2015. "A CRISPR/Cas9 Vector System for Tissue-Specific Gene Disruption in Zebrafish." *Developmental Cell* 32(6): 756–64. http://linkinghub.elsevier.com/retrieve/pii/S1534580715000751.

Alhamdi, Yasir et al. 2015. "Circulating Pneumolysin Is a Potent Inducer of Cardiac Injury during Pneumococcal Infection." *PLoS Pathogens* 11(5): e1004836. doi:10.1371/journal.ppat.1004836.

Allender, Matthew C., Daniel B. Raudabaugh, Frank H. Gleason, and Andrew N. Miller. 2015. "The Natural History, Ecology, and Epidemiology of *Ophidiomyces ophiodiicola* and Its Potential Impact on Free-Ranging Snake Populations." *Fungal Ecology* 17: 187–96. http://dx.doi.org/10.1016/j.funeco.2015.05.003.

Allert, Stefanie et al. 2018. "*Candida albicans*-Induced Epithelial Damage Mediates Translocation through Intestinal Barriers." *mBio* 9(3): 1–20. https://doi.org/10 .1128/mBio.00915-18.

Ashman, R B, and J M Papadimitriou. 1994. "Endothelial Cell Proliferation Associated with Lesions of Murine Systemic Candidiasis." *Infection and immunity* 62(11): 5151–53.

Bain, Judith, Neil Gow, and Lars-Peter Erwig. 2014. "Novel Insights into Host-Fungal Pathogen Interactions Derived from Live-Cell Imaging." *Seminars in Immunopathology* 37(2): 131–39. http://link.springer.com/10.1007/s00281-014-0463-3.

Bain, Judith M. et al. 2012. "Non-Lytic Expulsion/Exocytosis of *Candida albicans* from Macrophages." *Fungal Genetics and Biology* 49(9): 677–78. http://dx.doi.org/10.1016/j.fgb.2012.01.008.

Barker, Katherine S. et al. 2008. "Transcriptome Profile of the Vascular Endothelial Cell Response to *Candida albicans*." *The Journal of Infectious Diseases* 198(2): 193–202. https://academic.oup.com/jid/article-lookup/doi/10.1086/589516.

Basset, Christelle, John Holton, Rachel O'Mahony, and Ivan Roitt. 2003. "Innate Immunity and Pathogen-Host Interaction." *Vaccine* 21(S2): 12–23.

Ben-Ami, Ronen. 2018. "Treatment of Invasive Candidiasis: A Narrative Review." *Journal of Fungi* 4(3): 97. http://www.mdpi.com/2309-608X/4/3/97.

Ben-Ami, Ronen, Russell Lewis, Konstantinos Leventakos, and Dimitrios Kontoyiannis. 2009. "*Aspergillus fumigatus* Inhibits Angiogenesis through the Production of Gliotoxin and Other Secondary Metabolites." *Blood* 114(26): 5393–99. http://www.pubmedcentral.nih.gov/articlerender.fcgi?artid=2925388&tool=pmcentrez&rendertype=abstract.

Bergeron, Audrey C et al. 2017. "*Candida albicans* and *Pseudomonas aeruginosa* Interact To Enhance Virulence of Mucosal Infection in Transparent Zebrafis." 85(11): 1–18. https://doi.org/10 .1128/IAI.00475-17.

Bernut, A. et al. 2014. "*Mycobacterium abscessus* Cording Prevents Phagocytosis and Promotes Abscess Formation." *Proceedings of the National Academy of Sciences* 111(10): E943–52. http://www.pnas.org/cgi/doi/10.1073/pnas.1321390111.

Bernut, Audrey et al. 2016. "Mycobacterium Abscessus -Induced Granuloma Formation Is Strictly Dependent on TNF Signaling and Neutrophil Trafficking." *PLoS pathogens* 12(11): e1005986. doi:10.1371/journal.ppat.1005986.

Berthier, Erwin et al. 2013. "Low-Volume Toolbox for the Discovery of Immunosuppressive Fungal Secondary Metabolites." *PLoS pathogens* 9(4): e1003289. http://www.pubmedcentral.nih.gov/articlerender.fcgi?artid=3623715&tool=pmcentrez&rendertype=abstract.

Bojarczuk, Aleksandra et al. 2016. "*Cryptococcus neoformans* Intracellular Proliferation and Capsule Size Determines Early Macrophage Control of Infection." *Scientific Reports* 6: 21489. http://www.nature.com/articles/srep21489.

Bolcome, Robert E et al. 2008. "Anthrax Lethal Toxin Induces Cell Death-Independent Permeability in Zebrafish Vasculature." *Proceedings of the National Academy of Sciences of the United States of America* 105(7): 2439–44.

Brothers, Kimberly M., Zachary R. Newman, and Robert T. Wheeler. 2011. "Live Imaging of Disseminated Candidiasis in Zebrafish Reveals Role of Phagocyte Oxidase in Limiting Filamentous Growth." *Eukaryotic Cell* 10(7): 932–44. doi:10.1128/EC.05005-11.

Brothers, Kimberly M et al. 2013. "NADPH Oxidase-Driven Phagocyte Recruitment Controls *Candida albicans* Filamentous Growth and Prevents Mortality." *PLoS pathogens* 9(10): e1003634. http://www.pubmedcentral.nih.gov/articlerender.fcgi?artid=3789746&tool=pmcentrez&rendertype=abstract.

Brown, Gordon D et al. 2012. "Hidden Killers: Human Fungal Infections." *Science translational medicine* 4(165): rv13. http://www.ncbi.nlm.nih.gov/pubmed/23253612 (November 2, 2014).

Brunke, S. et al. 2015. "Of Mice, Flies - and Men? Comparing Fungal Infection Models for Large-Scale Screening Efforts." *Disease Models & Mechanisms* 8(5): 473–86. http://dmm.biologists.org/cgi/doi/10.1242/dmm.019901.

Bruserud, O. 2013. "Bidirectional Crosstalk between Platelets and Monocytes Initiated by Toll-like Receptor: An Important Step in the Early Defense against Fungal Infections?" *Platelets.* 24(2): 85–97. http://dx.doi.org/10.3109/09537104.2012.678426.

Burn, Thomas, and Jorge Ivan Alvarez. 2017. "Reverse Transendothelial Cell Migration in Inflammation: To Help or to Hinder?" *Cellular and Molecular Life Sciences* 74(10): 1871–81. DOI 10.1007/s00018-016-2444-2.

Carrillo, Simón A et al. 2016. "Macrophage Recruitment Contributes to Regeneration of Mechanosensory Hair Cells in the Zebrafish Lateral Line." *Journal of Cellular Biochemistry* 10(9999): 1–10. http://doi.wiley.com/10.1002/jcb.25487.

Chamilos, Georgios et al. 2006. "*Drosophila melanogaster* as a Facile Model for Large-Scale Studies of Virulence Mechanisms and Antifungal Drug Efficacy in Candida Species." *The Journal of infectious diseases* 193(7): 1014–22. http://www.ncbi.nlm.nih.gov/pubmed/16518764.

Chandra, Jyotsna et al. 2007. "Interaction of *Candida albicans* with Adherent Human Peripheral Blood Mononuclear Cells Increases *C. albicans* Biofilm Formation and Results in Differential Expression of pro- and Anti-Inflammatory Cytokines." *Infection and Immunity* 75(5): 2612–20.

Chao, Chun-Cheih et al. 2010. "Zebrafish as a Model Host for *Candida albicans* Infection." *Infection and immunity* 78(6): 2512–21. http://www.pubmedcentral.nih.gov/articlerender.fcgi?artid=2876552&tool=pmcentrez&rendertype=abstract (September 8, 2014).

Charlier, Caroline et al. 2009. "Evidence of a Role for Monocytes in Dissemination and Brain Invasion by Cryptococcus Neoformans." *Infection and immunity* 77(1): 120–27. http://www.pubmedcentral.nih.gov/articlerender.fcgi?artid=2612285&tool=pmcentrez&rendertype=abstract (September 8, 2014).

Chen, J N et al. 1996. "Mutations Affecting the Cardiovascular System and Other Internal Organs in Zebrafish." *Development (Cambridge, England)* 123: 293–302. http://www.ncbi.nlm.nih.gov/pubmed/9007249.

Chen, Yin Zhi et al. 2015. "Zebrafish Egg Infection Model for Studying *Candida albicans* Adhesion Factors." *PLoS ONE* 10(11): e0143048. doi:10.1371/journal. pone.0143048.

Cheng, Shih-Chin, Leo a B Joosten, Bart-Jan Kullberg, and Mihai G Netea. 2012. "Interplay between *Candida albicans* and the Mammalian Innate Host Defense." *Infection and immunity* 80(4): 1304–13. http://www.pubmedcentral.nih.gov/articlerender.fcgi?artid=3318407&tool=pmcentrez&rendertype=abstract.

Chin, Voon Kin, Tze Yan Lee, Basir Rusliza, and Pei Pei Chong. 2016. "Dissecting *Candida albicans* Infection from the Perspective of *C. albicans* Virulence and Omics Approaches on Host–pathogen Interaction: A Review." *International Journal of Molecular Sciences* 17(1643). doi:10.3390/ijms17101643.

Clay, Hilary et al. 2007. "Dichotomous Role of the Macrophage in Early *Mycobacterium marinum* Infection of the Zebrafish." *Cell host & microbe* 2(1): 29–39. http://www.pubmedcentral.nih.gov/articlerender.fcgi?artid=3115716&tool=pmcentrez&rendertype=abstract.

D'Amico, L a, and M S Cooper. 2001. "Morphogenetic Domains in the Yolk Syncytial Layer of Axiating Zebrafish Embryos." *Developmental dynamics : an official publication of the American Association of Anatomists* 222(4): 611–24. http://www.ncbi.nlm.nih.gov/pubmed/11748830.

Davis, Rachelle P, Sarah Miller-Dorey, and Craig N Jenne. 2016. "Platelets and Coagulation in Infection." *Clinical & Translational Immunology* 5(7): e89. http://www.nature.com/doifinder/10.1038/cti.2016.39.

Davison, Jon M et al. 2007. "Transactivation from Gal4-VP16 Transgenic Insertions for Tissue-Specific Cell Labeling and Ablation in Zebrafish." *Developmental biology* 304(2): 811–24. http://www.pubmedcentral.nih.gov/articlerender.fcgi?artid=3470427&tool=pmcentrez&rendertype=abstract.

Dejana, Elisabetta, Fabrizio Orsenigo, and Maria Grazia Lampugnani. 2008. "The Role of Adherens Junctions and VE-Cadherin in the Control of Vascular Permeability." *Journal of Cell Science* 121: 2115–22. doi:10.1242/jcs.017897.

Deng, Q., and A. Huttenlocher. 2012. "Leukocyte Migration from a Fish Eye's View." *Journal of Cell Science* 125: 3949–56. doi: 10.1242/jcs.093633.

Deng, Qing et al. 2011. "Dual Roles for Rac2 in Neutrophil Motility and Active Retention in Zebrafish Hematopoietic Tissue." *Developmental Cell* 21(4): 735–45. http://dx.doi.org/10.1016/j.devcel.2011.07.013.

Doyle, Timothy C et al. 2006. "Visualizing Fungal Infections in Living Mice Using Bioluminescent Pathogenic *Candida albicans* Strains Transformed with the Firefly Luciferase Gene." *Microbial pathogenesis* 40(2): 82–90. http://www.ncbi.nlm.nih.gov/pubmed/16426810.

Duggan, Seána, Ines Leonhardt, Kerstin Hünniger, and Oliver Kurzai. 2015. "Host Response to *Candida albicans* Bloodstream Infection and Sepsis." *Virulence*. http://www.tandfonline.com/doi/abs/10.4161/21505594.2014.988096.

Ellett, Felix et al. 2011. "Mpeg1 Promoter Transgenes Direct Macrophage-Lineage Expression in Zebrafish." *Blood* 117(4): e49-56. http://www.pubmedcentral.nih.gov/articlerender.fcgi?artid=3056479&tool=pmcentrez&rendertype=abstract.

Ellet, Felix et al. 2018. "Macrophages Protect *Talaromyces marneffei* Conidia from Myeloperoxidase-Dependent Neutrophil Fungicidal Activity during Infection Establishment *in vivo*." *PLoS pathogens* 14(6): e1007063. http://dx.doi.org/10.1371/journal.ppat.1007063.

Erwig, Lars P., and Neil A R Gow. 2016. "Interactions of Fungal Pathogens with Phagocytes." *Nature Reviews Microbiology* 14(3): 163–76. http://dx.doi.org/10.1038/nrmicro.2015.21.

Feldman, Michael B., Jatin M. Vyas, and Michael K. Mansour. 2018. "It Takes a Village: Phagocytes Play a Central Role in Fungal Immunity." *Seminars in Cell and Developmental Biology*. https://doi.org/10.1016/j.semcdb.2018.04.008.

Filler, Scott G. 2014a. "*In vitro* Models of Hematogenously Disseminated Candidiasis." *Virulence* 5(2): 240–42. http://www.pubmedcentral.nih.gov/articlerender.fcgi?artid=3956498&tool=pmcentrez&rendertype=abstract.

Fishelson, L. 1995. "Ontogenesis of Cytological Structures around the Yolk Sac during Embryologic and Early Larval Development of Some Cichlid Fishes." *Journal of Fish Biology* 47(3): 479–91. https://doi.org/10.1111/j.1095-8649.1995.tb01916.x.

Foley, Jonathan E et al. 2009. "Rapid Mutation of Endogenous Zebrafish Genes Using Zinc Finger Nucleases Made by Oligomerized Pool ENgineering (OPEN)." *PloS one* 4(2): e4348. doi:10.1371/journal.pone.0004348.

Fuchs, Beth Burgwyn, Elizabeth O'Brien, Joseph B El Khoury, and Eleftherios Mylonakis. 2010. "Methods for Using *Galleria mellonella* as a Model Host to Study Fungal Pathogenesis." *Virulence* 1(6): 475–82. https://doi.org/10.4161/viru.1.6.12985.

Gibson, Josie F et al. 2017. "Dissemination of *Cryptococcus neoformans* via Localised Proliferation and Blockage of Blood Vessels ." *bioRxiv*. doi: http://dx.doi.org/10.1101/184200.

Gilbert, Andrew S et al. 2017. "Vomocytosis of Live Pathogens from Macrophages Is Regulated by the Atypical MAP Kinase ERK5." *Science advances* 3(8): e1700898. doi: 10.1126/sciadv.1700898.

Glittenberg, Marcus T et al. 2011. "Wild-Type *Drosophila melanogaster* as an Alternative Model System for Investigating the Pathogenicity of *Candida albicans*." *Disease models & mechanisms* 4(4): 504–14. doi: 10.1242/dmm.006619.

Gow, Neil a R, Frank L van de Veerdonk, Alistair J P Brown, and Mihai G Netea. 2012. "*Candida albicans* Morphogenesis and Host Defence: Discriminating Invasion from Colonization." *Nature reviews. Microbiology* 10(2): 112–22. doi:10.1038/nrmicro271.

Gratacap, Remi L., Allison K. Scherer, Brittany G. Seman, and Robert T. Wheeler. 2017. "Control of Mucosal Candidiasis in the Zebrafish Swim Bladder Depends on Neutrophils That Block Filament Invasion and Drive Extracellular-Trap Production." *Infection* 85(9): e00276-17. https://iai.asm.org/content/85/9/e00276-17.

Gratacap, Remi L, John F Rawls, and Robert T Wheeler. 2013. "Mucosal Candidiasis Elicits NF-KB Activation, Proinflammatory Gene Expression and Localized Neutrophilia in Zebrafish." *Disease models & mechanisms* 6(5): 1260–70. http://dmm.biologists.org/lookup/suppl/doi:10.1242/dmm.012039/-/DC1.

Gray, Caroline et al. 2011. "Simultaneous Intravital Imaging of Macrophage and Neutrophil Behaviour during Inflammation Using a Novel Transgenic Zebrafish." *Thrombosis and Haemostasis* 105.5: 811–19. doi:10.1160/TH10-08-0525.

Griffith, Jason W., Caroline L. Sokol, and Andrew D. Luster. 2014. "Chemokines and Chemokine Receptors: Positioning Cells for Host Defense and Immunity." *Annual Review of Immunology* 32(1): 659–702. http://www.annualreviews.org/doi/10.1146/annurev-immunol-032713-120145.

Grubb, Sarah E W et al. 2008a. "*Candida albicans* -Endothelial Cell Interactions: A Key Step in the Pathogenesis of Systemic Candidiasis." *Infection and immunity* 76(10): 4370–77. https://doi.org/10.1128/IAI.00332-08.

Hall, Chris et al. 2007. "The Zebrafish Lysozyme C Promoter Drives Myeloid-Specific Expression in Transgenic Fish." *BMC Dev Biol* 7: 42. http://www.ncbi.nlm.nih.gov/pubmed/17477879.

Hall, Chris, Phil Crosier, and Kathryn Crosier. 2015. "Inflammatory Cytokines Provide Both Infection-Responsive and Developmental Signals for Blood Development: Lessons from the Zebrafish." *Molecular Immunology* 69: 113–22. http://dx.doi.org/10.1016/j.molimm.2015.10.020.

Hamm, E. E., D. E. Voth, and J. D. Ballard. 2006. "Identification of Clostridium Difficile Toxin B Cardiotoxicity Using a Zebrafish Embryo Model of Intoxication." *Proceedings of the National Academy of Sciences* 103(38): 14176–81. http://www.pnas.org/cgi/doi/10.1073/pnas.0604725103.

Harvie, Elizabeth a, Julie M Green, Melody N Neely, and Anna Huttenlocher. 2013. "Innate Immune Response to *Streptococcus iniae* Infection in Zebrafish Larvae." *Infection and immunity* 81(1): 110–21. doi: 10.1128/IAI.00642-12.

Hassel, David et al. 2008. "Deficient Zebrafish Ether-à-Go-Go-Related Gene Channel Gating Causes Short-QT Syndrome in Zebrafish Reggae Mutants." *Circulation* 117(7): 866–75. doi: 10.1161/CIRCULATIONAHA.107.752220.

Helmchen, Fritjof, and Winfried Denk. 2005. "Deep Tissue Two-Photon Microscopy." *Nature Methods* 2(12): 932–40. doi:10.1038/NMETH818.

Henry, Katherine M, Catherine a Loynes, Moira K B Whyte, and Stephen a Renshaw. 2013. "Zebrafish as a Model for the Study of Neutrophil Biology." *Journal of leukocyte biology* 94(4): 633–42. doi: 10.1189/jlb.1112594.

Holmes, Geoffrey R. et al. 2012. "Drift-Diffusion Analysis of Neutrophil Migration during Inflammation Resolution in a Zebrafish Model." *Advances in Hematology* 2012: 1–8. http://www.hindawi.com/journals/ah/2012/792163/.

Hortle, Elinor et al. 2018. "Inhibition of Thrombocyte Activation Restores Protective Immunity to Mycobacterial Infection." *bioRxiv*: 338111. https://www.biorxiv.org/content/early/2018/06/05/338111.

Hosseini, Rohola et al. 2016. "Efferocytosis and Extrusion of Leukocytes Determine the Progression of Early Mycobacterial Pathogenesis." *Journal of Cell Science*. doi: 10.1242/jcs.135194.

Hurley, Sinead M., Nataliya Lutay, Bo Holmqvist, and Oonagh Shannon. 2016. "The Dynamics of Platelet Activation during the Progression of Streptococcal Sepsis." *PLoS ONE* 11(9): e0163531. doi:10.1371/ journal.pone.0163531.

Johnson, C.J. et al. 2018. "Emerging Fungal Pathogen *Candida auris* Evades Neutrophil Attack." *mBio* 9(e01403-18). https://doi.org/10 .1128/mBio.01403-18.

Jones, R. A. et al. 2013. "Modelling of Human Wiskott-Aldrich Syndrome Protein Mutants in Zebrafish Larvae Using *in vivo* Live Imaging." *Journal of Cell Science* 126(18): 4077–84. http://jcs.biologists.org/cgi/doi/10.1242/jcs.128728.

Jung, Hyun Min et al. 2017. "Development of the Larval Lymphatic System in Zebrafish." *Development* 144(11): 2070–81. http://dev.biologists.org/lookup/doi/10.1242/dev.145755.

Kara, A. et al. 2018. "The Frequency of Infective Endocarditis in Candida Bloodstream Infections: A Retrospective Study in a Child Hospital." *Brazilian Journal of Cardiovascular Surgery* 33(1): 54–58. doi: 10.21470/1678-9741-2017-0049%0Amost.

Karbassi, a, J M Becker, J S Foster, and R N Moore. 1987. "Enhanced Killing of *Candida albicans* by Murine Macrophages Treated with Macrophage Colony-Stimulating Factor: Evidence for Augmented Expression of Mannose Receptors." *The Journal of Immunology* 139(2): 417–21. http://www.ncbi.nlm.nih.gov/pubmed/3298429.

Kimmel, Charles B et al. 1995. "Stages of Embryonic Development of the Zebrafish." 203: 253–310. https://www.ncbi.nlm.nih.gov/pubmed/8589427.

Knox, Benjamin P et al. 2014. "Distinct Innate Immune Phagocyte Responses to *Aspergillus fumigatus Conidia and Hyphae in Zebrafish Larvae." Eukaryotic cell 13(10): 1266–77. doi:10.112*8/EC.00080-14.

Koh, Andrew Y. et al. 2008. "Mucosal Damage and Neutropenia Are Required for *Candida albicans* Dissemination." *PLoS Pathogens* 4(2): e35. doi:10.1371/journal.ppat.0040035.

———. 2013. "Murine Models of Candida Gastrointestinal Colonization and Dissemination." *Eukaryotic Cell* 12(11): 1416–22. doi:10.1128/EC.00196-13.

Kondakova, Ekaterina Alexandrovna A., and Vladimir Ivanovich I. Efremov. 2014. "Morphofunctional Transformations of the Yolk Syncytial Layer during Zebrafish Development." *Journal of Morphology* 275: 206–16. DOI 10.1002/jmor.20209.

Krysan, Damian J., Fayyaz S. Sutterwala, and Melanie Wellington. 2014. "Catching Fire: *Candida albicans*, Macrophages, and Pyroptosis." *PLoS Pathogens* 10(6): e1004139. doi:10. 1371/journal.ppat.1004139 Editor:

Lawson, Nathan D., and Brant M. Weinstein. 2002. "*In vivo* Imaging of Embryonic Vascular Development Using Transgenic Zebrafish." *Developmental Biology* 248: 307–18. doi:10.1006/dbio.2002.0711.

Li, Ling et al. 2016. "*In vivo* Screening Using Transgenic Zebrafish Embryos Reveals New Effects of HDAC Inhibitors Trichostatin A and Valproic Acid on Organogenesis." *PLoS ONE* 11(2): e0149497. doi:10.1371/journal.pone.0149497.

Lin, Hui Feng et al. 2005. "Analysis of Thrombocyte Development in CD41-GFP Transgenic Zebrafish." *Blood* 106(12): 3803–10. DOI 10.1182/blood-2005-01-0179.

Lionakis, Michail S, Jean K Lim, Chyi-Chia Richard Lee, and Philip M Murphy. 2011. "Organ-Specific Innate Immune Responses in a Mouse Model of Invasive Candidiasis." *Journal of innate immunity* 3(2): 180–99. http://www.pubmedcentral.nih.gov/articlerender.fcgi?artid=3072204&tool=pmcentrez&rendertype=abstract.

Liu, Yaoping et al. 2015. "New Signaling Pathways Govern the Host Response to *C. albicans* Infection in Various Niches." *Genome Research* 25: 679–89. http://www.genome.org/cgi/doi/10.1101/gr.187427.114.

Liu, Yaoping, and Scott G. Filler. 2011. "*Candida albicans* Als3, a Multifunctional Adhesin and Invasin." *Eukaryotic Cell* 10(2): 168–73. doi:10.1128/EC.00279-10.

Longcore, Jerry R., Joyce E. Longcore, Allan P. Pessier, and William A. Halteman. 2007. "Chytridiomycosis Widespread in Anurans of Northeastern United States." *Journal of Wildlife Management* 71(2): 435–44. http://www.bioone.org/doi/abs/10.2193/2006-345.

Losse, Josephine et al. 2011. "Role of PH-Regulated Antigen 1 of *Candida albicans* in the Fungal Recognition and Antifungal Response of Human Neutrophils." *Molecular immunology* 48(15–16): 2135–43. http://www.ncbi.nlm.nih.gov/pubmed/21820180.

MacCallum, Donna M., and Frank C. Odds. 2005. "Temporal Events in the Intravenous Challenge Model for Experimental *Candida albicans* Infections in Female Mice." *Mycoses* 48(3): 151–61. doi: 10.1111/j.1439-0507.2005.01121.x.

Manoharan, Ranjith Kumar, Jin-Hyung Lee, Yong-Guy Kim, and Jintae Lee. 2017. "Alizarin and Chrysazin Inhibit Biofilm and Hyphal Formation by *Candida albicans*." *Frontiers in Cellular and Infection Microbiology* 7(447). http://journal.frontiersin.org/article/10.3389/fcimb.2017.00447/full.

Marjoram, Lindsay et al. 2015. "Epigenetic Control of Intestinal Barrier Function and Inflammation in Zebrafish." *Proceedings of the National Academy of Sciences of the United States of America* 112(9): 2770–75. http://www.pnas.org/content/112/9/2770.long#sec-3.

Martinez, Alejandra N, Smriti Mehra, and Deepak Kaushal. 2013. "Role of Interleukin 6 in Innate Immunity to *Mycobacterium tuberculosis* Infection." *The Journal of infectious diseases* 207(8): 1253–61. http://www.pubmedcentral.nih.gov/articlerender.fcgi?artid=3693587&tool=pmcentrez&rendertype=abstract.

Mattingly, Carolyn J. et al. 2009. "Perturbation of Defense Pathways by Low-Dose Arsenic Exposure in Zebrafish Embryos." *Environmental Health Perspectives* 117(6): 981–87. doi:10.1289/ehp.0900555 available.

McDonald, Braedon et al. 2012. "Intravascular Neutrophil Extracellular Traps Capture Bacteria from the Bloodstream during Sepsis." *Cell Host and Microbe* 12(3): 324–33. http://dx.doi.org/10.1016/j.chom.2012.06.011.

McKenzie, C G J et al. 2010. "Contribution of *Candida albicans* Cell Wall Components to Recognition by and Escape from Murine Macrophages." *Infection and immunity* 78(4): 1650–58. doi: 10.1128/IAI.00001-10.

Meara, Teresa R O et al. 2018a. "High-Throughput Screening Identifies Genes Required for *Candida albicans* Induction of Macrophage Pyroptosis." *mBio* 9: e01581-18. https://doi.org/10.1128/mBio .01581-18. Editor.

Milan, David J. et al. 2003. "Drugs That Induce Repolarization Abnormalities Cause Bradycardia in Zebrafish." *Circulation* 107(10): 1355–58. doi: 10.1161/01.CIR.0000061912.88753.87.

Mitra, Soumya, Kristy Dolan, Thomas H. Foster, and Melanie Wellington. 2010. "Imaging Morphogenesis of *Candida albicans* during Infection in a Live Animal." *Journal of Biomedical Optics* 15(1): e010504. http://biomedicaloptics.spiedigitallibrary.org/article.aspx?doi=10.1117/1.3290243.

Moyes, David L. et al. 2016. "Candidalysin Is a Fungal Peptide Toxin Critical for Mucosal Infection." *Nature* 532(7597): 64–68. http://dx.doi.org/10.1038/nature17625.

Moyes, David L., Jonathan P. Richardson, and Julian R. Naglik. 2015. "*Candida albicans* - Epithelial Interactions and Pathogenicity Mechanisms: Scratching the Surface." *Virulence* 6(4): 338–46. doi: 10.1080/21505594.2015.1012981.

Moyes, David L, and Julian R Naglik. 2011. "Mucosal Immunity and *Candida albicans* Infection." *Clinical & developmental immunology* 2011: 1–9. doi:10.1155/2011/346307%0AReview (July 23, 2014).

Naglik, Julian R, Paul L. Fidel, and Frank C. Odds. 2008. "Animal Models of Mucosal Candida Infection." *FEMS microbiology letters* 283(2): 129–39. doi:10.1111/j.1574-6968.2008.01160.x.

Naglik, Julian R, David L Moyes, Betty Wächtler, and Bernhard Hube. 2011. "*Candida albicans* Interactions with Epithelial Cells and Mucosal Immunity." *Microbes and infection* 13: 963–76. doi:10.1016/j.micinf.2011.06.009.

Netea, M G et al. 2015. "Immune Defence against Candida Fungal Infections." *Nat Rev Immunol* 15(10): 630–42. http://www.ncbi.nlm.nih.gov/pubmed/26388329.

Nolan, Sabrina J., Man Shun Fu, Isabelle Coppens, and Arturo Casadevall. 2017. "Lipids Affect the *Cryptococcus neoformans*-Macrophage Interaction and Promote Nonlytic Exocytosis." *Infection and Immunity* 85(12): e00564-17. doi: 10.1128/IAI.00564-17.

Nourshargh, Sussan, Stephen A. Renshaw, and Beat A. Imhof. 2016. "Reverse Migration of Neutrophils: Where, When, How, and Why?" *Trends in Immunology* 37(5): 273–86. http://dx.doi.org/10.1016/j.it.2016.03.006.

Novikov, Aleksey et al. 2011. "*Mycobacterium tuberculosis* Triggers Host Type I IFN Signaling To Regulate IL-1-Beta Production in Human Macrophages." *Journal of immunology* 187: 2540–47. www.jimmunol.org/cgi/doi/10.4049/jimmunol.1100926.

de Oliveira, Sofia, Emily E Rosowski, and Anna Huttenlocher. 2016. "Neutrophil Migration in Infection and Wound Repair: Going Forward in Reverse." *Nature reviews. Immunology* 16(6): 378–91. http://www.ncbi.nlm.nih.gov/pubmed/27231052.

Orozco, Alison S, Xiang Zhou, and Scott G Filler. 2000. "Mechanisms of the Proinflammatory Response of Endothelial Cells to *Candida albicans* Infection Mechanisms of the Proinflammatory Response of Endothelial Cells to *Candida* a*lbicans* Infection." *Infection and immunity* 68(3): 1134–41. doi: 10.1128/IAI.68.3.1134-1141.2000.

Ortega-Riveros, Marcelo et al. 2017. "Usefulness of the Non-Conventional *Caenorhabditis elegans* Model to Assess Candida Virulence." *Mycopathologia* 182: 785–95. DOI 10.1007/s11046-017-0142-8.

Otrock, Zaher K, Rami A R Mahfouz, Jawad A Makarem, and Ali I Shamseddine. 2007. "Understanding the Biology of Angiogenesis : Review of the Most Important Molecular Mechanisms." *Blood Cells, Molecules, and Diseases* 39: 212–20. doi:10.1016/j.bcmd.2007.04.001.

Page, Clive, and Simon Pitchford. 2013. "Neutrophil and Platelet Complexes and Their Relevance to Neutrophil Recruitment and Activation." *International Immunopharmacology* 17(4): 1176–84. http://dx.doi.org/10.1016/j.intimp.2013.06.004.

Pappas, Peter G. et al. 2018. "Invasive Candidiasis." *Nature Reviews Disease Primers* 4: 18026. http://dx.doi.org/10.1038/nrdp.2018.26.

Peters, Brian M. et al. 2014. "Fungal Morphogenetic Pathways Are Required for the Hallmark Inflammatory Response during *Candida albicans* Vaginitis." *Infection and Immunity* 82(2): 532–43. doi:10.1128/IAI.01417-13.

Pfaller, M A, and D J Diekema. 2007. "Epidemiology of Invasive Candidiasis : A Persistent Public Health Problem Epidemiology of Invasive Candidiasis : A Persistent Public Health Problem." *Clinical Microbiology reviews* 20(1): 133–63. doi:10.1128/CMR.00029-06.

Pisharath, Harshan, and Michael J Parsons. 2009. "Nitroreductase-Mediated Cell Ablation in Transgenic Zebrafish Embryos." *Methods in Microbiology* 546: 133–43. doi: 10.1007/978-1-60327-977-2_9.

Prajsnar, Tomasz K. et al. 2012. "A Privileged Intraphagocyte Niche Is Responsible for Disseminated Infection of *Staphylococcus aureus* in a Zebrafish Model." *Cellular Microbiology* 14(10): 1600–1619. http://doi.wiley.com/10.1111/j.1462-5822.2012.01826.x.

Rane, Hallie S. et al. 2014. "Candida Albicans VPS4 Contributes Differentially to Epithelial and Mucosal Pathogenesis." *Virulence* 5(8): 810–18. https://doi.org/10.4161/21505594.2014.956648.

Renshaw, Stephen a et al. 2006. "A Transgenic Zebrafish Model of Neutrophilic Inflammation." *Blood* 108(13): 3976–78. http://www.ncbi.nlm.nih.gov/pubmed/16926288.

Rivera, Amariliz, Mark C. Siracusa, George S. Yap, and William C. Gause. 2016. "Innate Cell Communication Kick-Starts Pathogen-Specific Immunity." *Nature Immunology* 17(4): 356–63. doi:10.1038/ni.3375.

Robert, R et al. 2000. "Adherence of Platelets to Candida Species *In vivo*." *Society* 68(2): 570–76. https://www.ncbi.nlm.nih.gov/pubmed/10639419.

Rosowski, Emily E., Qing Deng, Nancy P. Keller, and Anna Huttenlocher. 2016. "Rac2 Functions in Both Neutrophils and Macrophages To Mediate Motility and Host Defense in Larval Zebrafish." *The Journal of Immunology* 197(12): 4780–90. doi: 10.4049/jimmunol.1600928.

Rosowski, Emily E et al. 2018. "Macrophages Inhibit Aspergillus Germination and Neutrophil-Mediated Fungal Killing *in vivo*." *PLoS Pathogens* 14(8): e1007229. https://doi.org/10.1371/journal.ppat.1007229.

Roumenina, Lubka T., Julie Rayes, Marie Frimat, and Veronique Fremeaux-Bacchi. 2016. "Endothelial Cells: Source, Barrier, and Target of Defensive Mediators." *Immunological Reviews* 274: 307–29. doi: 10.1111/imr.12479.

Rubinstein, Amy L. 2006. "Zebrafish Assays for Drug Toxicity Screening." *Expert Opinion Drug Metabolism Toxicology* 2(2): 231–40. doi: 10.1517/17425255.2.2.231.

Santiago-Tirado, Felipe H. et al. 2017. "Trojan Horse Transit Contributes to Blood-Brain Barrier Crossing of a Eukaryotic Pathogen." *mBio* 8: e02183-16. https://doi.org/10.1128/mBio.02183-16.

Saralahti, A, and M Ramet. 2015. "Zebrafish and Streptococcal Infections." *Scandinavian Journal of Immunology* 82: 174–83. doi: 10.1111/sji.12320.

Schindelin, Johannes et al. 2012. "Fiji: An Open-Source Platform for Biological-Image Analysis." *Nature Methods* 9(7): 676–82. doi:10.1038/nmeth.2019%0A676.

Seider, Katja et al. 2010. "Interaction of Pathogenic Yeasts with Phagocytes: Survival, Persistence and Escape." *Current opinion in microbiology* 13: 392–400. DOI 10.1016/j.mib.2010.05.001.

Seman, Brittany G et al. 2018. "Yeast and Filaments Have Specialized, Independent Activities in a Zebrafish Model of *Candida albicans* Infection." *Infection and immunity* 86: e00415-18. https://doi.org/10.1128/IAI.00415-18.

Shelef, Miriam A., Sebastien Tauzin, and Anna Huttenlocher. 2013. "Neutrophil Migration: Moving from Zebrafish Models to Human Autoimmunity." *Immunological Reviews* 256: 269–81. doi: 10.1111/imr.12124.

Sheppard, Donald C, and Scott G Filler. 2014. "Host Cell Invasion by Medically Important Fungi." *Cold Spring Harbor perspectives in medicine* 5: a019687. doi: 10.1101/cshperspect.a019687.

Soares, Miguel P., Luis Teixeira, and Luis F. Moita. 2017. "Disease Tolerance and Immunity in Host Protection against Infection." *Nature Reviews Immunology* 17(2): 83–96. http://dx.doi.org/10.1038/nri.2016.136.

Speth, Cornelia et al. 2013. "Platelets as Immune Cells in Infectious Diseases." *Future Medicine* 8(11): 1431–51. doi: 10.2217/FMB.13.104.

Speth, Cornelia, Gunter Rambach, and Cornelia Lass-Florl. 2014. "Platelet Immunology in Fungal Infections." *Thrombosis and Haemostasis* 112: 632–39. http://dx.doi.org/10.1160/TH14-01-0074.

Stainier, D Y, R K Lee, and M C Fishman. 1993. "Cardiovascular Development in the Zebrafish. I. Myocardial Fate Map and Heart Tube Formation." *Development* 119: 31–40. https://www.ncbi.nlm.nih.gov/pubmed/8275863.

Sudbery, Peter, Neil Gow, and Judith Berman. 2004. "The Distinct Morphogenic States of *Candida albicans*." *Trends in microbiology* 12(7): 317–24. http://www.ncbi.nlm.nih.gov/pubmed/15223059.

Sullivan, Con, and Carol H Kim. 2008. "Zebrafish as a Model for Infectious Disease and Immune Function." *Fish & shellfish immunology* 25(4): 341–50. doi:10.1016/j.fsi.2008.05.005.

Sutton, Timothy a et al. 2003. "Injury of the Renal Microvascular Endothelium Alters Barrier Function after Ischemia." *American journal of renal physiology* 285: F191-8. http://www.ncbi.nlm.nih.gov/pubmed/12684225.

Swidergall, Marc, and Scott G Filler. 2017. "Oropharyngeal Candidiasis : Fungal Invasion and Epithelial Cell Responses." *PloS Pathogens* 13(1): e1006056. doi: 10.1371/journal.ppat.1006056.

Sykes, D. et al. 2016. "A Novel System for the Study of Neutrophil-Fungal Interactions." *Open Forum Infectious Diseases* 3(1): 2208. https://doi.org/10.1093/ofid/ofw172.1756.

Thwaites, Guy E., and Vanya Gant. 2011. "Are Bloodstream Leukocytes Trojan Horses for the Metastasis of *Staphylococcus aureus*?" *Nature Reviews Microbiology* 9(3): 215–22. http://www.nature.com/doifinder/10.1038/nrmicro2508.

Tobin, David M, Robin C May, and Robert T Wheeler. 2012. "Zebrafish: A See-through Host and a Fluorescent Toolbox to Probe Host-Pathogen Interaction." *PLoS pathogens* 8(1): e1002349. http://www.pubmedcentral.nih.gov/articlerender.fcgi?artid=3252360&tool=pmcentrez&rendertype=abstract.

Torraca, Vincenzo, Samrah Masud, Herman P Spaink, and Annemarie H Meijer. 2014. "Macrophage-Pathogen Interactions in Infectious Diseases: New Therapeutic Insights from the Zebrafish Host Model." *Disease models & mechanisms* 7(7): 785–97. http://www.ncbi.nlm.nih.gov/pubmed/24973749.

Torraca, Vincenzo, Claudia Tulotta, B. Ewa Snaar-Jagalska, and Annemarie H. Meijer. 2017. "The Chemokine Receptor CXCR4 Promotes Granuloma Formation by Sustaining a Mycobacteria-Induced Angiogenesis Programme." *Scientific Reports* 7: 45061. http://dx.doi.org/10.1038/srep45061.

Trinh, Le a et al. 2011. "A Versatile Gene Trap to Visualize and Interrogate the Function of the Vertebrate Proteome." *Genes & development* 25(21): 2306–20. doi: 10.1101/gad.174037.111%0ASupplemental.

Tucey, Timothy M et al. 2018. "Glucose Homeostasis Is Important for Immune Cell Viability during Candida Challenge and Host Survival of Systemic Fungal Infection." *Cell Metabolism* 27(5): 988–1006.e7. https://doi.org/10.1016/j.cmet.2018.03.019.

Vancraeyneste, Hélène et al. 2016. "Short Fungal Fractions of β-1,3 Glucans Affect Platelet Activation." *American journal of physiology. Heart and circulatory physiology* 311: H725–H734. doi:10.1152/ajpheart.00907.2015.

Vázquez-Torres, a, and E Balish. 1997. "Macrophages in Resistance to Candidiasis." *Microbiology and molecular biology reviews : MMBR* 61(2): 170–92. http://www.ncbi.nlm.nih.gov/pubmed/19121076.

Voelz, Kerstin, Remi L Gratacap, and Robert T Wheeler. 2015a. "A Zebrafish Larval Model Reveals Early Tissue-Specific Immune Responses to *Mucor circinelloides*." *Disease Models & Mechanisms DMM* 8(11): 1375–88. doi:10.1242/dmm.019992.

Vu, Kiem et al. 2014. "Invasion of the Central Nervous System by *Cryptococcus neoformans* Requires a Secreted Fungal Metalloprotease." *mBio* 5(3): e01101-14. doi:10.1128/mBio.01101-14.

Wächtler, Betty et al. 2012. "*Candida albicans* -Epithelial Interactions: Dissecting the Roles of Active Penetration, Induced Endocytosis and Host Factors on the Infection Process." *PloS one* 7(5): e36952. doi:10.1371/journal.pone.0036952.

Wang, Fengjun et al. 2005. "Interferon-γ and Tumor Necrosis Factor-α Synergize to Induce Intestinal Epithelial Barrier Dysfunction by up-Regulating Myosin Light Chain Kinase Expression." *American Journal of Pathology* 166(2): 409–19. http://dx.doi.org/10.1016/S0002-9440(10)62264-X.

Wang, M I N, Herman Friedman, and Julie Y Djeu. 1989. "Enhancement of Human Monocyte Function against *Candida albicans* by the Colony-Stimulating Factors: IL-3, Granulocyte-Macrophage-CSF, and Macrophage-CSF." *The Journal of Immunology* 143(2): 671–77. https://www.ncbi.nlm.nih.gov/pubmed/2661688.

de Wet, J R et al. 1987. "Firefly Luciferase Gene: Structure and Expression in Mammalian Cells." *Molecular and cellular biology* 7(2): 725–37. doi: 10.1128/MCB.7.2.725.

Woth, G et al. 2012. "Activated Platelet-Derived Microparticle Numbers Are Elevated in Patients with Severe Fungal (Candida Albicans) Sepsis." *Ann Clin Biochem* 49: 554–60. doi: 10.1258/acb.2012.011215.

Yaniv, Karina et al. 2006. "Live Imaging of Lymphatic Development in the Zebrafish." *Nature Medicine* 12(6): 711–16. doi:10.1038/nm1427.

Yeaman, Michael R. 2014. "Platelets: At the Nexus of Antimicrobial Defence." *Nature reviews. Microbiology* 12(6): 426–37. http://www.ncbi.nlm.nih.gov/pubmed/24830471.

Yoshida, Nagisa, Eva-Maria Frickel, and Serge Mostowy. 2017. "Macrophage – Microbe Interactions : Lessons from the Zebrafish Model." *Frontiers in Immunology* 8(1703). doi: 10.3389/fimmu.2017.01703%0AMacrophages.

Zhao, Dongying, Gang Qiu, Zhongcheng Luo, and Yongjun Zhang. 2015. "Platelet Parameters and (1, 3)-β-D-Glucan as a Diagnostic and Prognostic Marker of Invasive Fungal Disease in Preterm Infants." *PloS one* 10(4): e0123907. doi:10.1371/journal.pone.0123907.

Zhao, Xiaomin et al. 2004. "ALS3 and ALS8 Represent a Single Locus That Encodes a *Candida albicans* Adhesin; Functional Comparisons between Als3p and Als1p." *Microbiology* 150: 2415–28. DOI 10.1099/mic.0.26943-0.

Zhu, Weidong, and Scott G Filler. 2010. "Interactions of *Candida albicans* with Epithelial Cells." *Cellular microbiology* 12(3): 273–82. doi:10.1111/j.1462-5822.2009.01412.x.

BIOGRAPHY OF THE AUTHOR

Allison Scherer was born in Minneapolis, Minnesota on December 13, 1989. She was raised in Bloomington, Minnesota and graduated from John F. Kennedy High School in 2008. She then attended St. Cloud State University and graduated in May 2012 with a Bachelor's degree in Biology and a Supplementary Communications degree. She then attended graduate school at the University of Maine for a PhD in Microbiology. Upon graduation, she will be joining the Mansour lab at Massachusetts General Hospital to investigate neutrophil response to pathogenic fungi. Allison is a candidate for the Doctorate of Philosophy in Microbiology from the University of Maine in December 2018.